

UNIVERSIDADE DE LISBOA  
FACULDADE DE CIÊNCIAS  
DEPARTAMENTO DE BIOLOGIA VEGETAL



**Development of a new immunoliposome drug delivery system  
for treatment of pneumococcal meningitis**

Marta Lisete Santos da Silva

**Mestrado em Microbiologia Aplicada**

Dissertação orientada por:  
Doutor Frederico Aires da Silva (FMV-UL)  
Professora Doutora Raquel Sá-Leão (FCUL)



This Dissertation was fully performed at Faculty of Veterinary Medicine of the University of Lisbon under the direct supervision of Doutor Frederico Aires da Silva

Professora Raquel Sá-Leão was the internal supervisor designated in the scope of the Master in Applied Microbiology of the Faculty of Sciences of the University of Lisbon.

## **Agradecimentos**

*“Nothing in life is to be feared, it is only to be understood. Now, is the time to understand more, so that we may fear less.”*

Marie Curie

Tudo fica um pouco mais fácil quando partilhamos a nossa caminhada com pessoas excecionais e é a elas que quero agradecer pela colaboração neste projeto.

Gostaria de começar por agradecer ao meu orientador, Doutor Frederico Aires da Silva, por me ter aceite no seu laboratório, mas acima de tudo por todos os incentivos, todos os conhecimentos que me transmitiu e por me ter feito ambicionar sempre mais.

À Doutora Sandra Aguiar por me ter apresentado este projeto, por partilhar comigo este mundo que é a microbiologia, mas acima de tudo por toda ajuda, em cada etapa. Todos os incentivos, todos os conselhos e todos os conhecimentos fizeram com que este projeto progredisse, e isso não seria possível sem ti.

À professora Doutora Raquel Sá-Leão, a minha orientadora da FCUL, por me ter acompanhado nesta etapa e por toda a ajuda e disponibilidade prestada.

À Doutora Manuela Gaspar (FFUL) e à Magda Ferreira (FAS-Lab) pelo desenvolvimento dos lipossomas, que foram um ponto crucial neste projeto.

Ao Prof. José Melo Cristino e ao Prof. Mário Ramirez da Faculdade de Medicina por gentilmente nos terem cedido as estirpes isoladas de infeção.

À minha colega de laboratório Diana Martins, que participou ativamente na segunda parte deste projeto, por toda ajuda e incentivos prestados, assim como todas as conversas e todos os momentos que tornaram esta tese mais fácil. Sem ti, era mais difícil.

Às minhas colegas de laboratório Joana Dias, Ana André, Isa Moutinho, Cristina Rita e Maria Ogren por me terem integrado da melhor maneira no laboratório, pela partilha de conhecimentos pela entreaajuda, e por terem tornado esta caminhada mais fácil e mais feliz.

À minha amiga Alexandra Rocha, por estar presente em cada etapa da minha vida. Por partilhar comigo as minhas vitórias, e me incentivar nas derrotas. Por toda amizade, toda a motivação e por nunca me deixares desistir em nenhuma circunstância. Afinal, o que o Porto uniu, ninguém separa.

À minha amiga Esmeralda Ramos, por mesmo longe estar sempre tão perto. Obrigada, por mesmo tão diferentes conseguires sempre apoiar-me e nunca me deixar desistir, mesmo a uns bons kms de distância.

À Ana Rute Duarte, por toda amizade, por me ouvir e incentivar e nunca me deixar desamparada nesta cidade.

A todos os meus amigos e colegas que de uma forma ou de outra me apoiaram e me ajudaram nesta caminhada e que são fulcrais para que esta tese e cada etapa seja possível.

Ao Gabriel, porque todas as palavras sempre serão poucas para agradecer toda ajuda, todo o incentivo e todas as conversas. Foste sem dúvida um pilar no decorrer desta caminhada, e espero que assim continue, pela vida fora.

A toda a minha família, porque será sempre o que de melhor temos nesta vida. Aos meus pais, por serem a minha força incondicional, e o melhor exemplo de trabalho e dedicação que eu podia ter. Por apoiarem sempre nas minhas escolhas, estarem sempre do meu lado, mesmo nos piores momentos e acreditarem sempre em mim, sem nunca duvidar. As palavras nunca chegarão para agradecer tudo o que fizeram por mim.

Ao meu irmão, por ser a minha força para continuar, por me apoiar sempre, e por estar sempre do meu lado. Por toda amizade que partilhamos e por todos os momentos bons e menos bons, que alegraram esta caminhada.

O trabalho apresentado nesta dissertação obteve suporte financeiro da Fundação para a Ciência e Tecnologia (PTDC/BBB-BIO/0508/2014) e do CIISA (UID/CVT/00276/2019).

## **Abstract**

*Streptococcus pneumoniae* is the major cause of bacterial meningitis bringing morbidity and mortality as well as neurological sequelae. Following colonization, translocation across the blood-brain barrier (BBB) is a critical step in the pathogenesis of meningitis. Many pharmaceutical approaches have been developed in order to fight these bacteria. However, a major hurdle to the treatment of pneumococcal meningitis is the necessity of therapeutics able to cross the BBB. Thereby, besides the discovery of novel drugs to treat pneumococcal meningitis, the development of novel drug delivery systems that can cross the BBB and release the therapeutic molecule into the brain are urgently required. Since the structure of the BBB is known, many approaches for brain targeting have been developed based on physiological transport mechanisms. Thus, the aim of this project consists in the development of an immunoliposome as a drug delivery system to treat pneumococcal meningitis. To achieve this goal, potential of the encapsulated liposomes with penicillin, ceftriaxone and vancomycin was explored. For that, the minimum inhibitory concentrations of the three encapsulated antibiotics were determined in several serotypes of *S. pneumoniae*. Then, an immunoliposome was developed through attachment of a BBB translocating single-domain antibody to the liposome surface. Translocation studies were performed using a BBB *in vitro* model in order to prove the immunoliposome efficiency in crossing the BBB. This approach allowed the development of an immunoliposome able to target and cross the BBB, encapsulating antibiotics capable to fight *S. pneumoniae*. Briefly, the strategy developed in the present project resulted in an immunoliposome that could be a safer and more efficient approach to treat pneumococcal meningitis and a promising candidate in the treatment of other central nervous system diseases.

**Keywords:** meningitis; *S. pneumoniae*; antibiotics; single domain antibodies; blood-brain barrier; immunoliposome;

## Resumo alargado

A meningite pode ser definida como um processo inflamatório que envolve as meninges, quer as do sistema nervoso central quer as da medula espinal. Dos vários tipos de meningite descritos, a bacteriana é considerada o tipo mais severo. *Streptococcus pneumoniae* é considerado um dos principais agentes patogénicos responsáveis por este tipo de meningite causando uma alta taxa de mortalidade e morbilidade, e sequelas neurológicas nos sobreviventes. *S. pneumoniae* é um patógeno humano que coloniza essencialmente a nasofaringe em crianças, sendo uma causa importante de infeções na infância. *S. pneumoniae* é uma bactéria Gram-positiva, que frequentemente expressa uma cápsula polissacarídea, que constitui um dos seus principais fatores de virulência. Até ao momento, um total de 98 tipos de polissacarídeos capsulares foram descritos diferindo serológica e estruturalmente entre si. Após a colonização, a translocação através da barreira hematoencefálica (BHE) é uma das etapas cruciais para a patogénese da meningite.

Têm sido desenvolvidas várias abordagens farmacêuticas com o intuito de combater a infeção causada por *S. pneumoniae*. No entanto, um grande obstáculo ao tratamento da meningite pneumocócica é a necessidade de desenvolver terapêuticas capazes de atravessar a BHE. A estrutura da barreira hematoencefálica leva a concluir que para criar um tratamento eficiente para a meningite pneumocócica, é necessária uma abordagem constituída por duas partes essenciais: o desenvolvimento do medicamento com as propriedades antibacterianas e a tecnologia de direcionamento para permitir que a molécula atravesse a BHE e seja capaz de combater a infeção.

O foco atual é encapsular antibióticos em formulações lipossomais aumentando a atividade antibacteriana e as propriedades farmacocinéticas o que vai trazer várias vantagens ao sistema de administração de medicamentos como, por exemplo: diminuição da toxicidade, alta atividade antimicrobiana contra patógenos, seletividade do alvo e uma melhor biodistribuição. Desta forma, o principal objetivo deste projeto é desenvolver um sistema de administração de fármacos capaz de atravessar a BHE e libertar antibióticos para combater a meningite pneumocócica.

Para atingir esse objetivo, propomos uma nova abordagem que engloba as propriedades da administração de fármacos e o direcionamento específico de um imunolipossoma. Para que o imunolipossoma seja direcionado com sucesso para a BHE, dois anticorpos de pequeno domínio, nomeadamente FC5 [55] e G3 (um sdAb recentemente selecionado pelo nosso grupo que é capaz de atravessar a barreira hematoencefálica), foram acoplados na superfície do lipossoma, permitindo o transporte do lipossoma através da BHE. O uso de anticorpos de pequeno domínio tem várias vantagens relativamente ao uso de IgG, devido ao seu tamanho reduzido, o que facilita o acesso ao alvo. Adicionalmente, estas moléculas são mais estáveis quando em circulação permitindo uma administração mais eficiente. Em suma, ao conjugar a capacidade de um

anticorpo de pequeno domínio específico para o direcionamento e translocação da BHE e o encapsulamento de antibióticos no lipossoma é possível criar um sistema capaz de superar os dois obstáculos no desenvolvimento de um tratamento para a meningite pneumocócica: a necessidade de uma terapêutica capaz de atravessar a BHE e as propriedades antimicrobianas necessárias para combater *S. pneumoniae*. Dessa forma, a liberação gradual dos antibióticos no foco da infecção, resulta num sistema eficiente de administração de medicamentos para o tratamento da meningite pneumocócica.

Para o desenvolvimento do projeto foram encapsulados em lipossomas três dos antibióticos mais recorrentemente utilizados no tratamento desta infecção (penicilina, vancomicina e ceftriaxona) com o objetivo de explorar o seu potencial no tratamento da meningite pneumocócica. Para isso, a concentração inibitória mínima dos três antibióticos encapsulados foi determinada em vários serótipos de *S. pneumoniae*. Uma vez validada a eficiência dos lipossomas encapsulados, foi possível prosseguir para o desenvolvimento de um imunolipossoma.

O primeiro passo para o seu desenvolvimento consistiu na expressão dos anticorpos de pequeno domínio em bactérias, e, seguidamente, a sua purificação. Uma vez obtidos os anticorpos, estes foram ligados à superfície do lipossoma. Para esta ligação foram otimizados dois métodos diferentes amplamente utilizados para o efeito: o método da biotina e o método da maleimide. Uma vez otimizados os métodos de ligação, os imunolipossomas obtidos pelos dois métodos foram sujeitos a estudos de translocação para avaliar a sua capacidade de atravessar a BHE.

Os estudos de translocação foram realizados utilizando um modelo da BHE *in vitro*. Através destes estudos verificou-se que o método de ligação usando a biotina é um método de ligação mais eficaz permitindo uma maior translocação do imunolipossoma. Da mesma forma, foi possível concluir que o anticorpo G3 tem uma maior capacidade para atravessar a BHE quando comparado com o FC5.

Esta abordagem permitiu o desenvolvimento de um imunolipossoma capaz de atravessar a BHE encapsulando antibióticos capazes de combater *S. pneumoniae*. Resumidamente, a estratégia estudada no presente projeto resultou num imunolipossoma que poderá corresponder a uma abordagem mais segura e eficiente no tratamento da meningite pneumocócica e ser um candidato promissor no tratamento de outras doenças do sistema nervoso central.

**Palavras-chave:** meningite; *S. pneumoniae*; antibióticos; anticorpos de pequeno domínio; barreira hematoencefálica; imunolipossoma;

## Contents

Agradecimientos .....	II
Abstract .....	IV
Resumo alargado.....	V
Contents .....	VIII
List of tables.....	X
List of figures.....	XI
List of abbreviations.....	XIV
<b>Chapter 1 - Introduction .....</b>	<b>1</b>
1.1 Meningitis .....	1
1.2 Bacterial meningitis .....	2
1.3 <i>Streptococcus pneumoniae</i> - The pathogen.....	2
1.4 <i>Streptococcus pneumoniae</i> – Infection and colonization.....	3
1.5 <i>Streptococcus pneumoniae</i> – Central nervous system invasion.....	4
1.6 <i>Streptococcus pneumoniae</i> – Prevention and treatment.....	5
1.6.1 Pneumococcal meningitis treatment – The limitation of the blood brain barrier ..	6
1.6.2 Recombinant antibodies and single domain antibodies as promising BBB crossing scaffolds .....	8
1.7 Pneumococcal meningitis treatment: The therapeutic approach .....	9
1.8 Immunoliposomes – combining the therapeutic approach with the targeting technology .....	10
1.9 Objective.....	11
<b>Chapter 2 – Material and Methods .....</b>	<b>12</b>
2.1. Liposomes .....	12
2.2 <i>Streptococcus pneumoniae</i> growth curve.....	12
2.3 Determination of minimum inhibitory concentration using alamarBlue.....	12
2.3.1 AlamarBlue assay.....	12
2.3.2 AlamarBlue assay optimization .....	13
2.3.3 Minimum inhibitory concentration by broth dilution.....	13
2.4 Minimum inhibitory concentration by agar dilution method.....	14
2.5 Citotoxicity assays.....	14
2.5.1 Citotoxicity assays optimization .....	14
2.6 Antimicrobial liposomes efficacy in clinical isolates .....	14
2.7 Expression of sdAb- FC5 and G3.....	15
2.8 Immobilized metal ion affinity chromatography of sdAb – FC5 and G3.....	15

2.9 SDS-PAGE .....	16
2.9.1 Coomassie staining.....	16
2.9.2 Western blot .....	16
2.10 Size exclusion chromatography (SEC) of sdAb – FC5 and G3 .....	17
2.11 SdAb (FC5 and G3) coupling to the liposome surface .....	17
2.11.1 Biotin-streptavidin ligation .....	17
2.11.2 Antibody biotinylation .....	17
2.11.3 Liposome antibody conjugation.....	17
2.11.4 Thiol-Maleimide antibody-liposome conjugation .....	18
2.11.5 sdAb-liposome ligation efficiency .....	19
2.11.6 Bradford method .....	19
2.12 <i>In vitro</i> Blood brain barrier model .....	20
2.12.1 Translocation and integrity studies .....	20
2.13 Statistical analysis .....	20
<b>Chapter 3 – Results and discussion .....</b>	<b>21</b>
3.1 <i>Streptococcus pneumoniae</i> growth curve .....	21
3.2 AlamarBlue assay optimization.....	22
3.3 Minimum inhibitory concentration of the Antibiotics by broth dilution .....	23
3.4 Liposomal formulations with encapsulated antibiotics .....	23
3.5 Antibacterial activity of encapsulated liposomes in <i>S. pneumoniae</i> (TIGR4).....	25
3.5.1 Penicillin liposomes.....	25
3.5.2 Vancomycin liposomes.....	26
3.5.3 Ceftriaxone liposomes .....	27
3.6 Antimicrobial efficacy of the liposomes in clinical isolates .....	29
3.6.1 Penicillin liposomes.....	30
3.6.2 Vancomycin liposomes.....	31
3.6.3 Ceftriaxone liposomes .....	32
3.7 Cytotoxicity assays with free antibiotics and antibiotic-encapsulated liposomes .....	34
3.8 Development of an immunoliposome - Expression and purification of FC5 and G3 to liposome conjugation.....	35
3.9 SdAb (FC5 and G3) coupling to the liposome surface – Biotin approach .....	37
3.10 sdAb (FC5 and G3) coupling to the liposome surface – Maleimide approach .....	39
3.11 <i>In vitro</i> BBB model.....	40
3.12 <i>In vitro</i> BBB model- incubation time optimization .....	42
<b>Chapter 4 – Integrated analysis, main conclusions and future perspectives .....</b>	<b>44</b>
<b>Chapter 5 –Bibliography .....</b>	<b>47</b>

## List of tables

<b>Table 1.1:</b> Factors that influence invasive pneumococcal disease in young children .....	3
<b>Table 2.1:</b> Clinical isolates used for antibacterial efficacy .....	14
<b>Table 2.2:</b> BSA standard dilutions used for the determination of a standard curve.....	19
<b>Table 3.1:</b> MIC obtained for antibiotics in study. ....	23
<b>Table 3.2:</b> Physicochemical characterization of liposomal formulations.....	24
<b>Table 3.3:</b> MIC obtained for the antibiotic-encapsulated liposomes compared with the free antibiotic and the empty liposome. ....	28
<b>Table 3.4:</b> Resistance of the invasive <i>S. pneumoniae</i> serotypes isolated from IPD.....	29
<b>Table 3.5:</b> MIC obtained for the antibiotic-encapsulated liposomes, in several IPD isolated serotypes .....	33
<b>Table 3.6:</b> Yield of mAb (G3 and FC5) attachment on liposomes prepared by the biotin approach.....	39
<b>Table 3.7:</b> Yield of mAb (G3 and FC5) attachment on liposomes prepared by the maleimide approach .....	40
<b>Table 3.8:</b> Integrity of BBB in vitro model, after translocation of the sdAb in study (G3 and FC5). ....	41
<b>Table 3.9:</b> Integrity of BBB in vitro model, after translocation with an incubation time of 90 minutes of the immunoliposomes in study.....	41
<b>Table 3.10:</b> Integrity of BBB in vitro model, after translocation with an incubation time of 3, 6, and 24 hours of incubation with the immunoliposomes in study .....	43

## List of figures

<b>Figure 1.1:</b> Comparison between normal meninges and meninges affected by meningitis .....	1
<b>Figure 1.2:</b> Anatomical representation of the human brain and meningeal structures affected by bacterial meningitis .....	2
<b>Figure 1.3:</b> Morphology of <i>S. pneumoniae</i> . .....	2
<b>Figure 1.4:</b> Simplified description of colonization, infections and CNS invasion from <i>Streptococcus pneumoniae</i> . .....	4
<b>Figure 1.5:</b> <i>S. pneumoniae</i> serotypes covered in each pneumococcal conjugate vaccine.....	5
<b>Figure 1.6:</b> Blood-Brain barrier structure .....	6
<b>Figure 1.7:</b> Schematic representation of main routes for molecular traffic across the BBB.....	7
<b>Figure 1.8:</b> Receptor-mediated endocytosis .....	7
<b>Figure 1.9:</b> Schematic representation of a human IgG antibody and a single domain antibody..	8
<b>Figure 1.10:</b> Schematic illustration of a conventional liposome. ....	9
<b>Figure 1.11:</b> Schematic representation of a sterically stabilized liposome .....	9
<b>Figure 1.12:</b> Schematic representation of the Liposome- sdAb conjugates by two different methods .....	10
<b>Figure 1.13:</b> Schematic representation of the immunoliposome encapsulated with antibiotic proposed for this project. ....	11
<b>Figure 1.14:</b> Schematic representation of the main objectives aiming to develop the immunoliposome for pneumococcal meningitis. ....	11
<b>Figure 2.1:</b> REDOX reaction of resazurin to resorufin that produces fluorescence. ....	12
<b>Figure 2.2:</b> Alamarblue bacteria viability assay workflow .....	13
<b>Figure 2.3:</b> Minimum inhibitory concentration by broth dilutions of the antibiotics and the encapsulated liposomes with antibiotics workflow.....	13
<b>Figure 2.4:</b> Western blot sandwich order prepared to place in gel holder cassette. ....	16
<b>Figure 2.5:</b> Representation of the ELISA process and its components .....	18
<b>Figure 2.6:</b> Thiol-Maleimide conjugation:.....	18
<b>Figure 2.7:</b> Schematic representation of the in vitro BBB model .....	20

<b>Figure 3.1:</b> <i>S. pneumoniae</i> growth curve results.....	21
<b>Figure 3.2:</b> Alamar blue optimization assay .....	22
<b>Figure 3.3:</b> MIC determination, by a colorimetric method, of the antibiotics in study. ....	23
<b>Figure 3.4:</b> MIC determination by a colorimetric method using penicillin compounds. ....	25
<b>Figure 3.5:</b> CFU of <i>Streptococcus pneumoniae</i> after treatment with penicillin compounds .....	26
<b>Figure 3.6:</b> MIC determination by a colorimetric method using vancomycin compounds .....	26
<b>Figure 3.7:</b> CFU of <i>Streptococcus pneumoniae</i> after treatment with vancomycin compounds. 27	
<b>Figure 3.8:</b> MIC determination by a colorimetric method using ceftriaxone compounds. ....	27
<b>Figure 3.9:</b> CFU of <i>Streptococcus pneumoniae</i> after treatment with ceftriaxone compounds. .	28
<b>Figure 3.10:</b> MIC determination by a colorimetric method using penicillin compounds in five different serotypes.....	30
<b>Figure 3.11:</b> MIC determination by a colorimetric method using penicillin compounds in three different serotypes.....	30
<b>Figure 3.12:</b> MIC determination by a colorimetric method using vancomycin compounds in six different serotypes .....	31
<b>Figure 3.13:</b> MIC determination by a colorimetric method using vancomycin compounds in two different serotypes.....	31
<b>Figure 3.14:</b> MIC determination by a colorimetric method using ceftriaxone compounds in five different serotypes .....	32
<b>Figure 3.15:</b> MIC determination by a colorimetric method using ceftriaxone compounds in three different serotypes.....	32
<b>Figure 3.16:</b> Cytotoxicity assay - density cells optimization. ....	34
<b>Figure 3.17:</b> Antibiotic encapsulated liposomes cytotoxicity assays .....	34
<b>Figure 3.18:</b> SDS-PAGE with the several fractions collected from IMAC purification.....	35
<b>Figure 3.19:</b> SDS-PAGE with the several fractions collected from SEC purification.....	36
<b>Figure 3.20:</b> Chemical reactions involved in antibody biotinylation.....	37
<b>Figure 3.21:</b> Optimization of the sdAb-biotin ligation.....	37
<b>Figure 3.22:</b> FC5 and G3 biotinylation. ....	38
<b>Figure 3.23:</b> Optimization of the liposome-antibody conjugation .....	38

<b>Figure 3.24:</b> ELISA with the results of the conjugation of the sdAb with the liposomes .....	39
<b>Figure 3.25:</b> Optimization of the liposome-antibody conjugation .....	39
<b>Figure 3.26:</b> Translocation of the sdAb across a BBB model in the 90 minutes incubation time .....	40
<b>Figure 3.27:</b> Percentage of translocation for immunolipomes developed by maleimide conjugation .....	41
<b>Figure 3.28:</b> Percentage of translocation for immunolipomes developed by biotin approach at 3, 6 and 24h incubation times. ....	42
<b>Figure 3.29:</b> Translocation of the sdAb across a BBB model with several time points: 3,6 and 24 hours .....	42
<b>Figure 3.30:</b> Percentage of translocation for immunolipomes developed by biotin approach at 24h incubation time.....	44

## List of abbreviations

ABTS	2,2'-azino-bis(3-ethylbenzothiazoline-6-sulphonic acid)
AET	Active efflux transport
APS	Ammonium persulfate
BBB	Blood-brain barrier
BHI	Brain heart infusion
BSA	Bovine serum albumin
CFU	Colony forming units
CMT	Carrier-mediated transport
CNS	Central nervous system
CPS	Capsular polysaccharide
CSF	Cerebrospinal fluid
CTX	Ceftriaxone
DMEM	Dulbecco's modified eagle medium
DPPC	Dipalmitoyl phosphatidylcolin
DPPG	Dipalmitoyl phosphatidylglycerol
DTT	Dithiothreitol
E.E	Encapsulation efficiency
EDTA	Ethylenediamine tetraacetic acid
ELISA	Enzyme-linked immunosorbent assay
EUCAST	European committee on antimicrobial susceptibility testing
FBS	Fetal bovine serum
FT	Flow through
HEPES	4-(2-hydroxyethyl) -1-piperazineethanesulfonic acid
IMAC	Immobilized metal ion affinity chromatography
IPD	Invasive pneumococcal disease
MH	Muller-hinton

MIC	Minimum inhibitory concentration
O.D.	Optical density
P.I.	Polydispersity index
PBP	Penicillin binding protein
PBS	Phosphate buffer saline
PC	Phosphatidylcholine
PCV	Pneumococcal conjugate vaccine
PEG	Polyethylene glycol
PEN	Penicillin
PG	Phosphatidylglycerol
PPSV23	Pneumococcal polysaccharide vaccine 23
REDOX	Reduction-oxidation
RMT	Receptor-mediated transcytosis
sdAb	Single domain antibody
SDS-PAGE	Sodium dodecyl sulphate polyacrylamide gel
SEC	Size exclusion chromatography
TEMED	N, N, N', N'-tetramethylethylenediamine
THB	Todd Hewwit broth
VCM	Vancomycin
VH	Heavy chain
VL	Light chain

## Chapter 1 - Introduction

### 1.1. Meningitis

Meningitis is a central nervous system (CNS) disorder and can be defined as an inflammation of the meninges, the layered unit that covers the brain and the spinal cord responsible for maintenance and function of the central nervous system. The infection affects several parts of the CNS, particularly the arachnoid, the pia matter and the intervening cerebrospinal fluid (CSF). The clinical state of acute meningitis involves fever, headache, muscle pain, stomach cramps, vomiting, photophobia, diarrhea and chills. Some variations in symptoms occur according to the patient's age. In an advanced state some severe complications can result in the death of the patient, some hours after the appearance of the first symptoms [1].

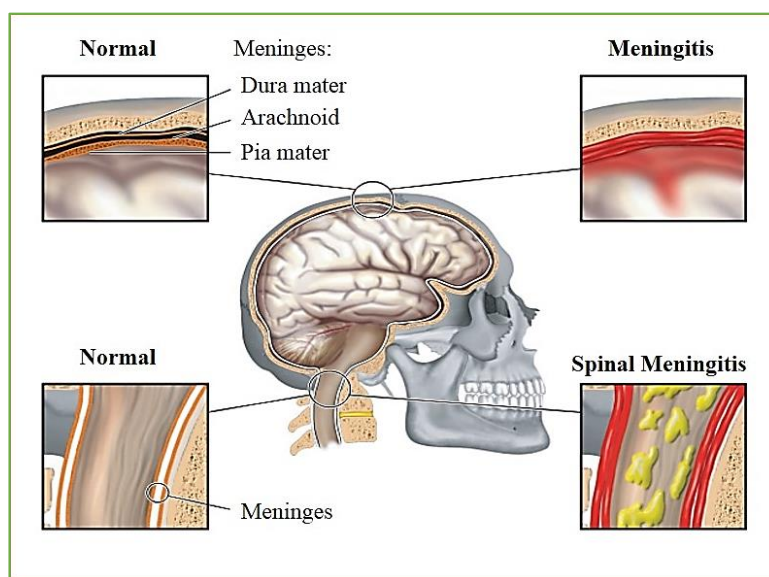


**Figure 1.1: Comparison between normal meninges and meninges affected by meningitis.**

Adapted from: [118].

Meningitis is normally the result of an infection but can also occur due to some non- infectious agents. Thus, this disease can be classified in two different categories: infectious meningitis, a severe condition of the CNS in consequence of a microbial infection or non-infectious meningitis, which represents a small percentage of the cases [2]. Regarding infectious meningitis, the most common agents are bacteria (*Haemophilus influenzae*, *Streptococcus pneumoniae* and *Neisseria meningitidis*) and viruses (principally enteroviruses, and in a smaller extent human immunodeficiency virus and herpes simplex viruses). A few meningitis cases can also be caused by parasites (*Strongyloides stercoralis*, *Naegleria fowleri* and *Acanthamoeba cantonensis*) [3]. In an infectious meningitis, the pathogen begins a localized infection, for example in the respiratory tract, the skin, the nasopharynx, the gastrointestinal tract or genitourinary tract of the host. Once in these sites, the microbial agents invade the surrounding host defences acquiring access to the CNS, spreading to the brain using different approaches: hematogenous spread ( through the blood vessels to the subarachnoid space), direct spread (travel through the nerves leading to the brain) or a defect on CNS structure allowing the microorganisms to easily enter the CNS [4]. Among all types of meningitis, bacterial meningitis is considered the most serious form of this disease.

## 1.2. Bacterial Meningitis

Bacterial meningitis is an important cause of mortality and morbidity, especially among children less than 5 years old [1]. This kind of meningitis can be acquired at the hospital, in consequence of invasive procedures, frequently called nosocomial bacterial meningitis, or spontaneously, in the community – due to community acquired bacteria. Regarding the community-acquired bacterial meningitis, this disease continues having a heavy toll, even in developed countries. The incidence of bacterial meningitis in children less than 5 years old is between 1:400 ( in less developed countries) and 1:2000 ( in developed countries) [5]. Although plenty antibacterial agents are being studied to fight this disease, meningitis fatality rates remain high. Additionally, in 10 to 20% of those who survive permanent sequelae are observed, such as mental retardation and epilepsy [6]. The most common agents of acute bacterial meningitis are *S. pneumoniae* (pneumococcus meningitis) and *Neisseria meningitidis* (meningococcus meningitis). Data from community-acquired bacterial meningitis show that *S. pneumoniae* is responsible for 50% of all cases, affecting all age groups and causing the most severe disease both in children and adults [7].

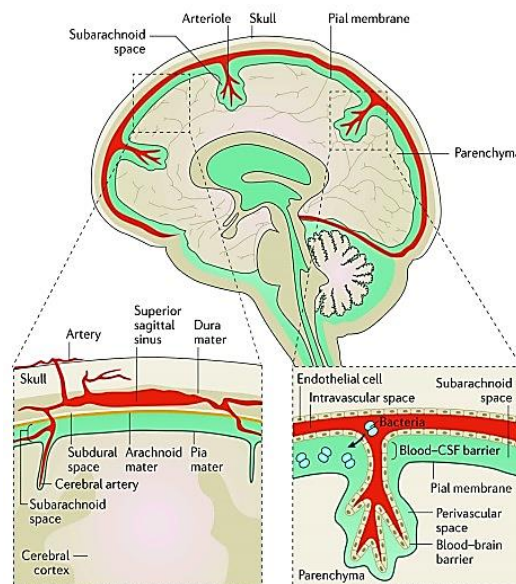


Figure 1.2: Anatomical representation of the human brain and meningeal structures affected by bacterial meningitis. Adapted from [119].

## 1.3. *Streptococcus pneumoniae* – The pathogen

Pneumococci is a human pathogen that colonizes the nasopharynx of young children being the main cause of childhood infections, predominantly on the respiratory tract, such as sinusitis and pneumonia. However, the pathogen can also develop an invasive disease such as bacteraemia, sepsis and meningitis. [7]. *S. pneumoniae* is currently the main pathogen associated with bacterial meningitis and belongs to the viridans group of streptococci, characterized by gram-positive cocci. Its optimum growth conditions need 5% carbon dioxide and a source of catalase,

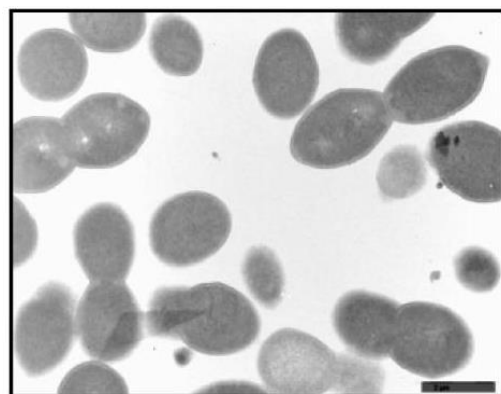


Figure 1.3: Morphology of *S. pneumoniae*. Adapted from: Orio *et al* [120].

requiring a complex media supplemented with blood [8]. Once in blood agar culture, *S. pneumoniae* develops colonies which are alpha-hemolytic, presenting a green halo [9].

The morphology of *S. pneumoniae* is described as lancet-shaped cocci frequently surrounded by a polysaccharide capsule. The capsule is the outermost layer of encapsulated *S.pneumoniae* and, to date, a total of 98 capsular polysaccharide (CPS) have been described based on serological differences [10]. According to previous studies, a serotype can be defined as pneumococcal strains that produce a CPS with unique properties, structurally and serologically. Instead, a serogroup is defined as a group of serotypes that share several serologic characteristics such as, for example, cross-reactive antibodies [10]. The CPS has long been considered indispensable for pneumococcal virulence [11]. Indeed, spontaneous nonencapsulated strains are almost avirulent, though some strains have been associated with some superficial infections [12]. The role of the capsule in virulence results from its antiphagocytic activity in non-immune hosts [13]. Additionally, the capsule is also responsible for colonization, inhibition of mechanical removal by mucus and is also crucial for preventing autolysis and decrease the susceptibility to antibiotics [14, 15].

#### 1.4. *Streptococcus pneumoniae* – Infection and colonization

*S. pneumoniae* is an important commensal of the human nasopharynx and its carriage is often asymptomatic. Although rare, pneumococcus colonization can develop into disease [16]. Transmission between individuals occurs essentially by sneezing and coughing. Once in its habitat, bacterial survival depends on several factors as: adherence, nutrition and replication. For a successful colonization in the niche, *S. pneumoniae* needs to overcome the host's immune system and to compete with the other microorganisms that inhabit the same niche [17]. Colonization of the nasopharynx requires that bacteria reach the epithelial cell layer followed by degradation of the mucus (to prevent mucus entrapment), using exoglycosidases [18]. Additionally, *S. pneumoniae* produces pneumolysin, a toxin which function is to decrease the movement of epithelial cell cilia and intensify the bacterial adherence [19]. Some enzymes are also responsible for the success of this process as such as N-acetylglucosamine-deacetylase A and O-acetyl-transferase that inhibit the lysozyme which provides the degradation of the pathogen's cell wall [20]. Progression to invasive pneumococcal disease (IPD) is influenced by some risk factors. First of all, in order to develop an infection, carriage is necessary and normally the infection occurs in a month after the acquisition of a new serotype [21]. The individuals with the highest carriage rates are the young children that commonly develop IPD owing to some factors directly associated with infection in this age group (table 1.1) [22].

Table 1.1: Factors that influence invasive pneumococcal disease in young children

	<b>Age (&lt; 2 years)</b>
<b>Host Factors</b>	Co-infection (essentially respiratory virus)
	Absence of pneumococcal vaccination
	Immunodeficiency
	Parental smoking
<b>Environmental factors</b>	Winter months
<b>Pathogen factors</b>	Acquisition of a new serotype

Over the years, several studies have focused on the distribution of pneumococcal serotypes in different geographic areas and age groups. Most, if not all, serotypes are apparently capable of causing serious disease in humans. However, just a small number of serotypes are usually responsible for the majority of IPD [23]. The reason why differences are observed in the incidence of IPD in several geographic areas and group age is still unclear. Nevertheless, the patient age is one of the most important factors when considering the serotype distribution, which is comproved when analysing the main serotypes that cause IPD in children and in adults, in the same period and geographical area [24]. Before the introduction of vaccines, IPD serogroups 6, 14, 18 and 19 were found essentially between young children, while serotype 3 was common among older adults [25]. In the case of serotype 11A, it is commonly carried in children but rarely causes IPD in this age group. On the other hand serotype 11A IPD is frequently found between adults and is also associated with a high mortality rate [26].

### 1.5. *Streptococcus pneumoniae* – Central nervous system invasion

Bacterial meningitis occurs when pathogenic virulence factors overwhelm host defense mechanisms. The mechanism by which *S. pneumoniae* crosses the blood brain barrier (BBB) is not fully understood. Recent studies have described some hypothesis for this process, namely : (1) the destruction of the endothelial cell layers by pneumolysin [27] and (2) bacterial crossing of the BBB by transcytosis, a route designed to transport molecules from the apical to the basolateral side [28]. Usually, a large number of bacteria circulating in the blood is necessary for CNS invasion. Pneumococci reach the CNS using a hematogenous route from a distant focus such as the lower airways for instance in a patient with pneumonia, or by direct spread to the cerebrospinal fluid, when the entrance of bacteria occurs from an infectious focus near the CNS, as in the case of an otitis media. Once in the CNS, *S. pneumoniae* quickly multiplies, inducing in a strong immunological response. The BBB becomes more permeable, allowing the influx of a high number of leukocytes into the brain causing brain edema, ischemia, neuronal damage, intracranial hypertension and in some cases leading to the death of the patient [29]. In consequence of bacterial growth in the meningeal spaces, a secondary bacteraemia can occur contributing to morbidity [30].

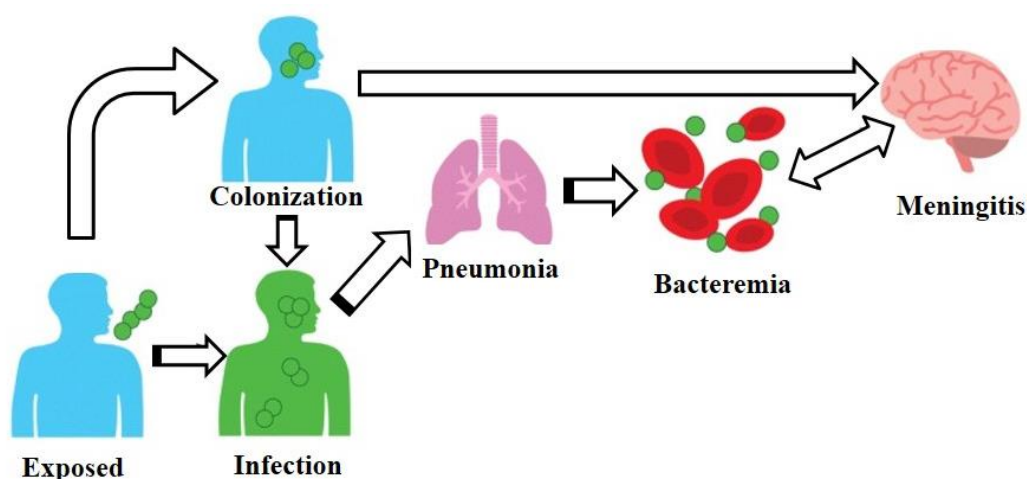


Figure 1.4: Simplified description of colonization, infections and CNS invasion from *Streptococcus pneumoniae*.

## 1.6. *Streptococcus pneumoniae* meningitis – Prevention and Treatment

During many years, infections caused by *S. pneumoniae*, mainly meningitis, have been treated using antibiotics. Therefore, the choice was essentially penicillin, a  $\beta$ -lactam, which binds to penicillin-binding proteins (PBPs) compromising their activity- PBPs are enzymes that catalyse the last steps of peptidoglycan synthesis [31]. However, it was noticed the emergence of resistance to penicillin and other  $\beta$ -lactam antibiotics in *S. pneumoniae*, due to the selective pressures associated with the disseminated use of antibiotics and the expansion of multiresistant *S. pneumoniae*. Consequently, other antibiotics have been used for pneumococcal meningitis treatment. For example, vancomycin, vancomycin inhibits polymerization (transglycosylation) and cross-linking (transpeptidation). In consequence of this inhibition the bacterial cell wall becomes weak and ultimately results in exposure of the intracellular components causing the death of bacteria [32]. The cephalosporins, such as ceftriaxone, are also used as an option to treat *S. pneumoniae* infections. Their mechanism of action is very similar to penicillin's, forming a covalent bond with PBPs and causing cell lysis [33]. Despite the efforts in using different antibiotics, the resistance levels increased, which combined with the high disease burden has led to the need for preventing strategies. This prevention was accomplished by immunization with conjugate vaccines.

Pneumococcal vaccines currently in use target the capsular polysaccharide of *S. pneumoniae*. Therefore, these vaccines provide specific protection against some specific serotypes [34]. Presently, there are several types of vaccines against *S. pneumoniae*. One of them is the 23-valent polysaccharide pneumococcal vaccine (PPSV23) that uses purified capsular polysaccharides [35]. This vaccine confers protection against 23 serotypes of *S. pneumoniae* 1, 2, 3, 4, 5, 6B, 7F, 8, 9N, 9V, 10A, 11A, 12F, 14, 15B, 17F, 18C, 19F, 19A, 20, 22F, 23F and 33F, and is given to adults with  $\geq 65$  years of age, in some countries such as USA, and its effectiveness is about 50-70% [36]. PPSV23 works providing T-cell independent immunity needing revaccination each 5 years after the first vaccination [37]. However, it was observed that PPSV23 has a low efficacy in infants and young children due to the poor immunogenicity of the capsular polysaccharide [38]. To overcome the PPSV23 low efficacy a new vaccine was produced. The pneumococcal conjugate vaccine (PCV) was designed by complexing the purified capsular polysaccharide with a carrier protein, CRM197 [39]. The first PCV approved was PCV7, containing seven purified capsular polysaccharides: 4, 6B, 9V, 14, 18C, 19F, 23F. These serotypes were chosen since they were the main cause of IPD among children in USA. After the introduction of this vaccine a significant decrease in IPD caused by the serotypes included in the vaccine has been reported [40]. Changes in the IPD incidence were evaluated after 7 years of PCV7 use in USA in children and it was reported that only 2% of IPD in children  $5\geq$  years old were due to PCV7 serotypes.

Additionally, other 6 non- PCV7 serotypes were responsible for 68% of IPD in this age group,

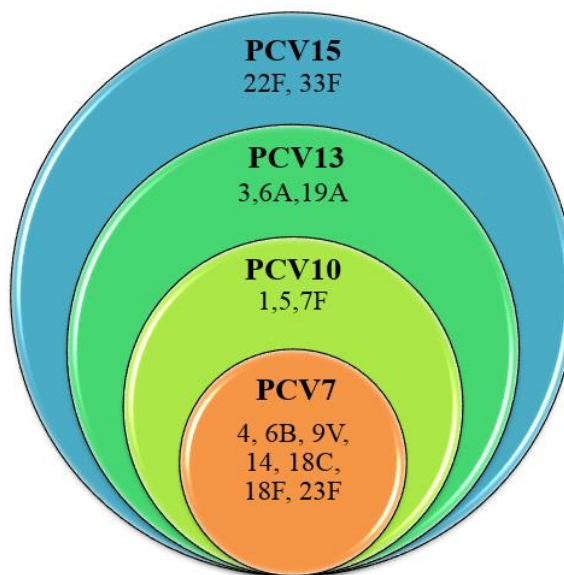


Figure 1.5: *S. pneumoniae* serotypes covered in each pneumococcal conjugate vaccine.

resulting in their inclusion on new vaccines [41]. In the following years the development of PCV with additional serotypes coverage was observed. PCV10 was launched in 2008 in USA and Europe and this vaccine includes all the serotypes present in PCV7 plus 3 additional serotypes: 1,5 and 7F. In 2010, PCV13 became available. It also includes all the serotypes in PCV7 plus 1, 3, 5, 6A, 7F and 19A. The introduction of these two PCV's was a consequence of epidemiological changes owing to serotype replacement. Recently, a new vaccine was launched, PCV15, which includes all the serotypes present in PCV13 and additionally 22F and 33F (figure 1.5) [42].

After the introduction of a pneumococcal conjugate vaccine a decreased in carriage of the serotypes included in the vaccine was observed. However, an increase of non-vaccine pneumococcal serotypes is occurring, in a process named serotype replacement [43]. Unfortunately, the number of serotypes that can be included in a vaccine produced by protein conjugation of pneumococcal polysaccharide is still limited. As a result, an universal vaccine has not been available, so far. This leads to conclude that besides the use of pneumococcal conjugates vaccines as prevention an effective treatment to pneumococcal meningitis is also necessary.

### 1.6.1. Pneumococcal meningitis treatment – The limitation of the blood brain barrier

Pneumococcal meningitis is a brain disorder, meaning that in order to develop an efficient treatment for this disease overcoming the blood BBB is required. The BBB is classified as a complex, dynamic and adaptable interface, which functions is to control the exchange of

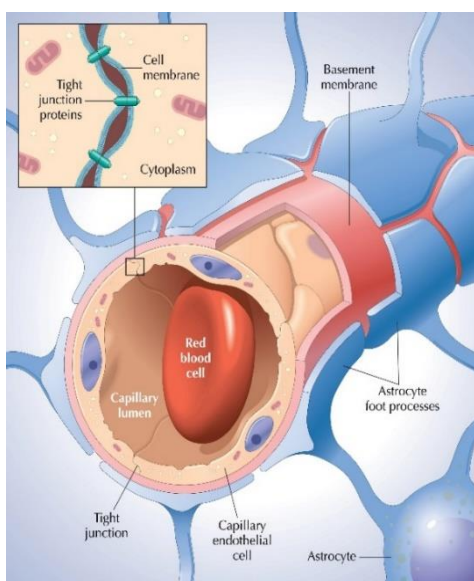


**Figure 1.6: Blood-Brain barrier structure.**  
Adapted from: [121].

substances between the CNS and the blood, being an important component regarding the regulation of the influx and efflux of ions, oxygen and nutrients[44]. The endothelial cells that compose the BBB are distinct from the endothelial cells present in the other tissues for the presence of BBB-specific transporters and receptor proteins to control the entrance and exit of metabolites. However, the complexity of the BBB formed by tight junctions between brain endothelial and endothelial cells limit the transport of therapeutic molecules between the blood and the CNS, creating the main obstacle for therapeutics delivery in the brain [45]. As a consequence, most pharmaceuticals are not able to cross the BBB in which are included >99% of large protein drugs and 98% of small-molecule drugs. To be able to penetrate the brain the molecule has to be lipid soluble, form < 8-10 hydrogen bonds with water and have a molecular weight between 400-500 Daltons [46].

The structure and the characteristics of the BBB lead to conclude that to create an efficient treatment for pneumococcal meningitis, the pharmaceutical approach requires two essential parts: the drug component, with the antibacterial properties and the targeting technology to allow the molecule to cross the BBB and to treat the infection.

Regarding the targeting technology, a controlled transport is demanding and should not cause damage to the BBB [47]. Currently, the methods used for improving CNS delivery of biologics involve neurosurgical intervention, and hospitalization, leading to the necessity of expensive equipment, and only a small group of patients can be treated since these interventions result in several side effects and a limited clinical benefit [48]. To develop a drug delivery system into the brain, in a safer and most efficient way, the use of the endogenous BBB transporters has been considered [50]. There are several categories of endogenous transporters, depending on the type of the transport they perform, and the size of the molecules transported. The carriers responsible for the transport of small molecules, for example glucose, amino acids and nucleoside, are normally highly specific, and can be divided into carrier-mediated transport (CMT), and active efflux transport (AET).

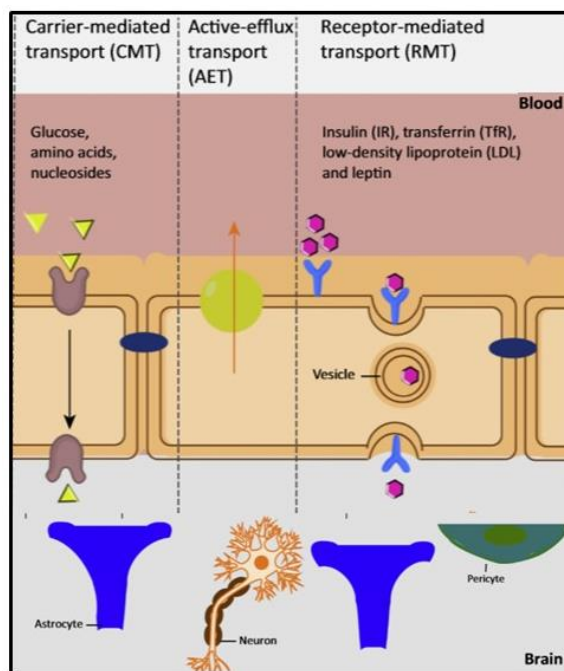


Figure 1.7: Schematic representation of main routes for molecular traffic across the BBB. Adapted from: [124].

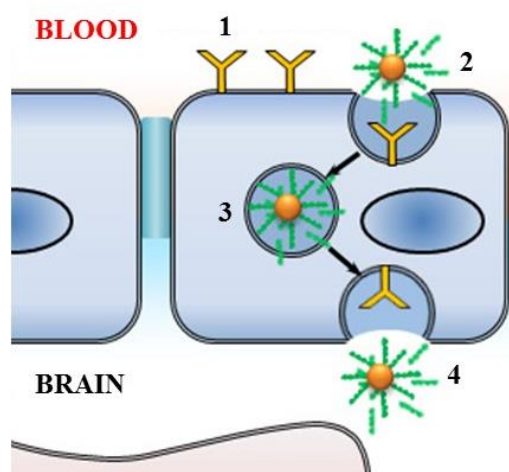


Figure 1.8: Receptor-mediated endocytosis. 1: Representation of the RMT receptors; 2: Ligand binding and receptor clustering; 3: Endocytosis and vesicles trafficking through the cell; 5: Exocytosis of payload;

Large molecules, such as insulin and transferrin are transported through receptor-mediated transcytosis (RMT) which relies on a vesicular transport through nonspecific micropinocytosis [49, 50]. This pathway is highly selective for BBB-expressed receptors and is activated by molecules able to bind the RMT receptors, as antibodies. When the ligand binds to the receptor, in the luminal side of the brain endothelial cells (blood side), a subsequent receptor clustering is triggered followed by an invagination of the membrane, resulting in the formation of intracellular transport vesicles. These vesicles are subject to classification in the endocytic compartments resulting in ligand release on the brain side (abluminal surface) and the recycling of the receptor (figure 1.8).

The currently RMT receptors used for targeting and BBB transport are due to the expression of several specific receptors, including insulin receptors, lactoferrin receptor, transferrin receptor, glutathione transporter and scavenger receptors class B type 1 [44]. Each of the different types of

transporters have different capacities and affinities to transport ligands from the blood to the brain [50, 51]. Currently, the focus is to discover ligands to these receptors. Several molecules, such as antibodies, are known as Trojan horses and specifically target the RMT receptors, allowing the transcytosis of macromolecules through the BBB. Antibodies targeting alternative RMT pathways are becoming a dominant drug-developing pipeline to increase the development of BBB penetrating therapeutics. However, the approaches currently available rely on targeting widely expressed receptors as the mentioned above which can in consequence mistargeting the drugs to other organs, generating safety risks. This leads to a weak selectivity resulting in a small fraction of the injected dose reaching the brain [52]. Therefore, in the last few years the focus is to identify new BBB RMT targets.

### 1.6.2. Recombinant antibodies and single domain antibodies as promising BBB crossing scaffolds

An IgG antibody is composed by a pair of similar light (VL) and heavy (VH) chains. The light chains contain a constant domain and a variable one and the heavy chains contain three constant domains and one variable domain. The Fc constant region is responsible for the recruitment of effectors from the immune system. Molecular biology tools allow the use of IgG fragments, as single domain antibodies (sdAb). These are antibodies fragments of the heavy or light chains present in the IgGs having a size of approximately 13 kDa (figure 1.9). Even if the formats with the antibody constant domains are very stable, the use of sdAb brings several advantages: the small size, the potential transvascular brain delivery capability, the low-specific interaction with tissues that express Fc receptors, the low immunogenicity, and the high stability in conditions of high temperature, and pH variations [53]. To discover new antigen-ligand systems that can be used to overcome the BBB, a study using llama sdAb phage-display library was performed [54]. Two sdAbs were selected, FC5 and FC44, that recognized the human cerebrovascular endothelial cells and had the capability to transmigrate the BBB [55]. Regarding to FC5, this sdAb has the advantage of presenting species cross reactivity and has been demonstrated to bind to rat, mouse and human endothelial cells [56]. FC5 starts the RMT process by binding the  $\alpha(2,3)$ -siaglycoprotein receptor and its endocytosis is classified as a clathrin-mediated process [57]. A panel of sdAbs were efficiently selected and showed promising BBB crossing characteristics as a result of a currently ongoing project with the goal to identify new vectors for BBB drugs. The chosen sdAbs were tested both in vitro and in vivo and G3 was selected as the sdAb with greatest BBB crossing properties.

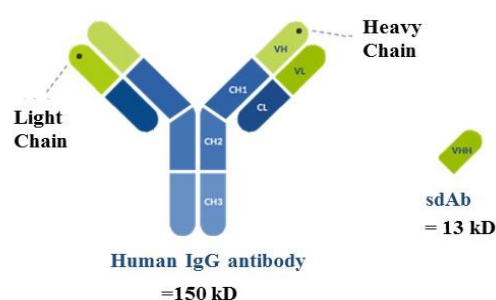


Figure 1.9: Schematic representation of a human IgG antibody and a single domain antibody.

## 1.7. Pneumococcal meningitis treatment – The therapeutic approach

Several studies have been focused on the drug development and delivery in all areas of clinical research. Commonly, the antimicrobial properties are brought by antibiotics. However with the increase of antibiotic resistance among bacterial pathogens and the antibiotic toxicity in the host body, some researchers are focused in the improvement of the current available therapy in a new form: liposomal formulations [58]. Liposomes can be described as spherical vesicles composed by one or more phospholipids bilayers enclosing a water space (figure 1.10). The liposomal formulations are normally composed by phospholipids, cholesterol and sometimes they also contain lipoproteins. The diameter of the liposomes is between 0.02 to 10  $\mu\text{m}$  [59]. The biophysical properties of the liposomes can be changed by modifying some aspects as the type and the composition of the lipids, the liposome fluidity, its size, the charge of the liposomal surface (positive, negative or neutral), and the sensitivity to temperature and pH [60, 61]. Due to their unique physicochemical features, liposomes are able to incorporate both hydrophilic and lipophilic molecules. The use of liposomes as a nanocarrier in drug delivery brings advantages once their outer lipophilic membrane increases the permeability across

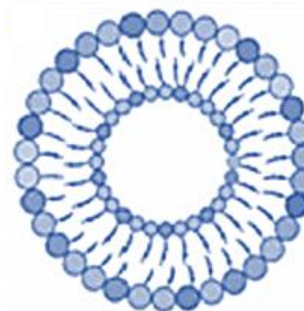


Figure 1.10: Schematic illustration of a conventional liposome.

Adapted from: [122].

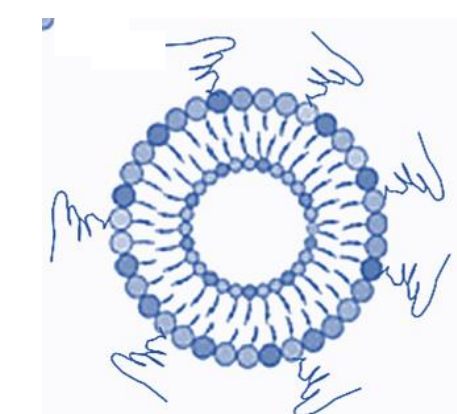


Figure 1.11: Schematic representation of a sterically stabilized liposome.

Adapted from: [122].

membranes. The current focus is to encapsulate antibiotics in liposomal formulations, increasing the antibacterial activity and pharmacokinetic properties, bringing several advantages to the drug delivery system as for example: decreased toxicity, the high antimicrobial activity against pathogens, the target selectivity, and the improved biodistribution [60, 62]. The diversity of liposomal formulations allows the encapsulation of different antibiotics leading to therapeutic success. However, there is a major drawback in the use of conventional liposomal formulations. Since they have a high systemic plasma clearance, liposomes are quickly removed from the circulation by macrophages, right after the intravenous administration [63]. The half-life of the liposome in the circulation can be enhanced by coating the liposome surface with some molecules as gangliosides or polyethylene glycol (PEG). When the liposomes are coated with PEG they are commonly referred as sterically stabilized liposomes (figure 1.11). The incorporation of PEG brings some advantages to the liposomal formulation, since it is presumed that it avoids the binding to opsonin's derived from the plasma, resulting in the prevention of the recognition by phagocytic cells, allowing a long-circulation in the blood stream [64, 65]. Liposomes can also be used featuring an active targeting, which is accomplished by coupling targeting ligands to the surface resulting in an immunoliposome.

## 1.8. Immunoliposomes – combining the therapeutic approach with the targeting technology

Immunoliposomes are a promising liposome approach designed to enhance the therapeutic effect of pharmaceutical agents as well as improve the *in vivo* targeting. For that, specific ligands are attached to the liposome surface, able to recognize cellular surface antigens or receptors in targeted tissues [66]. The immunoliposomes combine the use of a pharmaceutical agent encapsulated in liposomal formulations, acting as nanocarriers, with the biological targeting technology. Therefore, liposomes with antibodies on the surface are able to be selectively taken up by cells that overexpress the receptor for the ligand coupled, improving therapeutic outcome [67]. Currently, there are several strategies available for the preparation of long-circulating immunoliposomes, normally involving conjugation of antibodies or their fragments to the distal end on the PEG (figure 1.12). Different approaches have been developed for this objective, including covalent and non-covalent methods. The most applied approach belongs to the category of covalent methods and is based on the reaction of sulfhydryl groups with maleimide groups which is considered a clean, fast and efficient process. Regarding the non-covalent methods, the most widely used is the biotin-streptavidin-biotin method, that is based on the strong biomolecular binding between these two molecules. In previous studies, it was demonstrated that the conjugation of streptavidin to liposomes results in a flexible system, able to be conjugated with a wide variety of biotinylated proteins [68, 69]. The first successfully developed immunoliposome was used to localize in acute canine myocardial infarction [70]. Recent studies showed that immunoliposomes have successfully accomplished target delivery to brain tumours [71]. The conjugation of liposomes with specific antibodies or sdAb with targeting properties to the CNS increases their efficacy [72]. Previous studies using a murine monoclonal antibody, OX-26, specific against the transferrin receptor conjugated to a PEG-liposome showed that the use of an immunoliposome as a drug delivery system does not cause any damage to the BBB integrity [73]. Additionally, efficacy studies of the immunoliposome's, when loaded with daunorubicin, demonstrated that the OX-26-PEG-liposomes crossed the BBB faster when compared with free daunorubicin [74].

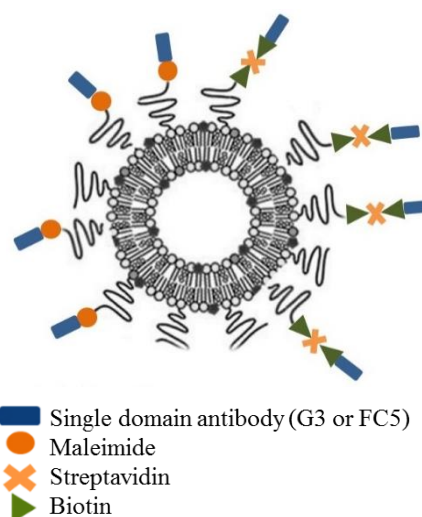


**Figure 1.12: Schematic representation of the Liposome- sdAb conjugates by two different methods.** A non-covalent method - Biotin-Streptavidin-Biotin - and a covalent method based on maleimide covalent ligation to sulfhydryl groups

## 1.9. Objective

The main goal of this project was to develop a drug delivery system able of crossing the BBB and release antibiotics in the CSF to clear pneumococcal infection. To achieve this goal, we proposed a novel approach by addressing the properties of drug delivery and targeting of an immunoliposome encapsulated with antibiotics (figure 1.13)

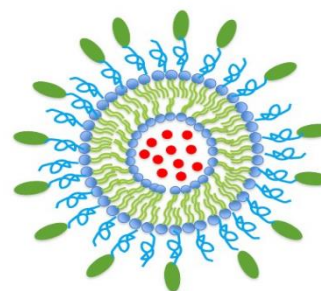


Figure 1.13: Schematic representation of the immunoliposome encapsulated with antibiotic proposed for this project.

Therefore, the first objective of this project was the optimization of the liposomal formulation in order to obtain the most appropriate properties to encapsulate the selected antibiotics. The second objective was the validation of the antimicrobial efficiency of these liposomes in *S. pneumoniae*. For that, the antimicrobial activity of the antibiotic-encapsulated liposomes was compared with that of the free drug by determining the minimum inhibitory concentration.

After liposome optimization and the activity studies, the following goal was to ensure its transport through the BBB. The ligation of two single domain antibodies, namely FC5 [55] and G3 to the liposome surface was optimized. Two different approaches were tested for the sdAb conjugation to the liposome. The most proficient developed immunoliposome was selected for *in vitro* studies. The final step of this project was an efficacy study, using the *in vitro* BBB model aiming to validate the immunoliposome system.

By conjugating the ability of a specific sdAb to cross the BBB, and encapsulation of antibiotics in the liposome, it was possible to create a system able to overcome the main obstacle in the development of a treatment for pneumococcal meningitis: the difficulty in cross the BBB and still have the antimicrobial properties required to fight *S. pneumoniae*. With this approach, we expect to be able to gradually release the antibiotics at the focus of the infection, creating an efficient drug delivery system for treatment of pneumococcal meningitis.

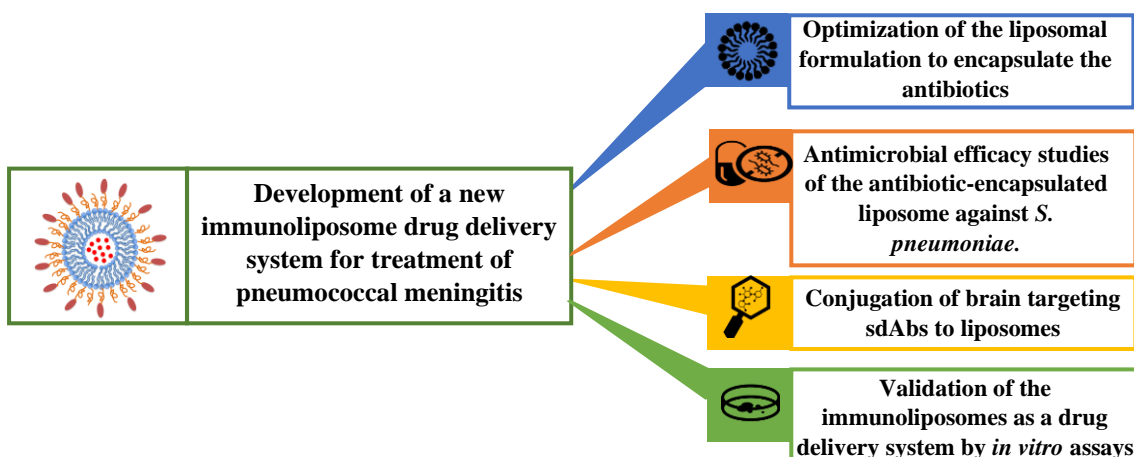


Figure 1.14: Schematic representation of the main objectives aiming to develop the immunoliposome for pneumococcal meningitis.

## Chapter 2 – Material and methods

### 2.1. Liposomes

The liposomes were formulated and prepared by Dra. Manuela Gaspar, in collaboration with the Galenic Pharmacy and Pharmaceutical Technology department from the Faculdade de Farmácia da Universidade de Lisboa (FFUL). The formulations were prepared using different proportions of dipalmitoyl phosphatidylglycerol (DPPG), phosphatidylcholine (PC), PEG, phosphatidylglycerol (PG), dipalmitoyl phosphatidylcholine (DPPC). Penicillin liposomes were prepared by an active method loading through a calcium acetate gradient. Vancomycin liposomes were prepared by a passive method. Both vancomycin and penicillin liposomes were prepared with 4-(2-hydroxyethyl)-1-piperazineethanesulfonic acid HEPES buffer, pH 7.4 Ceftriaxone liposomes were prepared by an active method using an ammonium sulphate gradient. These liposomes suspended in citrate buffer pH 5.0 (10 mM acid citric, 145 mM NaCl).

### 2.2. *Streptococcus pneumoniae* growth curve

The first step in this project was the elaboration of a growth curve with the reference strain in order to acquire knowledge about its growth conditions. *S. pneumoniae* (TIGR4) bacterial stock was cultured on Columbia agar + 5% sheep blood and incubated overnight at 37°C. Then, the colonies formed were inoculated in brain heart infusion (BHI) (Difco) medium and incubated at 37°C until the solution reached an optical density (O.D.) of approximately 0.1. The resulting inoculum was diluted in a proportion of 1:100, incubated at 37°C and the O.D. was measured every 30 minutes during approximately 8 hours.

### 2.3. Determination of minimum inhibitory concentration using alamarBlue

#### 2.3.1 AlamarBlue Assay

AlamarBlue is a ready-to-use resazurin-based solution which function is to measure the bacteria viability when exposed to different compounds. The assay incorporates a reduction-oxidation (REDOX) indicator that undergoes a colour change in consequence of cellular metabolic reduction (figure 2.1). The changes in viability can be measured by absorbance or fluorescence and the quantity formed is directly proportional to the number of living cells in the sample. AlamarBlue is added to the samples and incubated during 2 hours at 37°C. Then, absorbance is monitored at 570 nm and 600 nm (figure 2.2). The cell/bacteria viability is determined using the formula below (equation 2.1), calculating the percent difference in reduction between cells treated with antibiotics and control cells.

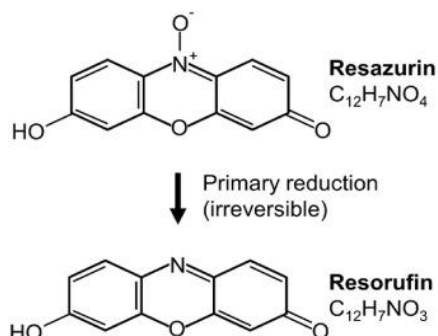


Figure 2.1: REDOX reaction of resazurin to resorufin that produces fluorescence

#### Equation 2.1:

$$\text{Cell/bacteria viability} = \frac{(\epsilon_{OX})_{\lambda_2} A_{\lambda_1} - (\epsilon_{OX})_{\lambda_1} A_{\lambda_2} \text{ of test agent dilution}}{(\epsilon_{OX})_{\lambda_2} A_{\lambda_1} - (\epsilon_{OX})_{\lambda_1} A_{\lambda_2} \text{ of untreated positive growth control}} \times 100$$

Where,

$\epsilon_{ox}$  = molar extinction coefficient of AlamarBlue oxidized form

A = absorbance of test wells

$A^\circ$  = absorbance of growth control well

$\lambda_1 = 570 \text{ nm}$

$\lambda_2 = 600 \text{ nm}$

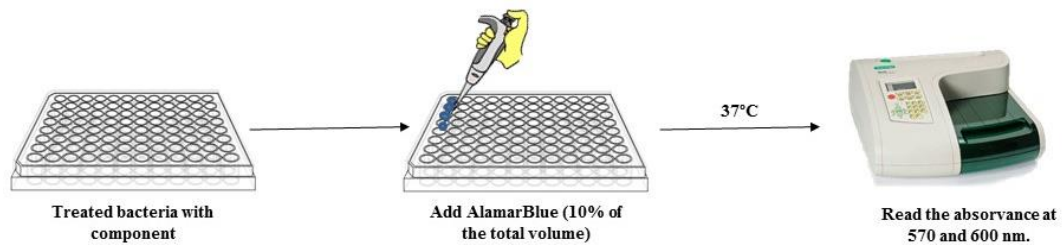


Figure 2.2: Alamarblue bacteria viability assay workflow.

### 2.3.2 AlamarBlue assay optimization

The conditions of the alamarBlue assay were optimized and for that *S. pneumoniae* was cultured in Columbia agar and incubated at 37°C, overnight. The colonies were transferred to several broths: BHI, Muller-Hinton (MH), Todd Hewitt broth (THB) and C+Y, using different initial O.D. 's: 0.1, 0.2, 0.3, 0.4, 0.5.

### 2.3.3 Minimum inhibitory concentration by broth dilution

A first assay was performed to determine the best range of concentrations for the determination of the minimum inhibitory concentration using the reference strain (*S. pneumoniae* TIGR4). For that, bacteria were inoculated into an agar medium (Columbia agar + 5% sheep blood) and incubated with antibiotic (penicillin, vancomycin and ceftriaxone) in several concentrations: 120 $\mu\text{g/ml}$ , 12 $\mu\text{g/ml}$ , 3 $\mu\text{g/ml}$ , 0.75 $\mu\text{g/ml}$ , 0.1875 $\mu\text{g/ml}$  and 0.0469 $\mu\text{g/ml}$ . The best range of concentrations determined for MIC determination were 0.09, 0.19, 0.38, 0.75, 1.5, 3, 6, 12, 24 and 120  $\mu\text{g/mL}$  for vancomycin (VCM) and ceftriaxone (CTX), instead for benzylpenicillin (PEN) two additional concentrations were determined 0.04 and 0.02  $\mu\text{g/mL}$  (Sigma-Aldrich). The MIC determination to penicillin, ceftriaxone and vancomycin were determined by broth

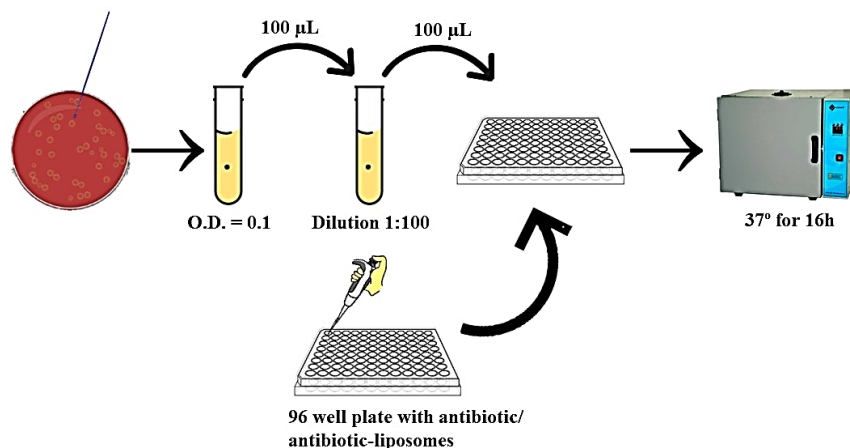


Figure 2.3: Minimum inhibitory concentration by broth dilutions of the antibiotics and the encapsulated liposomes with antibiotics workflow.

microdilution following CLSI procedures [75]. The plates were incubated for 16 hours and then 10% of AlamarBlue (Alfagene) was added to the plates in order to determine the antibacterial activity of the antibiotics. The encapsulated liposomes and the empty liposomes were also tested in the same conditions (figure 2.3).

#### **2.4. Minimum inhibitory concentration by agar dilution method**

Besides the assays performed with AlamarBlue, the liposomes efficacy was also determined by the agar dilution method, according to the described by Garcia et al.[76]. Bacteria were incubated in a 96-well plate containing different concentrations of antibiotic and antibiotic encapsulated liposomes of the three antibiotics in study, penicillin, vancomycin and ceftriaxone and incubated overnight in at 37°C. Then, the samples were diluted in a series of vials to 100×, 1,000× and 10,000×. In each agar plate, three drops of 10µl of the respective dilution were placed and incubated overnight at 37°C. In the following day, the colonies were counted and the colony forming units (CFU) per ml was determined using the formula below.

$$\text{Equation 2.2: CFU/ml} = \frac{\text{Number of colonies} \times \text{Dilution factor}}{\text{Volume of culture plate}}$$

#### **2.5. Cytotoxicity assays**

##### **2.5.1. Cytotoxicity assays optimization**

To investigate the *in vitro* cytotoxicity of the liposomes, a mouse brain endothelial cell line bEnd.3 (ATCC- CRL-2299) was used. The cells were cultured in Dulbecco's Modified Eagle Medium (DMEM) supplemented with 10% fetal bovine serum (Gibco) and 1% with penicillin-streptomycin (VWR) and incubated in a humidified atmosphere (37°C and 5% CO<sub>2</sub>) until it reached confluency. Cells were then seeded on 96-well plates, using 10,000 cells/well and 30,000 cells/well, and incubated in the same growth conditions for 24 hours. These cells were then treated VCM liposomes (120 µg/ml, 1.5µg/ml) and incubated for 24 hours. To determine the cell viability AlamarBlue was added, in a final concentration of 10%, followed by an additional incubation period of 24 hours. The measurements were performed at λ=570 nm and λ= 600 nm. Cell viability was presented as a percentage of viability when compared with the positive control (cells without treatment) as previously described. The previous experience was repeated with the optimized parameter - number of cells: 10,000, using the antibiotics and the encapsulated liposomes with the antibiotics in study: vancomycin, penicillin and ceftriaxone in all the study concentrations.

#### **2.6. Antimicrobial liposomes efficacy in clinical isolates**

After evaluating the efficacy of the liposomes in the reference strain *S. pneumoniae* (TIGR4), the same method was used in isolates recovered from IPD in Portugal presenting different serotypes (table 2.1). These strains were kindly provided by Prof. Mário Ramirez and Prof. José Melo Cristino from Faculdade de Medicina da Universidade de Lisboa.

**Table 2.1: Clinical isolates used for antibacterial efficacy**

<b>Clinical serotypes</b>
PP644 - Serotype 1
PP622- Serotype 3
PP491- Serotype 6B
PP537- Serotype 7F
2009V2540S- Serotype 14
2016V02555S- Serotype 15B/C
2008V1934S- Serotype 19A
2012V1441S- Serotype 24F

### **2.7. Expression of sdAb - FC5 and G3**

To obtain the sdAb necessary to link to the liposome and efficiently develop an immunoliposome, it was essential to express and purify the antibodies. For that, *Escherichia coli* BL21 (DE3) was transformed with the respective antibody clone in the pET21 vector and grown from a single fresh colony in SB medium (tryptone (PVL), yeast extract (PVL), MOPS (NZYtech), with 100 µg/mL of ampicillin and incubated overnight at 37°C with agitation. The cells were then diluted in a ratio of 1:30 in fresh medium containing ampicillin and incubated at 37°C until O.D.<sub>600nm</sub> reached 0.6-0.8. Protein expression was induced with 0.6 mM of isopropyl β-D-1thiogalactopyranoside (AppliChem) and incubated at 19°C overnight. After that, cells were centrifuged at 4°C for 20 minutes at 1700 G and the pellet was resuspended in binding buffer (20 mM phosphate buffer, 500mM NaCl, 5% glycerol and 5mM imidazole). To ensure a successful lysis, cells were sonicated (Bandelin, Sonoplus) for 8 minutes with 30 % output conditions during 6 cycles. The lysates were centrifuged at 16000 G for 15 minutes at 4°C. The supernatant (soluble fraction) was separated from the pellet and filtrated (with a 0.22µM filter (VWR)).

### **2.8. Immobilized metal ion affinity chromatography of sdAb - FC5 and G3**

The sdAb purification was performed using an immobilized metal ion affinity chromatography (IMAC). The purification process was done on an AKTA system (GE healthcare) using a His-tag protein purification column HisTrap HP 5ml (GE healthcare). The decrease of non-specific interactions between the proteins and the matrix was performed through washing the column with high salt concentration buffers, with low imidazole concentration. For that, the column was washed with binding buffer, followed by the sample application in the same conditions of the equilibration. To recover the intended protein, a gradient of imidazole was performed using sequential steps of elution buffer (20 mM phosphate buffer, 500mM NaCl, 5% glycerol and 500 mM of imidazole): 6%, 18%, 60% and 100%. The collected fractions were analysed sodium dodecyl sulphate polyacrylamide gel (SDS-PAGE) using two different techniques: coomassie staining and western blot.

## 2.9. SDS-PAGE

SDS-PAGE is an analytical method used to separate proteins according to their size. The system is composed by two different layers of acrylamide between glass plates. The stacking gel is the upper layer that includes the samples and is composed by 4% of acrylamide, 0.15M Tris-HCl pH 6.5, 0.20% sodium dodecyl sulfate (SDS), 0.10% ammonium persulfate (APS) and 0.01% of N, N, N', N'-tetramethylethylenediamine (TEMED, Aplichem). The separating (or resolving) gel is composed by 12.5% acrylamide, 0.5M Tris-HCl pH 8.8, 0.20% SDS, 0.10% APS and 0.01% TEMED. All the samples used in SDS-PAGE follow the same principles of denaturation which consist on adding loading buffer dye (1X) with 20 mM dithiothreitol (DTT) and heating for 10 minutes at 100° C. This allows the SDS to bind the hydrophobic regions and finish the denaturation process. After sample application, the electrophoresis was performed at 180 V using a Mini-Protean Electrophoresis System (Biorad). The gel was stained using to Coomassie Staining and Western Blot to detect the protein band.

### 2.9.1. Coomassie staining

Coomassie staining is a technique commonly used to detect proteins on gels. This technique can detect all the proteins with 0.2 µg or more, allowing to determine the quality of the purification. After running the SDS-PAGE, the resulting gel was covered with coomassie blue solution (Bio-rad) and incubated for 1 hour under gently shaking. The gel was destained overnight using 40% methanol, 10% acetic acid, and 50% H<sub>2</sub>O. The gel image was acquired using the Chemidoc™ XRS+ (Bio-Rad) system.

### 2.9.2. Western blot

Western blot refers to the separation of proteins by SDS-PAGE according to their size, followed by their transfer and immobilization to a membrane support, aiming to perform a selective detection with a specific antibody[77]. This technique is based on the transfer of proteins from a SDS-PAGE gel into a nitrocellulose membrane (Amersham). The components of the transfer cassette are: one piece of nitrocellulose membrane, two pieces of filter paper and two sponges per gel. The membrane is immersed in transfer buffer (25mM tris base, 192 mM glycine and 20% of methanol) for 5-10 minutes. The cassette was assembled for transfer as presented in figure 2.4.

The proteins were transferred to the membrane in a transfer tank (BioRad), for 1 hour at 250 mA. Following western blot transfer the membrane was blocked with 5% non-fat milk in PBS with 0.2% Tween 20 for 1 hour at room temperature under gently shaking. Afterwards, the membrane was washed 3 times with PBS 0.2% Tween 20 for 10 minutes. The membrane was then incubated with the primary antibody: anti-his (Roche) in a 1:3000 dilution during 1 hour at room temperature under gently shaking. Proteins were detected by chemiluminescence through Luminata Forte Western HRP (Merck Millipore, Darmstadt, Germany) and acquired using the ChemiDoc XRS+ imaging system (Bio-Rad).

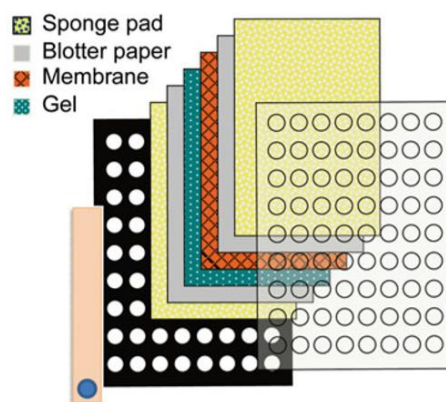


Figure 2.4: Western blot sandwich order prepared to place in gel holder cassette. Adapted from: [123]

## **2.10. Size exclusion chromatography (SEC) of sdAb - FC5 and G3**

Size exclusion chromatography separates molecules based on their size by filtration through a gel. Separation occurs when molecules of different sizes are included or excluded from the pores within the matrix, depending on the size of the pores [78]. The samples used in this purification were the collected fractions from the previous IMAC in which the sdAb was present in the correct size – positive fractions. Those fractions were then purified by SEC, using a Hiprep16/60 Sephacryl S-100 HR (GE Healthcare). The SEC process starts with the equilibration of the column with PBS, followed by loading the sample in the column. The resulted fraction was analysed by SDS-PAGE and western blot and concentrated using an Amicon® Ultra-4 (Merck) with a cut-off of 3 kDa.

## **2.11. sdAb- FC5 and G3 coupling to the liposome surface**

To choose the best/most efficient coupling protocol and to determine whether the chemical design may influence the biological performance, two different methods were evaluated: the biotin/streptavidin ligation and the thiol– maleimide, a covalent coupling.

### **2.11.1. Biotin – Streptavidin ligation**

A non-covalent method widely used is the biotin-streptavidin-biotin method, that is based on the strong biomolecular binding between these two molecules. Streptavidin is a homotetramer with approximately 56 kDa from *Streptomyces avidinini* that binds up until four biotin molecules with a  $K_d=10^{-14}$ M [79]. The biotin is bound in the active site of streptavidin by eight hydrogen bonds along with van der Waals interactions among non-polar groups [80].

### **2.11.2 Antibody biotinylation**

To link the antibody (G3 or FC5) to the liposome, the antibody has primarily to be linked to biotin which can be conjugated with some molecules such as avidin and streptavidin. The biotinylation of the antibody was performed using the kit “EZ-Link™ Sulfo-NHS-LC-Biotinylation Kit” (Thermoscientific). The molar ratio of Sulfo-NHS-LC-Biotin to protein was optimized to obtain the most efficient level of incorporation. In an initial phase we tested different molar ratios: 1:2.5, 1:5, 1:10, 1:20, 1:30. The first assays showed that the molar ratio 1:30 was the most efficient. To confirm the labelling of the protein, a western blot was done using Streptavidin-HRP antibody (Invitrogen) with a dilution of 1:7500.

### **2.11.3 Liposome antibody conjugation**

The biotin-antibody conjugate was mixed with streptavidin at a molar ratio of 3:1 (mole antibody/mole streptavidin) and the mixture was incubated at room temperature for 20 minutes. The mixture was then incubated with the pre-formed biotin-liposomes in a molar ratio of 1:1 (mole biotin in the liposome/ mole antibody biotinylated) at room temperature for 2 hours and later overnight at 4°C. Non-attached sdAb was removed by centrifugation using a 100K membrane filter (Amicon® Ultra-4, Millipore).

To confirm the ligation of the sdAb to the liposome two methods were performed: a SDS-PAGE followed by a western blot using Streptavidin-HRP antibody (at 1:7500 dilution) as primary antibody to properly identify the biotinylated proteins. In parallel, a Sandwich Enzyme-Linked Immunosorbent Assay (ELISA) was also performed. Briefly, polystyrene 96-well plates were coated with anti-PEG (abcam) antibody (10  $\mu\text{g/ml}$ ) for 1 h at room temperature. After washing 5 times with 100 $\mu\text{L}$  PBS and blocking with 3% bovine serum albumin (BSA) (1 h, room temperature) samples and known concentrations of biotinylated compounds were applied for 1 h at room temperature. This step was also followed by washing 5 times with PBS. Anti-His was added as second antibody (at 1:1000 dilution in 1 % BSA) during 1 hour at room temperature. 2,2'-azino-bis(3-ethylbenzothiazoline-6-sulphonic acid) (ABTS), (Sigma-Aldrich) and peroxidase (PVL) were added to each plate, incubated during 30 minutes at room temperature and the O.D. measured at 405 nm.

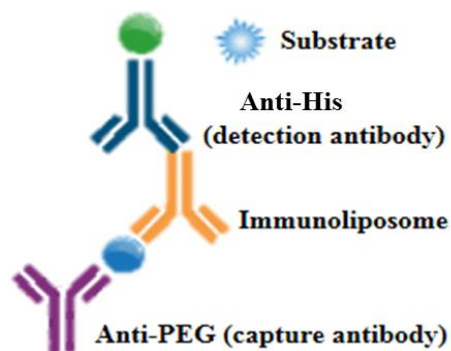


Figure 2.5: Representation of the ELISA process and its components.

#### 2.11.4 Thiol-Maleimide antibody-liposome conjugation

The thiol-maleimide conjugation is a ligation approach that belongs to the category of covalent methods and is based on the reaction of sulfhydryl groups with maleimide groups which is considered a clean, fast and efficient process [81] (figure 2.6).

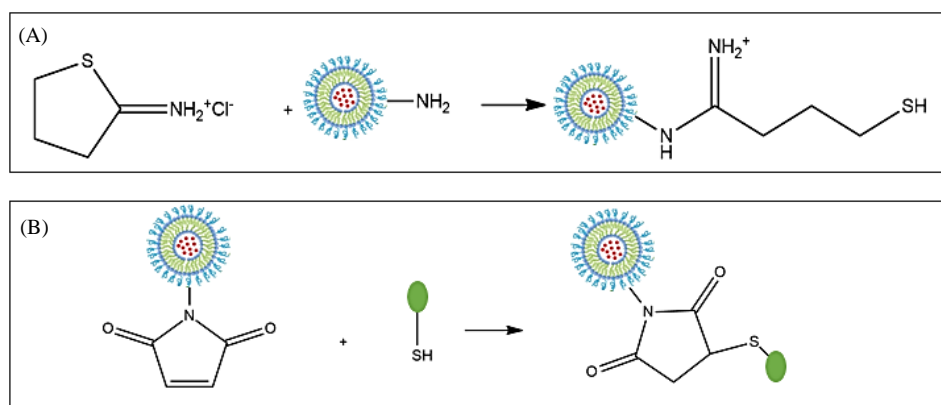


Figure 2.6: Thiol-Maleimide conjugation: (A) The liposome is prepared containing maleimide; (B) The liposome previously prepared is reacted with the sdAb containing a thiol group previously incorporated in the sdAb using the Traut's reagent.

The sdAbs FC5 and G3 were coupled to liposome employing the maleimide-thiol addition reaction. Thiol group (-SH) were introduced into the sdAbs by incubating with Traut's reagent at a molar ratio of 1:10 in 25 mM HEPES buffer, pH 8.0, containing 3mM EDTA. The reaction was incubated for 1 hour, in the dark, at room temperature under gentle shaking. The unreacted Traut's reagent was removed by using a desalting column (Zeba™ Spin Desalting Columns, Thermo Scientific). Thiolated sdAbs were then coupled to the pre-formed MAL-liposomes, in a molar

ratio of 3:1 (mole antibody/mole liposome). This reaction occurred with gentle shaking, in the dark at 4°C, overnight. Non-attached sdAb was removed by centrifugation using a 100K membrane filter. To confirm the ligation of the sdAb to the liposome through the thiol-maleimide conjugation method, SDS-PAGE followed by a western blot using Anti-His (at 1:3000 dilution) as primary antibody was performed to properly identify the biotinylated proteins.

### 2.11.5 SdAb-liposome ligation efficiency

The efficiency of the ligation between the antibodies and the liposome in both methods was determined through the quantification of the initial sdAb and the non-attached sdAb using the Bradford method. The calculations were performed using the formula below:

$$\text{Equation 2.3: Ligation efficiency} = \frac{\mu\text{g sdAb total} - \mu\text{g sdAb non attached}}{\mu\text{g sdAb total}} \times 100$$

### 2.11.6 Bradford Method

The Bradford method is a colorimetric method used for protein quantification, classified as rapid and accurate [82]. The protein concentration of the samples is estimated using a reference to absorbances determined for several standard BSA dilutions (table 2.2).

Table 2.2: BSA standard dilutions used for the determination of a standard curve

Dilution	Final BSA concentration (µg/mL)
A	2000
B	1500
C	1000
D	750
E	500
F	250
G	125
H	25
I	0 (Blank)

To construct the standard curve for BSA concentration, 10 µL of each standard were mixed with 300 µL of coomassie plus reagent (Thermofisher). The mixture was incubated for 10 minutes at room temperature and mixed in a plate shaker for 30 seconds. The absorbance was measured at 595 nm with a plate reader (BioRad). A standard curve was prepared by plotting the measurement for each BSA standard *versus* its concentration in µg/mL and was used to determine the protein concentration in unknown samples.

## 2.12. *In vitro* Blood-Brain Barrier Model

To study the efficiency of the immunoliposomes in crossing the BBB, an *in vitro* model was performed, according to [83]. In this model, bEnd.3 cells were cultured in DMEM supplemented with 10% FBS and 1% penicillin-streptomycin. When confluence was reached the cells were harvested with trypsin and were cultured 4000 cells/well in tissue culture inserts (VWR) with a pore size of 1  $\mu\text{m}$ . Aiming to reach a confluent monolayer, the cells were in culture for 11-14 days and the medium changed each two days. When in culture, the cells develop tight junctions responsible for restricting the passage of molecules between the apex and the base of the model, simulating the BBB [84].

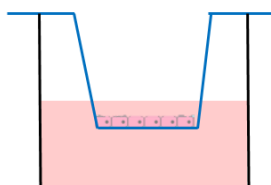


**Figure 2.7:** Schematic representation of the *in vitro* BBB model

### 2.12.1. Translocation and integrity studies

The integrity of the blood brain barrier was determined through the permeability of fluorescein isothiocyanate-conjugated dextran with molecular weight of 40 kDa (FD40). FD40 was diluted in transport buffer (glucose 1M,  $\text{MgCl}_2$  1M, HEPES 1M, BSA 3% and PBS 1X) to a final absorbance below 0.1. The probe was added to the apex and incubated for 2 hours. Then, the fluorescence intensity in the apex and in the base was measured at 495 excitation and 520 nm emission wavelengths using a microplate reader (FLUOstar OPTIMA BMG LABTECH). The percentage of FD40 translocation was used using the equation presented below.

$$\text{Equation 2.4: Translocation (\%)} = \frac{F_i}{F_T} \times 100$$

The cultures were only used for translocation studies when the integrity was higher than 95%. To study the transmigration capabilities of the immunoliposomes through the BBB, the immunoliposomes used were encapsulated with rhodamine, a fluorescent protein. The immunoliposomes were previously diluted in DMEM without phenol red (VWR). 1.15 ng of immunoliposomes (considering the ratio of antibody) were added to the apical side of the *in vitro* model. The apex volume and the base volume were collected after 90 min, 3, 6, 16 and 24 hours, the fluorescence in those samples was measured separately in a microplate reader (FLUOstar OPTIMA BMG LABTECH) and the translocation were calculated using the equation 2.4.

### 2.13. Statistical analysis

Each experiment was performed in triplicate, for three samples in each group. All data are presented as mean with standard error of the mean. A one-way ANOVA statistical test followed by a Dunnett's test or a Turkey's was used to compare the BBB fluorescence measurement with the respective controls and with each other considering  $P \leq 0.05$ .

## Chapter 3 – Results and discussion

### 3.1. *Streptococcus pneumoniae* growth curve

In order to be able to test the liposome activity in *S. pneumoniae*, the bacterial growth conditions were optimized. Bacterial growth is a process that involves several anabolic and catabolic reactions. These reactions result in cell division. The cell division process is dependent of the medium conditions. In ideal conditions, some bacterial cells can divide in about 20 minutes, however when in some environments the cells can take longer [85]. The elaboration of a growth curve in the conditions further used is an important step to determine the growth characteristics of the bacteria in study.

Four different growth phases can be observed within a bacterial growth curve: the lag phase, the log phase, the stationary phase and the death phase. The first one represents the phase in which the growth rate is essentially zero. This phase is thought to occur as a result of the physiological adaptation of the bacteria to the growth environment and is considered a transition to the exponential phase [86]. The second growth phase is the exponential or log phase that starts after the lag phase, in which an exponential growth is verified corresponding to the maximum growth rate [87]. The third phase is the stationary phase where the bacterial number in the culture remains constant because some cells continue to divide while others die [88]. This phase is followed by a death phase where the bacterial number decreases. Even though the *S.pneumoniae* growth curve presents all the discussed phases, in the growth curve assay (figure 3.1A) it was only possible to distinguish three phases: the lag phase that occurs during the first two hours of growth, the log

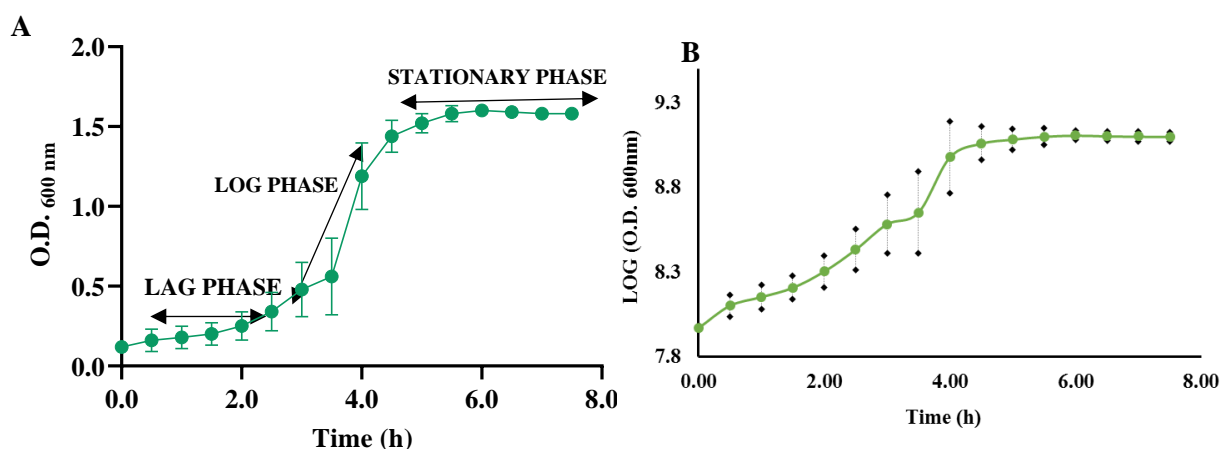


**Figure 3.1:** *S.pneumoniae* growth curve . (A) The optical density (O.D.<sub>600nm</sub>) values ( $\pm$  standard deviation) of *Streptococcus pneumoniae* cultures in BHI, at 37°C, are plotted as a function of time. (B) Growth curve in logarithmic scale.

phase during three hours and the stationary phase which occur the three final hours of the assay. Through the exponential phase it is possible to calculate the doubling time defined as the time it takes for a bacterial division to occur (figure 3.1 B). The mathematical principle behind the increase of the number of cells in a bacterial culture is given by the following equation:

- $N = N_0 e^{\mu t}$ , where N is the number of cells after each division event,  $N_0$  is the number of cells in the initial inoculum,  $\mu$  is the growth rate and t is the time that passed since the beginning of the experiment.
- $O.D. = O.D._0 e^{\mu t}$ , the previous formula can be converted in absorbance units. For data evaluation, the O.D. values obtained were converted in a logarithmic scale [89]. Using

the line equation ( $y = 0.0029e^{0.0251x}$ ) is possible to determine the growth rate,  $\mu$ . In *S. pneumoniae* growth curve, the growth rate is about  $0.0251 \text{ min}^{-1}$ .

- The doubling time,  $t_d$ , can be calculated using the following formula that relates the growth rate and the doubling time:  $\mu = \frac{\ln 2}{t_d}$ . For *S. pneumoniae* the calculated doubling time is 28 minutes. The theoretical value of *S. pneumoniae* is about 20-30 minutes which can vary accordingly to the growth conditions. For example, when cultured in C+Y growth medium the doubling time is about 30 minutes [90]. For the conditions tested, the value obtained is consistent with the theoretical value present in the literature.

### 3.2. AlamarBlue assay optimization

Currently, several different methods are provided to determine bacterial MIC of antibacterial agents. Broth microdilution is often used for MIC determination of many antibiotics. For MIC determination by broth microdilution bacteria are inoculated into a liquid growth medium with several concentrations of an antimicrobial compound. However, problems may occur when determining the endpoint given that the turbidity is measured visually or using absorbance [91]. The use of liposomes in these assays may lead to false interpretations when measuring the turbidity since the liposomes confer turbidity to the samples. This problem can be solved using a colorimetric MIC method. AlamarBlue is a resazurin compound normally used to determine the cell viability. As a result of bacterial growth and metabolism, alamarBlue changes colour from blue to pink. However, some media can interfere with alamarBlue, invalidating the results. Therefore, two conditions were tested in this assay: the initial O.D.<sub>600 nm</sub>, and the medium. Concerning the initial O.D.<sub>600 nm</sub>, the optimization presented in the figure 3.2B demonstrated that the initial number of bacteria does not interfere in the results. Accordingly, an initial O.D.<sub>600 nm</sub> of 0.1 was defined as the standard for the following assays. On the other hand, no differences were observed between the three media tested (figure 3.2A), so BHI was the medium selected since it is considered the reference medium for *S. pneumoniae*.

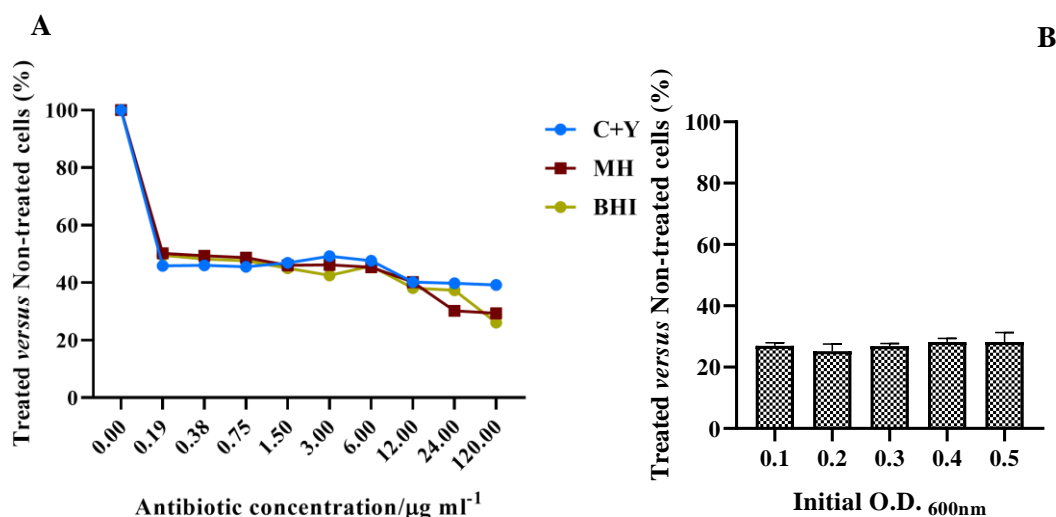


**Figure 3.2: Alamar blue optimization assay.** (A)- Difference in reduction between treated and control cells in viability assay with free ceftriaxone, in three different media: THB, BHI and MH; (B)- Percentage of Alamar blue reduced versus initial O.D. <sub>600nm</sub>;

### 3.3. Minimum inhibitory concentration of the antibiotics by broth dilution

The treatment of choice for pneumococcal meningitis has been penicillin, ceftriaxone or cefotaxime. However, due to the high incidence of resistance to penicillin G and 3rd generation cephalosporins it is recommended the administration of vancomycin along with penicillin or ceftriaxone [92]. Before liposome encapsulation the three antibiotics used in treatment of this infection were tested, using a range of concentrations between 0.09 -120 µg/ml. The aim of this assay was the validation of alamarBlue as a colorimetric broth dilution protocol as well as to confirm the antimicrobial activity of the selected antibiotics. The results are shown in figure 3.3.

The results are presented as the comparison between the growth in each concentration and the growth in the positive control. By comparing the antibacterial effect of the antibiotics in study at the same concentrations, it was observed that the antibiotics have a high growth inhibition of the bacteria. The obtained MICs for each antibiotic tested are summarized in table 3.1.

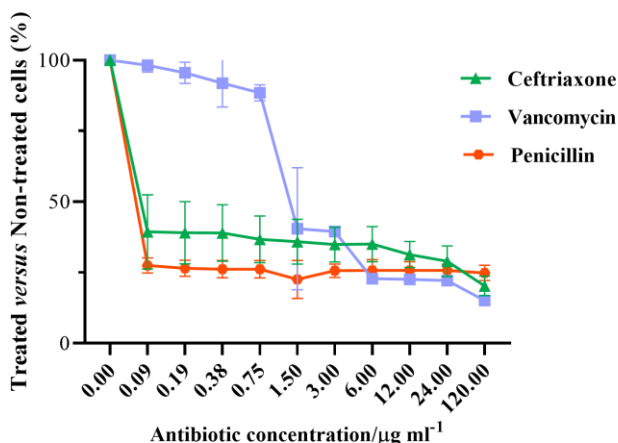


Figure 3.3: MIC determination, by a colorimetric method, of the antibiotics in study. Difference in reduction between treated and control cells in viability assay ( $\pm$ standard deviation) with free antibiotic (ceftriaxone, penicillin and vancomycin), in BHI medium.

Table 3.1: MIC obtained for antibiotics in study.

Antibiotic	MIC obtained (µg/ml)
Penicillin	< 0.9
Vancomycin	1.5
Ceftriaxone	< 0.9

The results obtained above allowed the validation of the broth dilution protocol, using alamarBlue to measure the bacterial viability enabling to proceed to antibiotic encapsulation in liposomes. The next step had

the main goal of providing a better option for clinical treatment, since the liposomes, in theory, possess lower cytotoxicity than the free antibiotics.

### 3.4. Liposomal formulations with encapsulated antibiotics

Once the antimicrobial efficacy of the selected antibiotics was verified, the next step was its encapsulation. This process was performed in collaboration with Dra. Manuela Gaspar (FFUL) that optimized the liposome composition to obtain the maximum encapsulation efficiency. The physicochemical characteristics of the liposomal formulations obtained are presented in table 3.2.

**Table 3.2: Physicochemical characterization of liposomal formulations.**

Formulation	Lipid Composition (molar ratio)	(AB /Lip) i (µg/µmol)	(AB/Lip) f (µg/µmol)	E.E. (%)	Ø (µm) (P.I.)	Zeta Potencial (mV)
<b>Loaded PEN</b>	PC: PG: PEG (76:19:5)	138±2	64±2	46±2	0.12 (<0.1)	-8 ± 1
<b>Unloaded</b>	PC: PG: PEG (76:19:5)	n.a.	n.a.	n.a.	0.12 (<0.1)	-5 ± 1
<b>Loaded VCM</b>	DPPC: DPPG: PEG (76:19:0.5)	121±4	25±1	21±1	0.13 (<0.1)	-5 ± 1
<b>Unloaded</b>	DPPC: DPPG: PEG (76:19:0.5)	n.a.	n.a.	n.a.	0.12 (<0.1)	-7± 1
<b>Loaded CTX</b>	PC:PG: PEG (8:2:0.5)	99±3	11±3	11±3	0.13 (<0.2)	-18 ± 2

**Abbreviations:** Encapsulation efficiency (E.E); Mean size (Ø); Polydispersity Index (P.I.) Antibiotic (AB); Liposome (Lip); Non applicable (n.a);

The main chemical compounds in liposome compositions are lipids and phospholipids. In the prepared formulations two different compositions were observed: in ceftriaxone and penicillin liposomes the lipids present were PC, PG and PEG. Vancomycin liposomes were composed by DPPC, DPPG and PEG. Another relevant characteristic when the liposomes are intended for therapeutic use is the mean size, which influences the pharmacokinetics of the vesicles. According to previous studies [94], the appropriated particle size range for long-circulating carriers when targeting the brain is between 50-200 nm. The formulations used for this study presented a particle size of about 120-130 nm, meaning that is they were in the recommend range. Besides the particle size, a successful liposomal formulation requires stability, which needs the preparation of homogenous populations of liposomes of a certain size. Thus, the polydispersity index (P.I.) is used to define the size range of the liposomes. Basically, the P.I. is a representation of the distribution of size populations in a given sample. The P.I. varies in a range of 0.0 and 1.0, where 0.0 represents a uniform sample, regarding the particle size and 1.0 is a polydisperse sample with multiple particle sizes [95]. When considering drug delivery liposomal formulations, the P.I. should be around 0.3 or less, indicating a homogenous population of lipid-based carriers [96, 97], which is verified in all liposomal formulations in study since the maximum value obtained for P.I. was 0.2.

The zeta potential is also a strong component in a liposome characterization. This parameter is described as the total charge that a particle acquires. The value of the zeta potential is normally used to conclude about the stability of a colloidal system. When the particles involved in the system have a large negative or positive zeta potential they will repel each other, inhibiting the aggregation process. Low zeta potential values will result in aggregation. The ideal value of zeta potential is about > +30 mV or < -30mV[98]. The zeta potential values obtained for the prepared liposomes were not consistent with the ideal values meaning that the liposomes have some tendency for aggregation. The ceftriaxone liposomes were considered the most stables.

The last parameter to consider is the encapsulation efficiency (E.E) which is defined as the total amount of encapsulant antibiotic found in the liposome solution versus the total initial input of

encapsulant. In table 3.2 these values are expressed in  $\mu\text{g}$  of antibiotic per  $\mu\text{mol}$  of liposomes. The encapsulation efficiency depends of multiple factors regarding the liposome and the antibiotic. Concerning the encapsulated antibiotic, the encapsulation efficiency is affected by the hydrophilic and lipophilic properties, which can be observed in the liposomes prepared for this study where, for the same liposomal formulation, ceftriaxone and penicillin liposomes have different encapsulation efficiencies. Moreover, the liposome properties also influence the encapsulation efficiency, as for example the aqueous volume, the surface area and the preparation methods [99]. Different encapsulation efficiencies were obtained for the different liposomes prepared. Penicillin liposomes had the highest E.E. of 46%, followed by vancomycin liposomes with 21% and finally ceftriaxone liposomes with an E.E. of about 11 %.

The previous analyses led us to conclude that the liposomal formulations encapsulated with the antibiotics were successfully prepared, allowing to proceed for the next step: the efficacy studies.

### 3.5. Antibacterial activity of encapsulated liposomes in *S. pneumoniae* (TIGR4)

#### 3.5.1 Penicillin liposomes

By comparing the antibacterial effect of the penicillin-encapsulated liposome at the same concentration of the free antibiotic (figure 3.4), it was verified that the free antibiotic has a lower MIC. This result is expected since the antibiotic is immediately in contact with the bacteria and the encapsulated liposome requires the release process. Nevertheless, the encapsulated liposomes efficiently inhibit the bacterial growth at concentrations above  $1.50\mu\text{g}/\text{ml}$ . The empty liposome was also tested, and we also observed some inhibitions of the bacterial growth at the maximum concentrations tested.

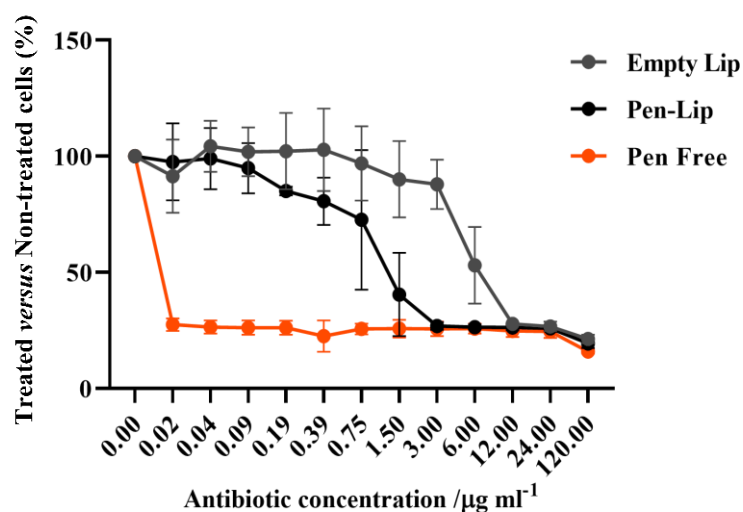


**Figure 3.4:** MIC determination by a colorimetric method, using penicillin compounds. The results are plotted as the difference in reduction between treated and control cells in viability assay ( $\pm$ standard deviation) with free antibiotic, empty liposome and liposome encapsulated antibiotic, in BHI medium. The amount of empty lip was equal to the encapsulated liposome.

The colony-forming results were performed to validate the alamarBlue assay. The results can be analyzed with the log CFU/mL values obtained for each concentration. As presented in figure 3.5, the free antibiotic has a higher efficacy when compared to the penicillin-encapsulated liposome. In all the antibiotic concentrations tested where it was seen bacterial growth, the log values for free penicillin and penicillin-encapsulated liposomes were very close, meaning that the inhibition efficacy of the two compounds was similar.

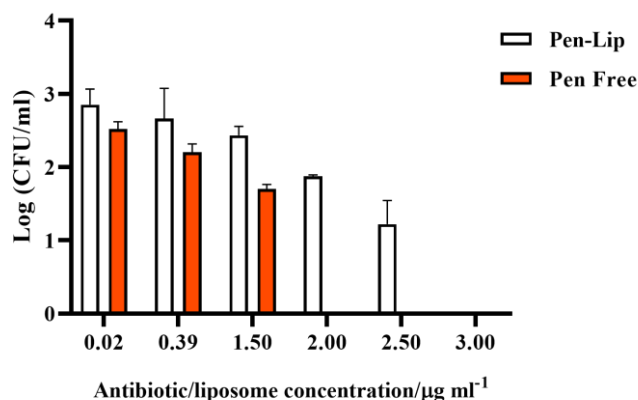


Figure 3.5: CFU of *Streptococcus pneumoniae* after treatment with penicillin compounds. The free Pen and Pen-Liposomes were incubated with the bacteria for 8 hours.

### 3.5.2 Vancomycin liposomes

Currently, there are no reports of *S. pneumoniae* with patterns of resistance to vancomycin. So, vancomycin is used for pneumococcal meningitis treatment along with beta-lactam and cephalosporin to fight resistant strains that cause infection. The antibacterial efficacy of the vancomycin liposome is presented in figure 3.6. By comparing the antibacterial effect of the free antibiotic and vancomycin-encapsulated liposomes in the same concentrations, it was observed that in almost every case, the vancomycin liposomes presented efficacy similar to that of the free antibiotic. However, the MIC for the free antibiotic is about 1.50 µg/mL and for the vancomycin liposomes is 3.00 µg/mL. In a previous *in vivo* study [100], aiming to fight *S. pneumoniae* the results showed that the liposomes promoted an increased amount of antibiotic near the bacteria. These previous results combined with the low cytotoxicity of the liposomes and the targeting for the BBB is a promising therapeutic approach, even with a low efficacy of the vancomycin-encapsulated liposomes when compared with the free antibiotic.

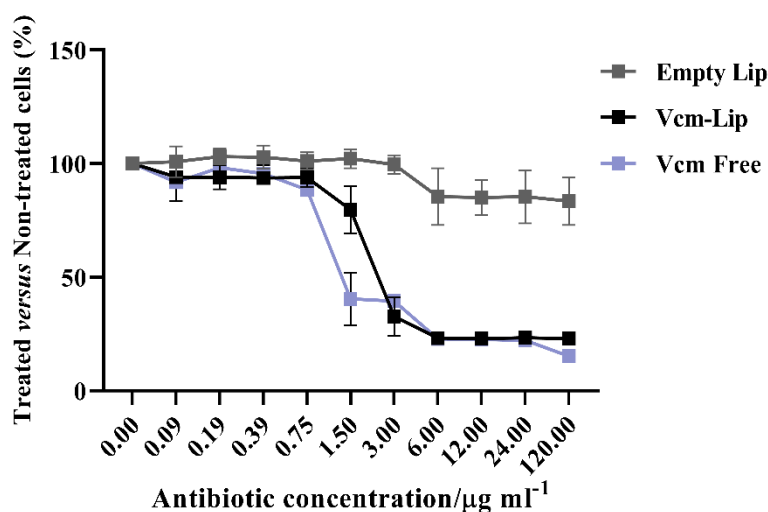


Figure 3.6: MIC determination by a colorimetric method using vancomycin compounds. The results are plotted as the difference in reduction between treated and control cells in viability assay ( $\pm$ standard deviation) with free antibiotic, empty liposome and vancomycin-encapsulated liposome, in BHI medium.

The colony-forming unit assay confirmed the results obtained in the efficacy study using alamarBlue. It is observed that for all the concentrations tested the antibacterial effect of the vancomycin liposome was better than the free antibiotic. A higher efficacy of the alamarBlue was noticed in comparison with the previous assay which is expected since the assay in agar plates is more sensitive.

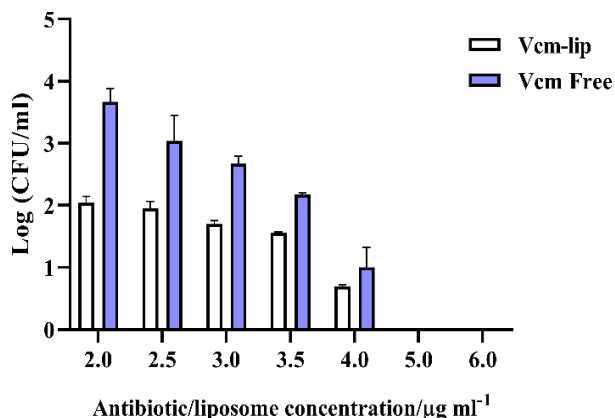


Figure 3.7: CFU of *Streptococcus pneumoniae* after treatment with vancomycin compounds. The free VCM and VCM-Liposomes were incubated with the bacteria for 8 hours.

### 3.5.3 Ceftriaxone liposomes

By comparing the antibacterial effect of the ceftriaxone liposome at the same concentration of the free antibiotic (figure 3.8), it was verified that, similar to penicillin, the free antibiotic has a lower MIC when compared to the encapsulated liposome. The ceftriaxone-encapsulated liposomes efficiently inhibit the bacterial growth at concentrations above 1.50 µg/ml and the free antibiotic exhibits a MIC between 0.00 and 0.09 µg/ml. The empty liposome was also tested and in this case an increase of the bacterial growth was noticed.

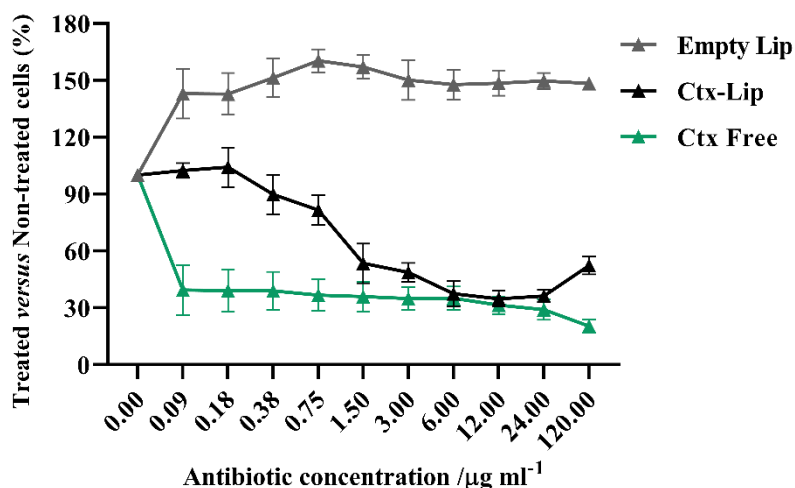


Figure 3.8: MIC determination by a colorimetric method using ceftriaxone compounds. The results are plotted as the difference in reduction between treated and control cells in viability assay ( $\pm$ standard deviation) with free antibiotic, empty liposome and ceftriaxone-encapsulated liposome, in BHI medium.

The colony-forming units results showed that the ceftriaxone liposomes have an antibacterial effect much lower than the free antibiotic, which supported the results obtained in the alamarBlue assays. This can be due to the lower encapsulation efficacy of this antibiotic. However, the ceftriaxone liposomes showed efficacy against *S. pneumoniae* in concentrations higher than 1.50 µg/ml concluding that the liposomal formulations encapsulated with ceftriaxone are also a promising therapeutic approach for pneumococcal meningitis.

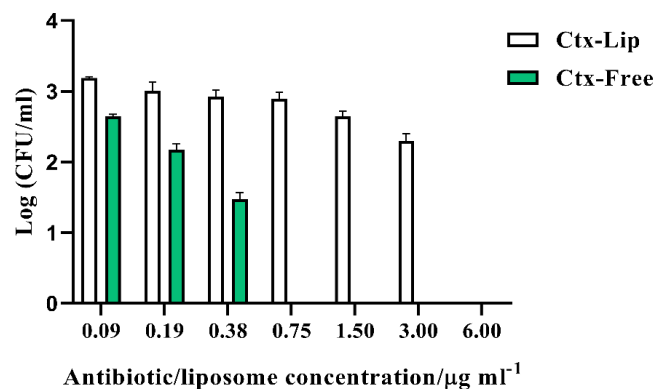


Figure 3.9: CFU of *Streptococcus pneumoniae* after treatment with ceftriaxone compounds. The free CTX and CTX-Liposomes were incubated with the bacteria for 8 hours.

Overall, the results obtained with AlamarBlue showed a good agreement with the results obtained by the colony-forming units, as already observed in previous studies [101]. AlamarBlue has already been successfully utilized to determine the susceptibility of several microorganisms to antibiotics, including gram-positive bacteria [102]. In our assay, the colorimetric method developed for the MIC determination by AlamarBlue was tested with three different antibiotics – penicillin, ceftriaxone and vancomycin. Considering the results, the colorimetric MIC method is a reliable method for the determination of antibiotic’s susceptibility in *S. pneumoniae*.

Concerning the antimicrobial effect of the encapsulated liposomes, it was observed that in the three antibiotic-encapsulated liposomes, the determined MIC was higher than the MIC obtained for the free antibiotic. The obtained results are summarized in table 3.3.

Table 3.3: MIC obtained for the antibiotic-encapsulated liposomes, compared with the free antibiotic and the empty liposome.

	MIC obtained ( $\mu\text{g/ml}$ )		
	Free antibiotic	Antibiotic encapsulated liposome	Empty liposome
<b>Penicillin</b>	< 0.02	1.50	12.00
<b>Vancomycin</b>	1.50	3.00	-
<b>Ceftriaxone</b>	< 0.09	1.50	-

Several liposomal formulations with encapsulated antibiotics have been previously evaluated for the treatment of bacterial infections. For example, for *Staphylococcus aureus* infections many vancomycin-encapsulated liposomes were prepared. One of the studies also obtained a lower efficacy for the liposomal preparation when compared to the free antibiotic [103]. Another study evaluated the *in vitro* and *in vivo* efficacy of vancomycin-encapsulated liposome in *S. aureus*. The *in vitro* results showed that the vancomycin-encapsulated presented a similar MICs when compared with the free vancomycin, but seemed to be more efficient in the *in vivo* studies [104]. The presented study does not address the comparison of the pharmacokinetics and biodistribution of the antibiotics-encapsulated liposomes and the free antibiotics. However, the liposome stability has been demonstrated to depend on the liposomal formulation characteristics, which already was discussed and proved to be a satisfactory formulation in all the cases.

The mechanism by which the liposomal formulations prepared inhibit *S. pneumoniae* growth is not established yet. The liposome can interact with the bacterial cell wall allowing an increased quantity of antibiotic to reach the cytoplasm. However, the time and process that leads to the antimicrobial activity of the liposome is not completely understood. The main advantages of the liposomes as nanocarriers for the pneumococcal meningitis is their ability to decrease the antibiotic toxicity and improve delivery of antibiotics to the brain[105]. The obtained MICs for the antibiotics-encapsulated liposome represent an auspicious approach for the treatment of pneumococcal meningitis. The most proficient liposomes developed are vancomycin-encapsulated liposomes since the difference between the efficacy of the free antibiotic and the encapsulated liposome is lower when compared with the other two formulations prepared. It is also important to note that these encapsulated liposomes will be coupled with a ligand for the BBB, improving the amount of bacteria reaching the focus of infection.

### 3.6 Antimicrobial efficacy of the liposomes in clinical isolates

*S. pneumoniae* is a gram-positive bacterium surrounded by capsule that can differ in the polysaccharides, dividing *S. pneumoniae* in serotypes [10]. To further elucidate if the differences between the serotypes affect the interaction between the bacteria and the liposome and consequently the antibacterial efficacy of the liposome, the MIC was determined by broth dilution method for several serotypes recovered from IPD. The first goal of this study was to determine the MIC of the invasive *S. pneumoniae* strains isolated for the free antibiotic. These data allowed monitoring the efficacy of the liposomes accordingly to the patterns of resistance.

Eight *S. pneumoniae* strains were collected from patients with IPD. The interpretation of MIC breakpoints was performed using the European Committee on Antimicrobial Susceptibility Testing (EUCAST) breakpoints. By evaluating the antimicrobial susceptibility (table 3.4), we observed that all strains were susceptible to vancomycin. On the contrary, two serotypes (19A and 14) showed antimicrobial resistance to ceftriaxone (MIC  $\geq 2$   $\mu\text{g/ml}$ ) and benzylpenicillin MIC  $\geq 2$   $\mu\text{g/ml}$ ). Serotype 19A is one of the most resistant serotypes to several antimicrobial agents, including ceftriaxone and penicillin which is supported by earlier reports. In accordance with the obtained results, serotype 14 is normally associated with a high resistance to penicillin antibiotics [106] [107]. Since the resistances of the strains were elucidated, the efficacy studies of the liposomes encapsulated with the three antibiotics in study were performed aiming to conclude about the influence of the several capsules in the presented therapeutics.

**Table 3.4: Resistance of the invasive *S. pneumoniae* serotypes isolated from IPD.** The interpretation of the MIC breakpoints was performed using EUCAST breakpoints. The MIC breakpoints were determined by broth dilution as described in the material and methods section.

<i>S. pneumoniae</i> serotype	MIC (mg/L)			Interpretation of MIC breakpoints		
	PEN	VCM	CTX	PEN	VCM	CTX
<b>1</b>	0.09	1.50	0.09	S	S	S
<b>3</b>	0.04	0.75	0.38	S	S	S
<b>6B</b>	0.02	1.50	0.19	S	S	S
<b>7F</b>	0.04	1.50	1.50	S	S	S
<b>14</b>	3.00	1.50	6.00	R	S	R
<b>15 B/C</b>	0.04	0.75	0.75	S	S	S
<b>19A</b>	120	1.5	12.0	R	S	R
<b>24F</b>	0.19	1.5	0.09	S	S	S

### 3.6.1 Penicillin liposomes

By comparing the minimum inhibitory concentration of the penicillin- encapsulated liposomes of the several serotypes it was possible to divide the serotypes in three groups according to the efficacy of the penicillin-encapsulated liposomes. The first group is composed by the serotypes 7F and 15 B/C, both penicillin susceptible, and the results of the assay are similar to the results of the reference strain described above. The MIC for the free antibiotic calculated previously was about 0.04  $\mu\text{g/ml}$ . The results of these two serotypes are presented in figure 3.10, where is possible to observe that the MIC for the two serotypes is about 0.75  $\mu\text{g/ml}$ .

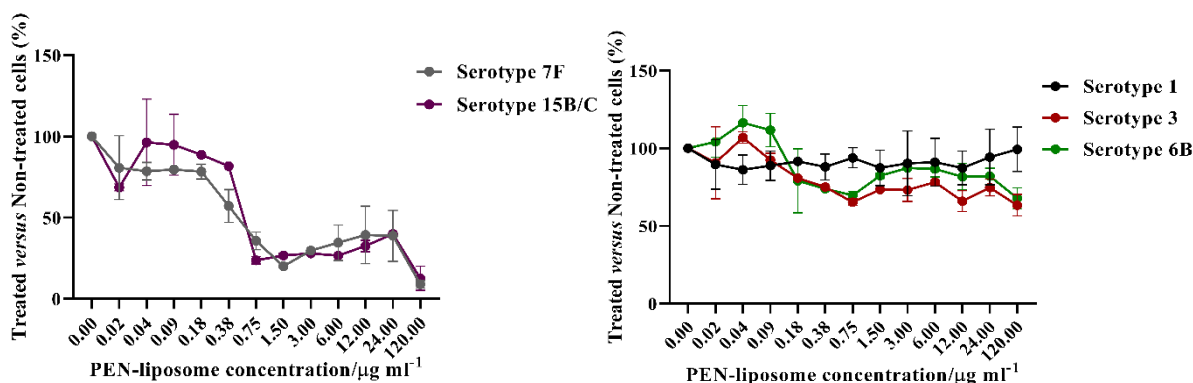


Figure 3.10: MIC determination by a colorimetric method using penicillin compounds in five different serotypes. Differences in reduction between treated and control cells in viability assay ( $\pm$ standard deviation) with penicillin-encapsulated liposomes, in serotype 7F and 15B/C (left image); in serotype 1,3 and 6B (right image)

According to these results it is possible to conclude that the penicillin-encapsulated liposomes are a promising therapeutic choice when considering meningitis caused by serotype 7F and serotype 15B/C.

The second group of serotypes with similarities between the results are serotypes 1, 3, and 6B. All of them are also penicillin susceptible with a MIC between 0.02-0.09  $\mu\text{g/ml}$ , as described in table 3.2. However, the results of the minimum inhibitory concentration by broth dilution have shown that the penicillin liposomes do not have an antibacterial effect on these serotypes, in all range of concentrations tested (figure 3.11). Since these strains are penicillin susceptible and the penicillin-encapsulated liposomes had high efficacy in the reference strain and in serotypes 7F and 15 B/C the results can be an effect of the differences between the capsular polysaccharide, which can improve the interaction between the liposome and the bacteria or in these cases inhibit this process.

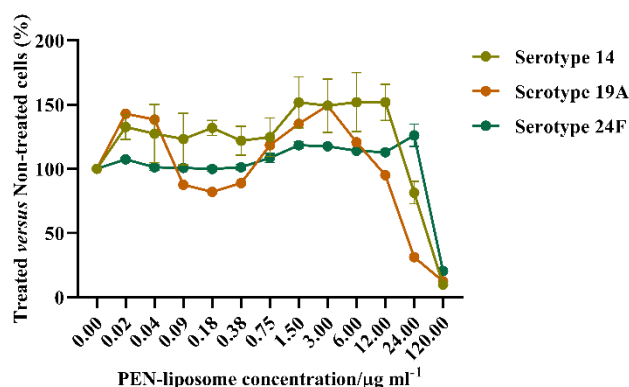


Figure 3.11: MIC determination by a colorimetric method using penicillin compounds in three different serotypes. Differences in reduction between treated and control cells in viability assay ( $\pm$ standard deviation) with penicillin-encapsulated liposomes, in serotypes 14, 19A, and 24F.

The final three serotypes with similar results are serotypes 14, 19A and 24F. Serotypes 14 and 19A are resistant to penicillin while serotype 24F is susceptible. The penicillin-encapsulated liposomes have similar antibacterial activity in the three serotypes, as observed in figure 3.11. In most of the concentrations the antibacterial effect of the liposomes was not noticed, except for the two higher concentrations. The MIC for these three serotypes was between 24-120  $\mu\text{g/ml}$ .

### 3.6.2. Vancomycin liposomes

The antimicrobial effect of the encapsulated liposomes was also tested in the serotypes for vancomycin. In this case, none of the serotypes in study presented resistance patterns which imply that the differences in the results between the several serotypes are only a consequence of the differences in the biochemical characteristics of the polysaccharide capsule.

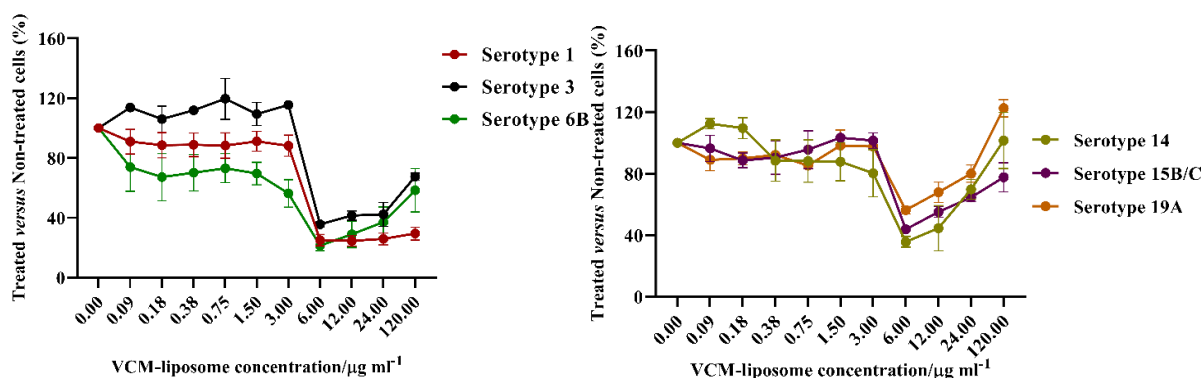


Figure 3.12: MIC determination by a colorimetric method using vancomycin compounds in six different serotypes. Differences in reduction between treated and control cells in viability assay ( $\pm$ standard deviation) with vancomycin-encapsulated liposomes: in serotypes 1,3 and 6B (left image); in serotypes 14, 15B/C and 19A;

The results of the minimum inhibitory concentration with the vancomycin-encapsulated antibiotics (figure 3.12) show that this nanocarrier can inhibit the growth of six different serotypes. However, in the case of serotypes 1, 3 and 6B, it is noticed that the maximum growth inhibition occurs at a concentration of 6.00  $\mu\text{g/ml}$  with a slight decrease in the inhibition in the higher concentrations. In the case of serotypes 14, 15B/C and 19A the maximum growth inhibition is also verified at 6.00  $\mu\text{g/ml}$  but the decrease of the inhibition in the higher

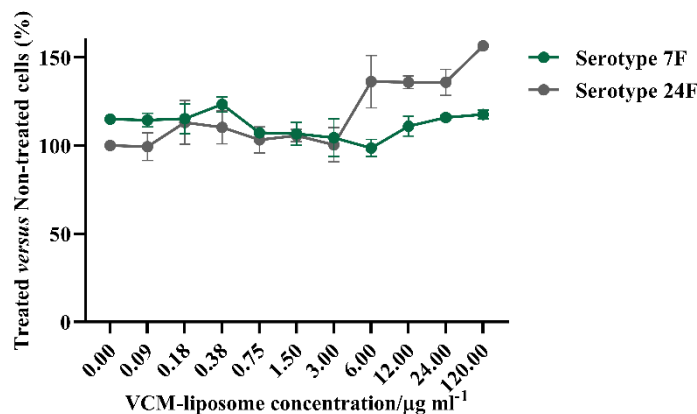


Figure 3.13: MIC determination by a colorimetric method using vancomycin compounds in two different serotypes. Differences in reduction between treated and control cells in viability assay ( $\pm$ standard deviation) with vancomycin-encapsulated liposomes: in serotypes 1,3 and 6B (left image); in serotypes 14, 15B/C and 19A;

concentrations is more pronounced. At a vancomycin encapsulated liposome concentration of 120  $\mu\text{g/ml}$  the antibacterial efficacy of the liposomes become negligible. On the other hand, the results for the serotypes 7F and 24F are presented in figure 3.13. In these cases, the vancomycin-encapsulated liposomes do not affect the bacterial growth in any concentration tested, when compared with the positive control.

### 3.6.3. Ceftriaxone liposomes

Similar to penicillin liposomes, the comparison between the minimum inhibitory concentration of the ceftriaxone-encapsulated liposomes of the several serotypes resulted in a serotype division according to the efficacy of the ceftriaxone-encapsulated liposomes. In figure 3.14 the results for the strains of serotypes 1, 3 and 6B, all of them susceptible to ceftriaxone, are presented. The antimicrobial effect of the encapsulated liposomes was similar to the case of the penicillin., The antimicrobial efficacy of the ceftriaxone-encapsulated liposomes was detected in concentrations higher than 3.0  $\mu\text{g/ml}$ , which represent a satisfactory result in fighting these serotypes.

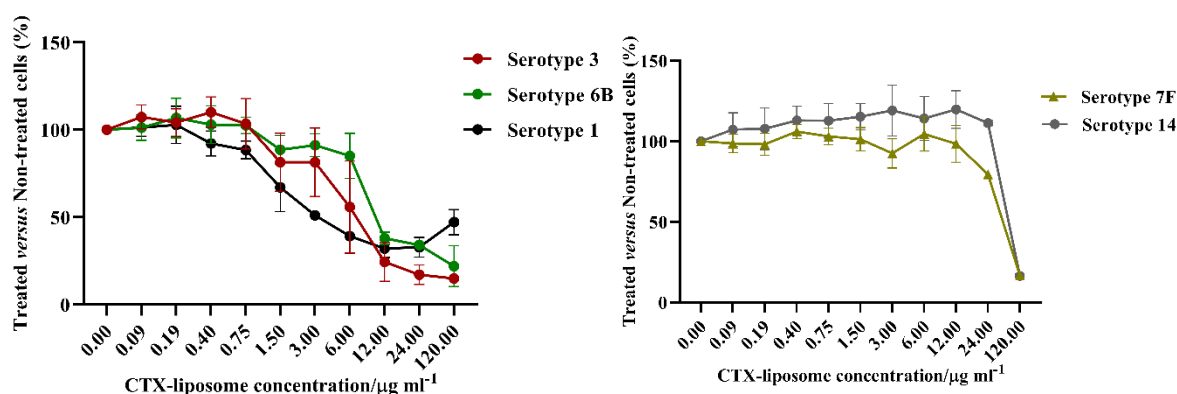


Figure 3.14: MIC determination by a colorimetric method using ceftriaxone compounds in five different serotypes. Differences in reduction between treated and control cells in viability assay ( $\pm$ standard deviation) with ceftriaxone-encapsulated liposomes: in serotypes 1,3 and 6B (left image); in serotype 7F and 14 (right image);

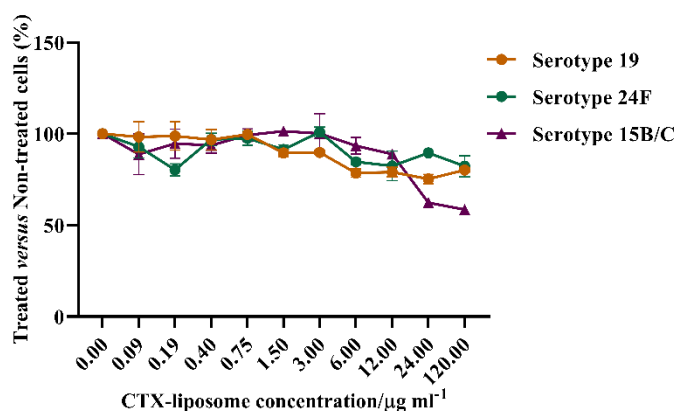


Figure 3.15: MIC determination by a colorimetric method using ceftriaxone compounds in three different serotypes. Differences in reduction between treated and control cells in viability assay ( $\pm$ standard deviation) with ceftriaxone-encapsulated liposomes, in serotypes 1,3 and 6B.

In contrast, the effect of the ceftriaxone encapsulated liposomes in serotype 7F and serotype 14 respectively, susceptible and resistant to ceftriaxone, are only noticed in the highest concentration tested (120  $\mu\text{g/ml}$ ), which was expected for serotype 14 due to the resistance patterns but not in the case of serotype 7F. Once more, the low efficacy of the encapsulated liposomes can be a result

of the capsule characteristics that limits the interaction with the liposome. Finally, the antimicrobial effect of the encapsulated liposomes with ceftriaxone in the serotypes 19A, 24F and 15B/C is presented in figure 3.15. The results show that the ceftriaxone-encapsulated liposomes are inefficient in all the range of the concentrations tested.

The study of the antimicrobial efficacy of the encapsulated liposomes in clinical serotypes led to conclude that the efficacy of the nanocarrier is different according to the serotype in study. For the interpretation of the results it is necessary to take into consideration several factors than can affect the interaction between the liposome and the bacteria. The first factor to consider is the characteristics of the liposome. Besides the characteristics already discussed in chapter 3.4., some physicochemical characteristics are crucial, as for example: the surface charge (cationic, anionic or neutral), the proportion and type of lipids in the composition and the presence of long-circulating molecules [108]. Concerning the bacteria, the role of the CPS in the interaction with the liposome is not fully understood. The assay with several serotypes was performed aiming to conclude about this interaction. The results obtained are summarized in table 3.5.

**Table 3.5: MIC obtained for the antibiotic-encapsulated liposomes, in several IPD isolated serotypes.**

<i>S. pneumoniae</i> serotype	Antibiotic- encapsulated liposome MIC (µg/mL)		
	PEN	VCM	CTX
<b>1</b>	n.a.	6	12
<b>3</b>	n.a.	6	12
<b>6B</b>	n.a.	6	12
<b>7F</b>	0.75	n.a.	120
<b>14</b>	120	6	n.a.
<b>15 B/C</b>	0.75	6	n.a.
<b>19A</b>	24	6	n.a.
<b>24F</b>	120	n.a.	n.a.

These results obtained above showed that the different capsules influence the results for the same liposomal formulation. For example, in the liposomal formulation developed for encapsulation of penicillin characterized as a negative charged formulation composed by PC, PG and PEG, three susceptible serotypes do not get any inhibition of the bacterial growth. On the contrary, in two other serotypes the calculated MIC was 0.75 µg/ml, revealing a high efficacy of the tested encapsulated liposome formulation. These results proved that the CPS influence the antibacterial effect of the developed liposomes.

### 3.7 Cytotoxicity assays with free antibiotics and antibiotics-encapsulated liposomes

Cytotoxicity assays are one of the most important parameters for biological evaluations since drugs have several cytotoxic mechanisms [109]. Aiming to evaluate the potential cytotoxicity effects of the free antibiotics and antibiotics-encapsulated liposomes on brain endothelial cells (bend.3), cells were treated with vancomycin-encapsulated liposomes with two different initial density of cells/per well, in order to find the best conditions for the cytotoxicity assay. The effect of the tested compound on cell viability was measured using alamarBlue as described in the material and methods section and three antibiotic concentrations (0.0, 1.5 and 120.0  $\mu\text{g/ml}$ ). The results of the density cells optimization presented in figure 3.16 showed that the initial cells density does not affect the results and 10000 cells/per well was defined as the cell density standard for the assay.

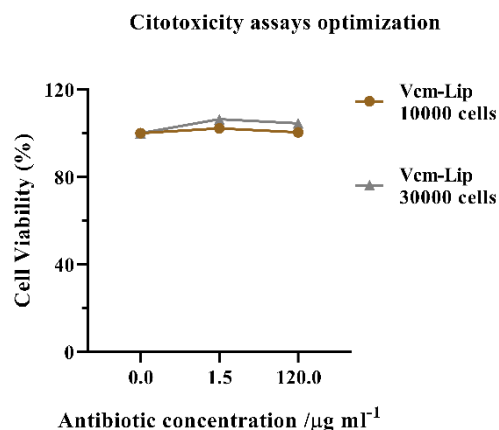


Figure 3.16: Cytotoxicity assay - density cells optimization. Two different initial density cells were tested using three concentrations of vancomycin encapsulated liposomes.

The same method was used to evaluate the cytotoxicity effects of all the compounds in study and are presented in figure 3.17. Regarding the vancomycin formulation and free antibiotics, it is possible to observe that there's no evidence of toxicity in the range of concentrations tested. The

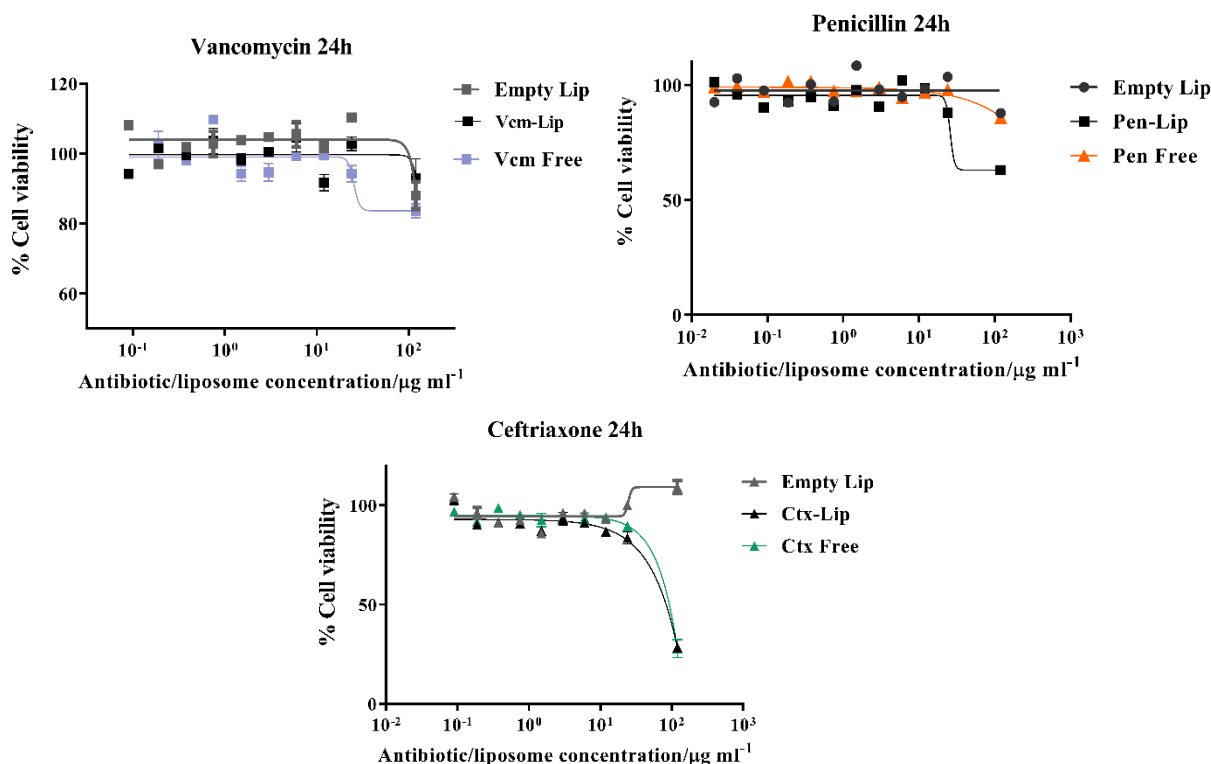


Figure 3.17: Antibiotic encapsulated liposomes cytotoxicity assays. Bend.3 cells were subjected to the concentrations in study of each liposomal formulation of the chosen antibiotics (vancomycin, penicillin and ceftriaxone). After 24 h treatment, cell viability was evaluated with AlamarBlue. Three replicate wells were used to determinate each data point and three independent experiments were carried out in different days.

data obtained clearly demonstrate that the viability of the bend.3 cells is maintained with a small decrease in the highest concentration in the cells treated with free vancomycin. The results for penicillin showed that no cytotoxicity effects are detected in the case of the empty liposome and the free antibiotic. In the data of penicillin-encapsulated liposomes we observed a small decrease in cell viability, though the viability remains higher than 85%. On the contrary, in the ceftriaxone cytotoxicity results it is observed the maintenance of the cell viability in most of the concentrations tested in the three compounds: the free antibiotic, the ceftriaxone-encapsulated liposome and the empty liposome. However, at the highest concentration were verified a sudden decrease of the cell viability in the cells treated with free antibiotic and with ceftriaxone-encapsulated liposomes. This toxicity seems to be due to the antibiotic toxicity since the empty liposome does not affect the cell viability.

The cytotoxicity assays are required for estimation and characterization of potentially toxic effects of the developed liposomes [110], meaning that when in the organism, healthy living brain cells will not be induced in cell death. The results discussed above lead to conclude that the antibiotics-encapsulated liposomes are safe nanocarriers, allowing to proceed for the development of the immunoliposome, knowing that no toxic effects will be detected.

### 3.8 Development of an immunoliposome - Expression and purification of FC5 and G3 to liposome conjugation

After validating the antimicrobial efficacy of the liposomes in *S. pneumoniae* strains, the next step was the coupling of the target technology to cross the BBB and reach the bacteria. The development of an immunoliposome started with the expression and purification of the antibodies chosen to cross the BBB. High quantities of protein containing a His-Tag were recovered from the lysate extract using an IMAC. The elution fractions were analyzed by SDS-PAGE followed by coomassie staining and western blot (figure 3.18).

The coomassie staining method is required to evaluate the protein purity. In the obtained results (figure 3.18A/B) it was possible to observe the intended antibody with a molecular weight of

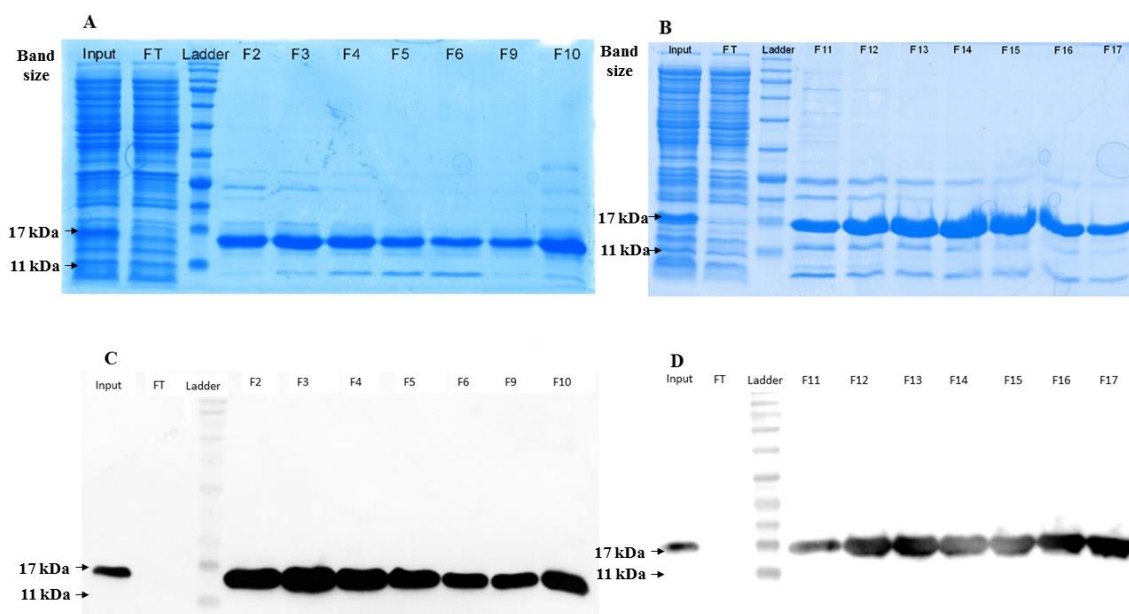


**Figure 3.18: SDS-PAGE with the several fractions collected from IMAC purification.** (A) Coomassie staining technique with the results of G3 purification; (B) coomassie staining with the FC5 purification results; (C) western blot with the results of G3 purification; (D) western blot with the results of FC5 purification.

15kDa in the fractions collected in both sdAb purifications. The flow through (FT) corresponding to the protein unbound to the column does not contain the sdAb, meaning that the antibodies successfully bound to the column. The analyzed fractions corresponding to the higher concentration registered on the IMAC purification contain a high number of undesirable proteins due to the elution of the proteins weakly bound to the column. Simultaneously, a western blot was performed with the collected fractions in order to reveal the desired protein, using an Anti-His as primary antibody for the process. This revealed the presence of a protein of about 15 kDa, in both cases corresponding to the desired single domain antibodies. To improve the purity of the antibodies, a second chromatography was performed. This time, a size exclusion chromatography was performed in order to separate the proteins according to their size. The collected fractions were also analyzed in a SDS-PAGE by two techniques: coomassie staining and western-blot. The results obtained are shown in figure 3.19.

Aiming to obtain the antibodies with high purity, the results presented above shown that the SEC was successfully performed. In the coomassie staining results (figure 3.19A/B) is possible to observe that the undesired proteins presented in the fractions collected from the IMAC were now eliminated, since in both purifications (FC5 and G3) only one band is present in the coomassie gel. The western blot was made to confirm the presence of the intended antibodies, using anti-His

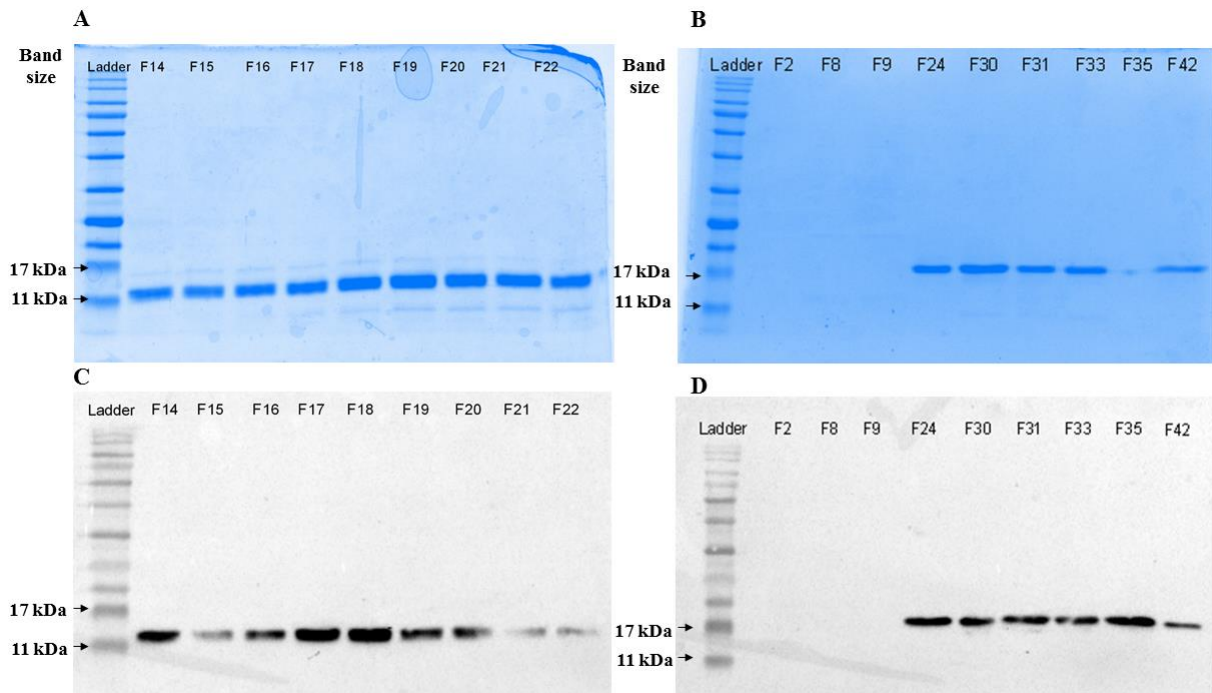


**Figure 3.19: SDS-PAGE with the several fractions collected from SEC purification.** (A) Coomassie staining technique with the results of G3 purification; (B) coomassie staining with the FC5 purification results; (C) western blot with the results of G3 purification; (D) western blot with the results of FC5 purification.

as primary antibody shown that in G3 purification (figure 3.19 C) all the fractions analyzed contain the antibody. However, in FC5 western blot (figure 3.19 D) three fractions do not contain the desired antibody.

The expression and purification of the sdAb was successfully achieved enabling to proceed with the immunoliposome development. The following step was the conjugation of the antibodies to the liposome surface, to efficiently create an immunoliposome.

### 3.9 SdAb (FC5 and G3) coupling to the liposome surface – Biotin approach

The coupling of the sdAb to the liposome surface was performed using two different approaches: the biotin approach and the maleimide approach. Regarding the biotin approach the distinguishing feature that lead to consider a promising method was the affinity of the noncovalent interaction. The affinity is only compared with systems involving ligand metal ions. The reaction between the biotin and streptavidin is almost irreversible ensuring a good conjugation between the liposome and the sdAb's.

The biotin method starts with the antibody biotinylation where the sulfo-NHS-LC-biotin supplied with the biotinylation kit (material and methods section) possess an active ester group that reacts with the primary amines or the  $\epsilon$ -amino of the lysine in an antibody (figure 3.20). For each lysine residue, this reaction results in a molecular weight increase of 339.161 Da, as previously demonstrated [111]. The determination of the best ratio for the sdAb biotinylation reaction was performed using FC5 that contains 41 lysine residues.

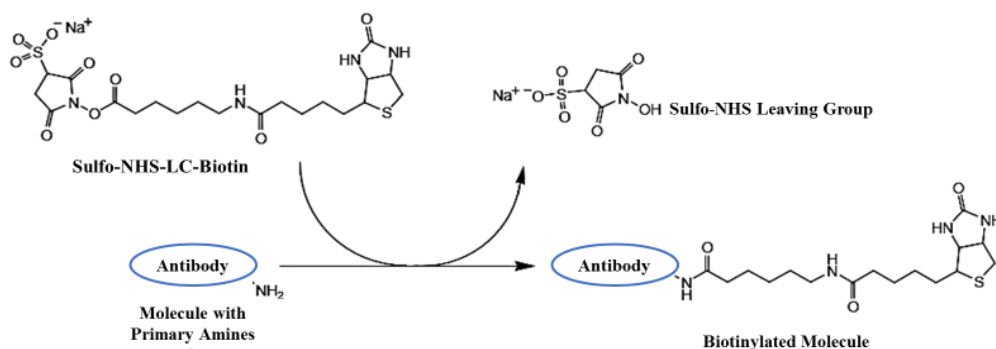


Figure 3.20: Chemical reactions involved in antibody biotinylation.

The analysis of the biotinylated antibodies by SDS-PAGE is presented on figure 3.21. In the first assay 4 different sdAb:biotin ratios were tested and the sdAb biotinylations were confirmed by biotin detection in western blot analysis employing HRP-conjugated streptavidin. The ligation between the sdAb and the biotin occurred in all the ratios tested since biotin was detected in all the reactions. However, a significant increase of the molecular weight between the several ratios tested was not verified, meaning that the biotinylation level was similar in all the ratios. Additionally, it was also possible to conclude that the biotinylation was not very high considering that the molecular weight was similar to the control.

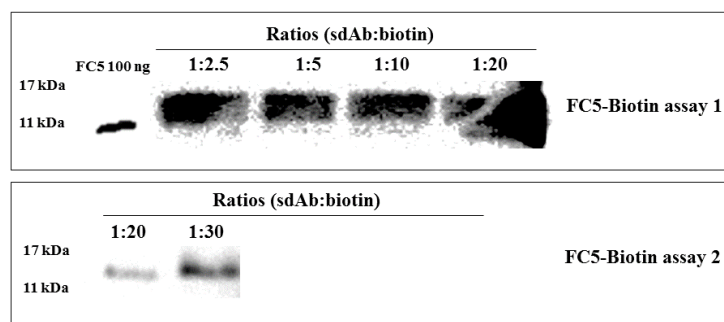
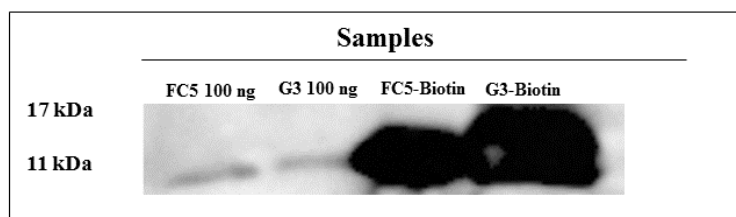


Figure 3.21: Optimization of the sdAb-biotin ligation. The first assay was performed with four different ratios and the second assay was performed with the best ratio obtained in the first assay and a second ratio.

A second assay was performed using two ratios 1:20 and 1:30 and it was verified that the ratio 1:30 had a better incorporation level since the detection is stronger for the same antibody concentration. An increase of the molecular weight was also observed suggesting that the number of biotin molecules linked to the lysine residues was higher. The biotinylation level should be enough to the subsequent reactions, which was achieved in the 1:30 molecular ratio

The biotinylation was also performed with G3, a sdAb that contains 44 lysine residues. We expected that using the same ratio used for FC5, the biotinylation level remained equivalent to the results obtained above, which is proven by the WB presented in figure 3.22.



**Figure 3.22: FC5 and G3 biotinylation.** The biotinylation process was performed using the best ratio previously evaluated: 1:30. The results were analysed in a western blot comparing with a positive control: 100 ng of the sdAb previously purified.

Since biotinylation of both sdAb was successfully achieved, the next step was the conjugation of the biotinylated sdAb to the streptavidin in order to be possible to link to the biotinylated liposomes. The two processes were made in one step with the incubation with streptavidin followed by the incubation with the liposomes containing PEG-biotin. The ratio sdAb: biotin (considering the ratio of biotin presented in the liposomes – supplementary information) was optimized in order to find the best ratio. The results were evaluated in a western blot after the separation of the sdAb unbound to the liposome.

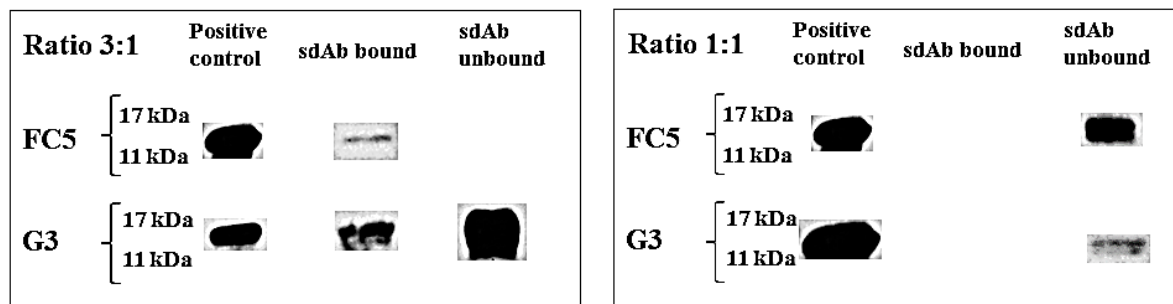


**Figure 3.23: Optimization of the liposome-antibody conjugation.** The ratio sdAb: PEG-biotin was optimized with two different ratios: 3:1 and 1:1 and analysed in a western blot using anti-his as primary antibody

The western blot showed that the best ratio to link the biotin-liposomes to the sdAb was 3:1(sdAb:biotin), since in the ratio 1:1, it was not detected sdAb bound, in either of the sdAb tested. In the 3:1 ratio, ligation of both sdAb to liposomes could be detected. Simultaneously, the best ratio was also tested by an ELISA to confirm the ligation of the sdAb to the liposome, using as capture antibody anti-PEG to link to the liposomes and as detection antibody anti-His to efficiently detect the antibodies.

The ELISA data (figure 3.24) confirmed the results obtained in the western blot. We used as negative control the liposome-PEG (without sdAb and biotin). The two developed immunoliposomes presented a higher absorbance when compared with the negative control, proving the success of the conjugation of the sdAb to the biotin-liposomes, since it was confirmed the presence of the liposomes and the antibodies in the reaction solution.

The results obtained showed that development of the immunoliposomes using the biotin approach was successfully achieved. However, it is also important to determine the efficiency of the ligation between the sdAb to the biotin-liposomes. The sdAb attachment efficiency was determined by the Bradford method (supplementary information), quantifying the unbound antibody and comparing with the quantity of initial antibody added to the reaction, since the quantification of the antibody attached to the liposome is uncertain owing to streptavidin interference.

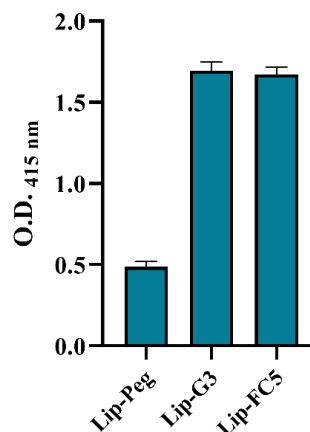


**Figure 3.24: ELISA confirming the conjugation of the sdAb with the liposomes.** The presented results presented are the means of three independent assays ( $\pm$ standard deviation).

**Table 3.6: Yield of sdAb (G3 and FC5) attachment on liposomes prepared by the biotin approach.** The yield was calculated after measuring the sdAb by a bradford technique. Each value is the mean from n samples (and the standard deviation is presented)

sdAb-liposome	Yield of sdAb attachment (%)		
	Yield of sdAb attachment (%)	Range of values	n
G3-liposome	75 $\pm$ 12	68.2-82.5	3
FC5-liposome	70 $\pm$ 7	63.4-76.8	3

The obtained yield attachment for the two sdAb tested (table 3.6) was 70% and 75%, showing a high ligation efficiency between the biotin liposome and the antibodies. This proves that the biotin approach is promising for the development of immunoliposomes. These values are similar to a recent study where the same procedure was used to develop immunoliposomes [112].

### 3.10 SdAb (FC5 and G3) coupling to the liposome surface – Maleimide approach

The maleimide approach is widely used in bioconjugation and is based on the reaction between a sulfhydryl group with maleimide groups. The maleimide is conjugated in the liposome formulation and the sulfhydryl group is added to the sdAb after the reaction with the Traut's reagent. The process starts with the thiolation of the sdAb followed by the incubation with the

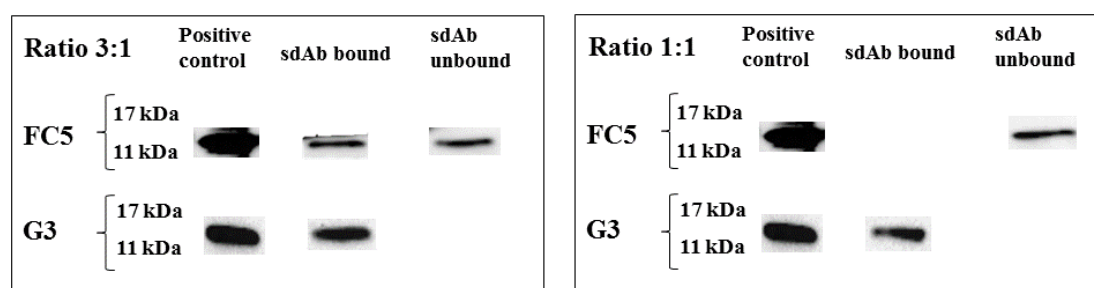


**Figure 3.25: Optimization of the liposome-antibody conjugation.** The ratio sdAb: PEG-maleimide was optimized with two different ratios: 3:1 and 1:1 and analysed in a western blot using anti-his as primary antibody

liposomes, containing PEG-maleimide. The ratio sdAb: maleimide (considering the ratio of maleimide presented in the liposomes – supplementary information) was optimized in order to find the best ratio. The results were evaluated in a western blot after the separation of the sdAb unbound to the liposome.

In the western blot it is possible to observe that the best ratio to link the maleimide-liposomes to the sdAb is 3:1(sdAb:maleimide), since in the ratio 1:1 it was only detected sdAb bound in G3, while in FC5 the reaction did not occur. In the ratio chosen, we detected the ligation in both sdAb tested. The efficiency of the sdAb attachment in the ratio 3:1 was also determined. The obtained results are presented in table 3.7.

**Table 3.7: Yield of sdAb (G3 and FC5) attachment on liposomes prepared by the maleimide approach.** The yield was calculated after measuring the sdAb by a bradford technique. Each value is the mean from n samples (and the standard deviation is presented)

sdAb-liposome	Yield of sdAb attachment (%)		
	Yield of sdAb attachment (%)	Range of values	N
G3-liposome	78±2	76.8-80.5	3
FC5-liposome	45 ±3	42.5-48.3	3

The calculated yield attachment for the sdAb tested was equal to 78% in the case of G3 and 45% in the case of FC5, showing a high ligation efficiency between the maleimide liposome and G3. FC5- maleimide liposomes presented the lowest efficacy when compared to all the immunoliposomes developed.

According to the results presented in this chapter the development of the immunoliposomes aiming to cross the BBB was successfully achieved, by two methods that differ in the conjugation properties. Since the yield of the conjugation techniques was confirmed to be promising, it was necessary to test the ability of the immunoliposomes in crossing the BBB.

### 3.11 *In vitro* BBB model

The BBB model was performed in order to determine the ability of the developed immunoliposomes in crossing the BBB. In this model brain endothelial cells were grown on the apical size of a porous membrane positioned between the apical side and the basolateral size. Two parameters were evaluated along the studies: the translocation of the immunoliposomes that was determined by fluorescence of the encapsulating rhodamine in the liposomes, and the BBB integrity, through FD40 translocation (material and methods section).

The first assay was carried out using the two sdAb in study, and the immunoliposomes previously developed by the two methods (biotin and maleimide) with 90 minutes of incubation.

Regarding the sdAb, the western blot results (figure 3.26) showed that after 90 minutes, both sdAb tested translocate the BBB, independently of the translocation mechanism, since it was detected in the basolateral side. The translocation of the two antibodies was similar. Furthermore, the analysis of the BBB integrity showed that the sdAb had minimal influence on the BBB model permeability (table 3.8).

**Table 3.8: Integrity of BBB in vitro model, after translocation of the sdAb in study (G3 and FC5).** The yield was calculated using FD40 as presented in material and methods sections. Each value is the mean from 2 samples (and the standard deviation is presented)

sdAb	BBB integrity (%)
G3	88.8 ± 3.77
FC5	93.8 ± 0.9

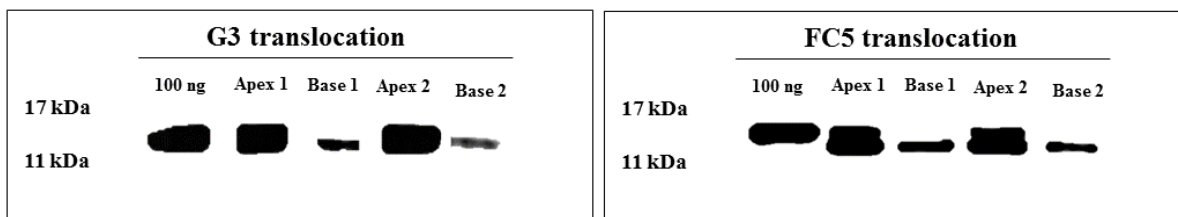


**Figure 3.26: Translocation of the sdAb across a BBB model in the 90 minutes incubation time.** The collected apical and basolateral sides were analysed in a western blot using anti-His (1:3000) as primary antibody. Two replicates wells for each sdAb were analysed.

Concerning the immunoliposomes, the results (figure 3.27) showed that after 90 minutes of incubation, a low percentage of the immunoliposomes added to the apical side translocate the BBB. The translocation of FC5-biotin-Lip and G3-biotin-LIP was 3.8 and 4.1 times higher respectively, than the biotin-lip without the sdAb. Instead, the translocation of FC5-maleimide-Lip and G3-maleimide-Lip was 1.2 and 1.7 times higher than the maleimide-lip without the sdAb, respectively(figure 3.27). The evaluation of the translocation between the two different immunoliposomes developed led us to conclude that the biotin-liposomes were more efficient in crossing the BBB when compared with the maleimide liposomes. Furthermore, the evaluation of BBB integrity (table 3.9) revealed that all immunoliposomes developed had minimal effect on the barrier permeability proving to be a promising system for drug delivery to the brain. However, the translocation of the immunoliposomes remains low and in order to improve the translocation a new assay was performed with higher incubation times, using the immunoliposomes developed though biotin conjugation. A incubation time higher than 90 minutes can be necessary for the translocation of nanocarriers with a higher size than the sdAb as already discussed in previous studies [113].

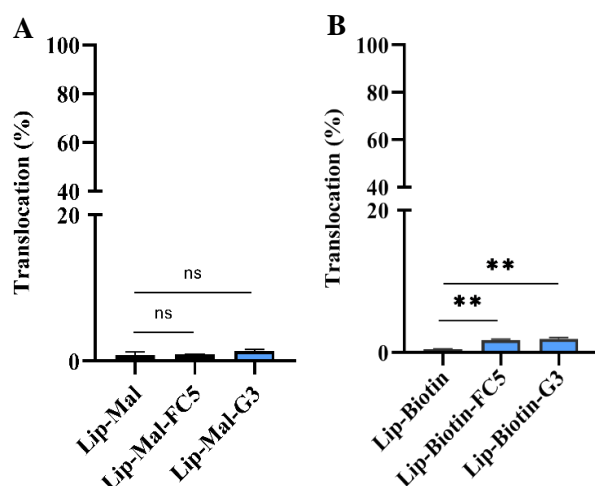


**Figure 3.27: Percentage of BBB translocation by immunoliposomes developed by maleimide conjugation.** (A) immunoliposomes developed by biotin conjugation (B)The percentage of translocation was, determined by fluorescence intensity measurements of rhodamine-loaded liposomes detection. A one-way ANOVA statistical test followed by a Dunnet's test was used to compare each immunoliposome fluorescence measurement with the respective liposome without sdAb (\*\*  $p \leq 0.01$ ; n.s., not significant); The values were obtained from duplicates of one experiment.

**Table 3.9: Integrity of BBB in vitro model, after translocation with an incubation time of 90 minutes of the immunoliposomes in study.** The yield was calculated using FD40 as presented in material and methods sections. Each value is the mean from 2 samples (and the standard deviation).

Lip	BBB integrity (%)
Control (+)	89.4 ± 1.0
Biotin-Lip	94.7 ± 1.1
FC5-Biotin-Lip	90.6 ± 0.9
G3-Biotin-Lip	87.9 ± 0.5
Mal-Lip	93.2 ± 4.2
FC5-Mal-Lip	95.5 ± 1.4
G3-Mal-Lip	88.9 ± 5.7

### 3.12. *In vitro* BBB model – incubation time optimization

Aiming to improve the translocation of the immunoliposomes, several incubation times were tested. The immunoliposomes developed through the biotin method were added to the apical side of the BBB model and the basolateral side was collected after 3, 6 and 24 h of incubation. The translocation was measured using rhodamine fluorescence and it was also analysed by western blot using Anti-His (1:300) as primary antibody.

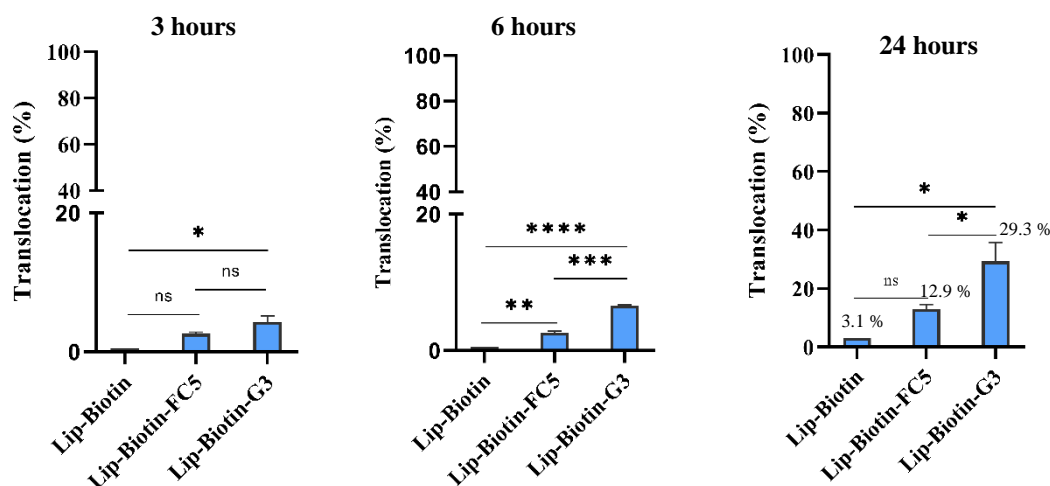


**Figure 3.28: Percentage of translocation for immunoliposomes developed by biotin approach at 3, 6 and 24h incubation times.** The percentage was determined by rhodamine fluorescence intensity detection. A one-way ANOVA statistical test followed by a Turkey's test was used to compare each immunoliposome fluorescence measurement with the respective liposome without sdAb and the two sdAb between each other (\*\*\*\* $p < 0.0001$ ; \*\*\* $p \leq 0.001$ ; \*\* $p \leq 0.01$ ; \* $p \leq 0.05$ ; n.s., not significant); The values were obtained from duplicates of one experiment.

The results (figure 3.28) showed that the highest translocation percentage was observed at 24 hours of incubation. With this incubation time the translocation reached a maximum of  $29.3 \pm 6.5\%$  using the G3-biotin-liposome, which is 9.4 times higher than the liposomal formulation without the sdAb. Concerning the liposome linked with FC5 the translocation is about  $12.9 \pm 1.6\%$ , that is 4.2 times higher than the liposomal formulation, which is similar to the results previously obtained in the incubation time of 90 minutes. Independently of the incubation time, the immunoliposome with G3 presented consistently a better translocation when compared with FC5 immunoliposomes, which can be due to the translocation mechanism of G3 that is still unknown.

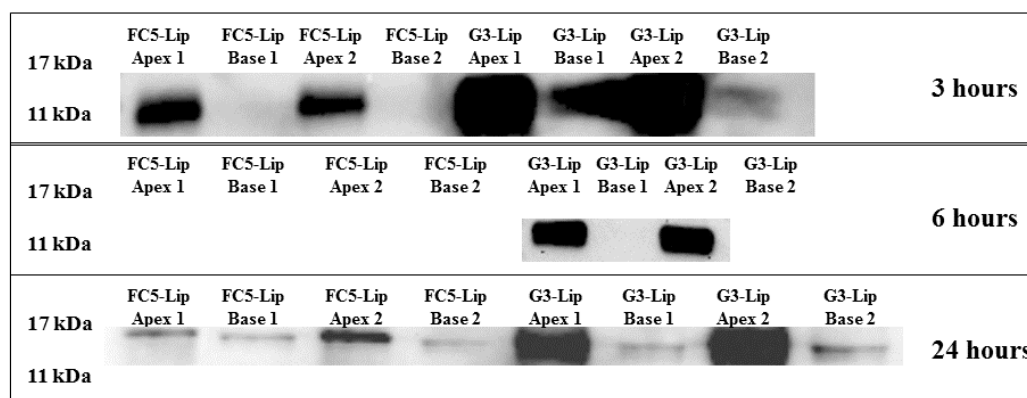


**Figure 3.29: Translocation of the sdAb across a BBB model with several time points: 3,6 and 24 hours.** The collected apical and basolateral sides were analysed in a western blot using Anti-His (1:3000) as primary antibody. Two replicates wells for each sdAb were analysed.

The western blot results (figure 3.29) of the three time points support the fluorescence data. The incubation time with the best results was the 24 hours where the immunoliposome was detected on the basolateral side collected in both cases (with FC5 and G3), in all the duplicates. In the first time point (3 hours) it is only achievable to detect the immunoliposome in the basolateral side in G3 immunoliposomes. Additionally, in the incubation time of 6 hours, it was only possible to detect the G3 immunoliposomes in the apical side which implies that the translocation was negligible. The absence of bands in the both sides of the *in vitro* BBB model in the case of FC5 immunoliposomes can be a consequence of the loss of the His-Tag during the conjugation procedure.

Based on the western blot and the fluorescence measurements results, the incubation time of 24 hours revealed to be the most adequate incubation time for the translocation of the immunoliposomes through the BBB. Noteworthy, the translocation of G3 immunoliposomes through the BBB on this incubation time showed a high *in vitro* efficacy, revealing these immunoliposomes as a promising therapeutic for *S. pneumoniae* overtaking the obstacle in translocate the BBB.

Additionally, the integrity of the BBB does not present any effect on the permeability, validating the immunoliposomes in a higher incubation time (table 3.10).

**Table 3.10: Integrity of BBB in vitro model, after translocation with an incubation time of 3, 6, and 24 hours of incubation with the immunoliposomes in study.** The integrity was calculated using FD40 as presented in material and methods sections. Each value is the mean from 2 samples (and the standard deviation).

<b>Lip</b>	<b>BBB integrity (%)</b>
<b>Control (+)</b>	90.4 ± 1.0
<b>Biotin-Lip (3h)</b>	87.4 ± 0.3
<b>FC5-Biotin-Lip (3h)</b>	94.1 ± 5.2
<b>G3-Biotin-Lip (3h)</b>	97.9 ± 0.8
<b>Biotin-Lip (6h)</b>	87.4 ± 0.3
<b>FC5-Biotin-Lip (6h)</b>	95.8 ± 2.9
<b>G3-Biotin-Lip (6h)</b>	90.7 ± 0.6
<b>Biotin-Lip (24h)</b>	95.2 ± 1.0
<b>FC5-Biotin-Lip (24h)</b>	92.2 ± 3.0
<b>G3-Biotin-Lip (24h)</b>	95.2 ± 1.5

Therefore, to further ensure the results obtained above, two independent assays were performed in the same conditions used before, with an incubation time of 24 hours. The results of these assays (figure 3.30) showed that both immunoliposomes have a high translocation, about 24.8±1.2% for FC5 immunoliposomes and 34±4.1% for G3 immunoliposomes.

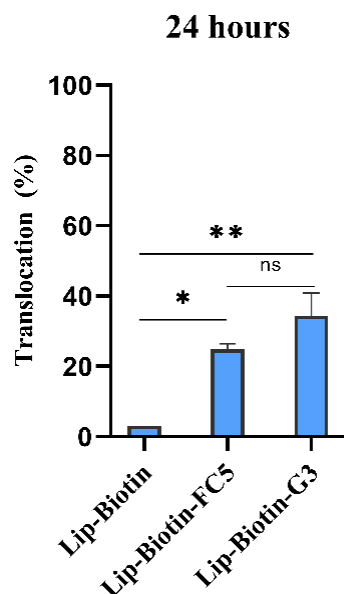


**Figure 3.30: Percentage of translocation for immunoliposomes developed by biotin approach at 24h incubation time.** The percentage was determined by rhodamine fluorescence intensity detection. A one-way ANOVA statistical test followed by a Turkey's test was used to compare each immunoliposome fluorescence measurement with the respective liposome without sdAb and the two sdAb between each other (\*\*  $p \leq 0.01$ ; \*  $p \leq 0.05$ ; n.s., not significant); The values were obtained from the mean of duplicates of two independent experiment and the standard deviations are presented.

#### **Chapter 4 - Integrated analysis, main conclusions and future perspectives.**

Bacterial meningitis caused by *S. pneumoniae* is a severe cause of meningitis, affecting all ages and often resulting in sequelae or death of the patient. The main challenge for the treatment of this disease is the low permeability of the BBB to most of the pharmaceuticals. Therefore, the treatment of pneumococcal meningitis requires the incorporation of a target technology for the BBB and an antimicrobial compound to fight bacteria.

Nanocarriers are the most commonly studied as drug delivery vehicles for BBB translocation with the advantage of selectively targeting the brain [114]. The approach presented in this study has the purpose to develop an immunoliposome as a drug delivery system for the treatment of pneumococcal meningitis. Otherwise stated, the treatment purpose combines the antibiotic's encapsulation as the antimicrobial compound and the conjugation of a sdAb to the liposome surface, aiming to target the BBB.

The first step of this study was the validation of the antimicrobial efficiency of the liposome encapsulated with antibiotic against *S. pneumoniae* TIGR4 (reference strain). This task was performed by determining the minimum inhibitory concentration of the three liposome-encapsulated antibiotics: ceftriaxone, penicillin and vancomycin. The results for this assay confirmed the antimicrobial efficacy of the three liposomal-encapsulated formulations and were interpreted as positive indicators to the development of a treatment of a pneumococcal meningitis. The MIC of the liposome-encapsulated antibiotics was higher than the free antibiotics in all cases, however, it is important to note that these encapsulated liposomes represent a better option for clinical treatment since they possess lower cytotoxicity and a targeting technology [115]. Between the three different formulations the vancomycin-encapsulated liposomes were the most efficient ones. This is proved since the differences between the MIC of the free antibiotic and the

vancomycin-encapsulated liposome is much lower when compared with other formulations. However, the comparison between the efficacy of the three encapsulated-liposomes have shown that the ceftriaxone-encapsulated liposomes and the penicillin-encapsulated liposomes have a lower MIC, considering a promising option for pneumococcal meningitis treatment.

In order to validate the liposomal formulations their potential was also evaluated in clinical isolates. Each described serotype holds different capsule characteristics. The interaction between the liposome and the bacterial capsule seems to occur, since different serotypes resulted in different antimicrobial efficacy of the antibiotics-encapsulated liposomes. For example, serotype 1 has a zwitterionic capsule that can interact either with anionic liposomes or cationic. On the other hand serotype 7F produces neutral polysaccharides which leads to a non-charge capsule [116]. In summary, the differences between the polysaccharides in each CPS result in distinct charges. These differences interfere with the interaction between the liposome and the bacteria and consequently the results obtained differ according to the serotype. In further studies, it will be crucial to test different liposomal formulations with singular characteristics, aiming to discover a formulation that enhances the interaction between the liposome and the different serotypes CPS. For example, the use of a fusogenic liposome, described as pH-sensitive with a high capacity to fuse with the bacteria membrane and promote intracellular drug release [76]. This is a promising approach for pneumococcal meningitis since this type of liposomes is able to interact with the bacteria and perhaps annul the interference of the CPS.

Before the development of an immunoliposome the toxicity of the antibiotics-encapsulated liposomes was tested using cytotoxicity assays, which is considered a crucial step of any pharmaceutical development [117]. The results of the cytotoxicity assays proved that none of the developed encapsulated liposomes decreased the viability of the brain endothelial cells suggesting that the nanoparticle proposed is a safer way to treat pneumococcal meningitis.

Since the antimicrobial efficacy and the safety of the developed liposomal formulations were tested, the following step was the development of the immunoliposome, which started with a successful expression and purification of the two sdAb used to conjugate in the liposomal surface: FC5 that is widely used to target the BBB and G3 that was selected by our laboratory as a promising sdAb that targets the BBB. The conjugation of the liposome and the sdAb were tested by two often used methods: the biotin-streptavidin method and the maleimide method. The development of the immunoliposome was optimized and it was possible to obtain high yields for this process through the two tested methods.

The main purpose of this project was the development of an immunoliposome able to cross the BBB. Consequently, an *in vitro* BBB model was developed to evaluate the translocation of the immunoliposomes through the BBB. The immunoliposomes developed by the biotin method demonstrated a higher translocation when compared with the immunoliposomes developed by the maleimide method being chosen as the best conjugation method. The *in vitro* model was then optimized concerning the incubation time with the immunoliposomes, and 24 hours was selected as the best incubation time where the translocation is high without loss of integrity. Between the two sdAb used is possible to conclude that G3-immunoliposomes have a higher translocation when compared with FC5-immunoliposomes.

The overall results from this work showed that an immunoliposome as a drug delivery system for treatment of pneumococcal meningitis is a promising approach, since it was possible to validate the antimicrobial efficacy of the encapsulate-liposome antibiotics against *S.pneumoniae* and it was achievable the development of an immunoliposome able to cross the BBB.

As in this work only the *in vitro* translocation of the immunoliposomes was tested, to strengthen these results, the execution of an *in vivo* biodistribution of the immunoliposomes, in which the translocation of the immunoliposomes through the brain will be tested along with the accumulation of the immunoliposomes in several organs will also prove the low toxicity of the developed immunoliposomes. Besides that, the biodistribution and efficacy of the immunoliposomes in a pneumococcal meningitis mouse model will provide important conclusions about the developed drug delivery system.

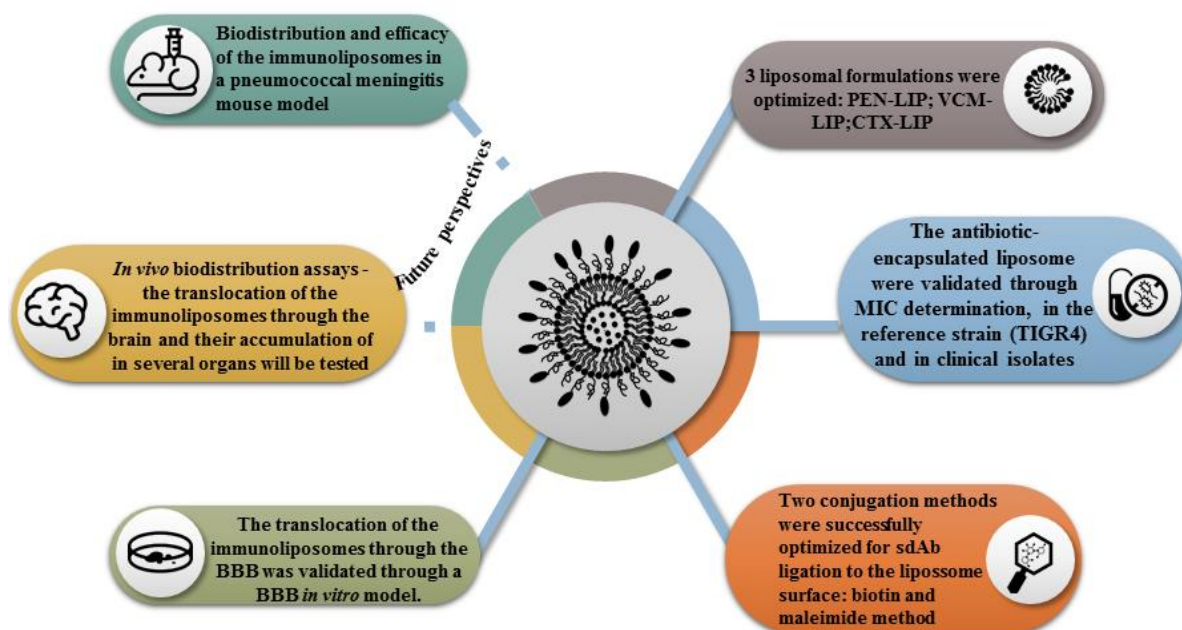


Figure 4.1: Schematic representation of the main results of this project and the future perspectives

In conclusion this work is an essential first step in the pneumococcal meningitis treatment, validating a novel therapeutic approach. We hope that this work also contributes to the infinite steps required for the treatment of several brain diseases limited by the BBB impermeability.

## Chapter 5 - Bibliography

1. Swartz, M. N., & Nath, A. (2012). *Meningitis: bacterial, viral, and other. Goldman's Cecil Medicine, 24/e* (Twenty Fou.). Elsevier Inc. doi:10.1016/B978-1-4377-1604-7.00420-6
2. Torpy, J. ., Lynn, C., & Glass, R. M. (2007). Meningitis. *JAMA*, *297*, 122.
3. Zueter, A. M. (2018). Infectious Meningitis. *Clinical Microbiology Newsletter*, *37*(6), 43–51. doi:10.1016/j.clinmicnews.2015.02.004
4. Tille, P. M., Lynn.C., & Glass, R. M. (2014). *Bailey & Scott's diagnostic microbiology. Bailey & Scott's diagnostic microbiology.*
5. Gans, J. De, Tunkel, A. R., & Wijdicks, E. F. M. (2006). Community-Acquired Bacterial Meningitis in Adults, 44–53.
6. Thigpen, M. C. (2007). Bacterial Meningitis in the United States. *New England Journal of Medicine*, *364*, 2016–2025.
7. Weisfelter, M., Van de Beek, M., & Spaanjar, L. (2006). Clinical features complications and outcome in adults with pneumococcal meningitis: a prospective cause series. *Lancet Neurology*, *5*(123–129).
8. Ruoff, K., Whiley, R., & Beighton, D. (2003). Streptococcus. In *Manual of Clinical Microbiology* (8th, voll ed., pp. 411–421). Washington: ASM press.
9. Lund, E. (1978). Laboratory Diagnosis, serology and epidemiology of Streptococcus pneumoniae. In T. Berman & J. R. Norris (Eds.), *Methods in Microbiology*, vol 12 (pp. 242–263). London: Academic Press.
10. Geno, K., Saad, J., & Nahm, M. (2017). Pneumococcal capsules and their types: past, present and future. *J Clinical Microbiology*, *55*, 1416–1425.
11. Austrian, R. (1981). Some observations on the pneumococcus and on the current status of pneumococcal disease and its prevention. *Rev infect Dis*, *3*, 183–189.
12. Kadioglu, A., Weiser, J. N., Paton, J. C., & Andrew, P. W. (2008). The role of Streptococcus pneumoniae virulence factors in host respiratory colonization and disease. *Nat Rev Microbiol*, *6*, 288–301.
13. Jonsson, S., Musher, D., Chapman, A., Goree, A., & Lawrence, E. (1985). phagocytosis and killing of common bacterial pathogens of the lung by human alveolar macrophages. *Journal Of Infectious Disease*, *152*, 4–13.
14. Nelson, A., Roche, A., Gould, J., Chim, K., Ratner, A., & Weiser, J. (2007). Capsule enhances pneumococcal colonization by limiting mucus-mediated clearance. *Infect Immun*, *75*, 83–90.
15. Van der poll, T., & Opal, S. (2009). Pathogenesis, treatment, and prevention of pneumococcal pneumonia. *Lancet*, *374*, 1543–1556.
16. Iovino, F., Seinen, J., Henriques-normark, B., & Dijn, J. M. Van. (2016). How Does Streptococcus pneumoniae Invade the Brain? *Trends in Microbiology*, *24*(4), 307–315. doi:10.1016/j.tim.2015.12.012
17. Aas, J., Paster, B., Stokes, L., Olsen, I., & Dewhirst, F. (2005). Defining the normal bacterial flora of the oral cavity. *J Clinical Microbiology*, *43*, 5721–5732.
18. Burnaugh, A., Frank, L., & King, S. (2008). Growth of Streptococcus pneumoniae on human glycoconjugates is dependent upon the sequential activity of bacterial

exoglycosidases,. *Journal of Bacteriology*, 190, 221–230.

19. Feldman, C., Mitchell, T., Andrew, P., Boulnois, G., Read, R., Todd, H., ... Wilson, R. (1990). The effect of *Streptococcus pneumoniae* pneumolysin on human respiratory epithelium in vitro. *Microb.Pathog.*, 9, 275–284.
20. Davis, K., Akinbi, H., Standish, A., & Weiser, J. (2008). Resistance to mucosal lysozyme compensates for the fitness deficit of peptidoglycan modifications by *Streptococcus pneumoniae*. *PLOS pathogens*.
21. BM, G., GM, C. 3rd, & HC, D. J. (1980). Epidemiologic studies of *Streptococcus pneumoniae* in infants: acquisition, carriage and infection during the first 24 months of life. *Journal Of Infectious Disease*, 142, 923–33.
22. Mehr, S., & Wood, N. (2012). *Streptococcus pneumoniae* – a review of carriage, infection, serotype replacement and vaccination. *Paediatric Respiratory Reviews*, 13, 258–264.
23. I, J., Harwell, M., & Brown, R. B. (1999). The Drug-Resistant Pneumococcus. *FCCP*.
24. Brueggemann, A. B., Peto, T. E. A., Crook, D. W., Butler, J. C., & Kristinsson, K. G. (2004). Temporal and Geographic Stability of the Serogroup- Specific Invasive Disease Potential of *Streptococcus pneumoniae* in Children, (November). doi:10.1086/423820
25. Scott, J. A. G., Hall, A. J., Dagan, R., & Dixon, J. M. S. (n.d.). Serogroup-Specific Epidemiology of *Streptococcus pneumoniae*: Associations with Age , Sex , and Geography in 7 , 000 Episodes of Invasive Disease, 973–981.
26. AM, B., JJ, C., J, Y., KA, G., GR, C., & MH, N. (2014). Low invasiveness of pneumococcal serotype 11A is linked to ficolin-2 recognition of O-acetylated capsule epitopes and lectin complement pathway activation. *Journal Of Infectious Disease*, 210, 1155–1165.
27. Marriot, H., Mitchell, T., & Dockerll, D. (2008). Pneumolysin: a double-edge sword during the host-pathogen interaction. *Curr Mol Med*, 8, 497–509.
28. Ring, A., Weiser, J., & Tuomanen, E. (1998). Pneumococcal trafficking across the blood-brain barrier. Molecular Analysis of a novel bidirectional pathway. *J Clin Invest*, 102, 347–360.
29. Ohga, S., Aoki, T., Okada, K., Akeda, H., & Fujioka, K. (1994). Cerebrospinal fluid concentrations of interleukin-1 beta, tumour necrosis factor alpha and interferon gamma in bacterial meningitis. *Arch Dis Child*, 70, 123–125.
30. Pfister, H., Fontana, A., Tauber, M., Tomasz, A., & Sheld, W. (1994). Mechanisms of brain injury in bacterial meningitis: workshop summary. *Clinical Infectious Diseases*, 16, 463–479.
31. Miller, E. L. (2002). The penicillins: a review and update. *Journal of Midwifery & Wome's Health*, 47(6), 426–434.
32. Alexander, M. R. (n.d.). A review of Vancomycin.
33. Richards, D. M., Heel, R. C., Brogden, R. N., Speight, T. M., & Avery, G. (1984). Ceftriaxone A Review of its Antibacterial Activity. *Pharmacological properties and Therapeutic use*, 527, 469–527.
34. Obaro, S. K. (2002). The new pneumococcal vaccine. *Clinical Microbiology and Infection*, 8, 623–633.
35. JC, B., RF, B., JF, C., HB, L., CV, B., & RR, F. (1993). Pneumococcal polysaccharide vaccine efficacy: An evaluation of current recommendations. *JAMA*, 270, 1826–1831.

36. Musher Daniel M. (2015). Pneumococcal Vaccination in Adults. <http://www.uptodate.com/contents/pneumococcal-vaccination-in-adults>.
37. Whitehouse Station, N. (2014). US Food and Drug Administration. Pneumovax 23 Prescribing Information. *Merck Sharp & Dohme Corp., a subsidiary of Merck & Co., Inc.* Retrieved April 25, 2019, from <https://www.fda.gov/downloads/BiologicsBloodVaccines/Vaccines/ApprovedProducts/UCM257088.pdf> (Accessed: March 27, 2017).
38. Bonten, M., Huijts, S., Bolkenbaas, M., Webber, C., Patterson, S., & Gault, S. (2015). Polysaccharide conjugate vaccine against pneumococcal pneumonia in adults. *New England Journal of Medicine*, *372*, 1114–1125.
39. Westerink, M., Schroeder, H. J., & Nahm, M. (2012). Immune responses to pneumococcal vaccines in children and adults: rationale for age-specific vaccination. *Aging Dis*, *3*, 51–67.
40. Hanage, W. P., Huang, S. S., Lipsitch, M., Bishop, C. J., Godoy, D., Pelton, S. I., Finkelstein, J. A. (2007). Diversity and antibiotic resistance among nonvaccine serotypes of *Streptococcus pneumoniae* carriage isolates in the post-heptavalent conjugate vaccine era. *Journal Of Infectious Disease*, *195*, 347–352.
41. Pilishvili, T., Lexau, C., Farley, M., Hadler, J., Harrison, L., & Bennett, N. (2010). Sustained reductions in invasive pneumococcal disease in the era of conjugate vaccine. *Journal Of Infectious Disease*, *201*, 32–41.
42. Brito, M. J., Silva-Costa, C., Aguiar, S., Lopes, J. P., Ramirez, M., & Melo-Cristino, J. (2019). The increasing importance of non-culture methods in diagnosis and serotyping of invasive pediatric pneumococcal infections revealed the continuous dominance of vaccine serotypes in the era of PCV13 vaccination. *International Journal of Infectious Diseases*, *79*.
43. Frazão, N., Brito-Avô, A., Simas, C., Saldanha, J., Mato, R., Nunes, S., ... Lencastre, H. de. (2005). Effect of the sevenvalent conjugate pneumococcal vaccine on carriage and drug resistance of *Streptococcus pneumoniae* in healthy children attending day-care centers in Lisbon. *Pediatr Infect Dis J*, *24*, 243–252.
44. Banks, W. A. (2016). From blood-brain barrier to blood-brain interface: new opportunities for CNS drug delivery. *Nature Reviews*, *15*, 275–292.
45. Neuweit, E. (2008). Strategies to advance translational research into brain barriers. *Lancet Neurology*, *7*, 84–96.
46. Pardrige, W. M. (2005). The Blood Brain Barrier: Bottleneck in brain drug development. *NeuroRx*, *2*, 3–14.
47. Patel, M. M. (2009). Getting into the brain: approaches to enhance brain drug delivery. *CNS Drugs*, *23*, 35–58.
48. Gabathuler, R. (2009). Blood-brain barrier transport of drugs for the treatment of brain diseases. *CNS & Neurological Disorders: Drug Targets*, *8*, 195–204.
49. Spencer, B. J., & Verma, I. (2007). Targeted delivery of proteins across the blood-brain barrier. *Proceeding of the National Academy of Sciences of the United States of America*, *104*, 7594–7599.
50. Jones, A. R., & Shusta, E. V. (2007). Blood-brain barrier transport of therapeutics via receptor-mediation. *Pharmaceutical Research*, *24*, 1759–1771.
51. Smith, M. W., & Gumbleton, M. (2006). Endocytosis at the blood-brain barrier: From

- basic understanding to drug delivery strategies. *Journal of Drug Targeting*, *14*, 191–214.
52. JA, C., YJ, Y., Y, Z., JM, T., RN, F., WJ, M., ... RJ, W. (2013). Addressing safety liabilities of TfR bispecific antibodies that cross the blood-brain barrier. *Scientific translational medicine*, *5*, 1–12.
  53. Muyldermans, S. (2001). Single domain camel antibodies: current status. *J. Biotechnol.*, *74*, 277–302.
  54. Tanha, J., Dubue, G., Hiramata, T., Narang, S. A., & Mackenzie, C. R. (2002). Selection by phage display of llama conventional VH fragments with heavy chain antibody VHH properties. *J. Immunol. Meth.*, *263*, 97–109.
  55. Tanha, J., Muruganandam, A., & Stanimirovic, D. (2003). Phage Display technology for identifying specific antigens on brain endothelial cells. *Med. Meth. Mol.*, *89*, 438–444.
  56. Muruganandam, A., Tanha, J., Narang, S., & Stanimirovic, D. (2002). Selection of phage-display llama single domain antibodies that transmigrate across human blood brain barrier endothelium. *FAS-EB J.*, *16*, 240–242.
  57. Abulrob, A., Sprong, H., Henegouwen, P. van B. en, & Stanimirovic, D. (2005). The blood-brain barrier transmigrating single domain antibody: mechanisms of transport and antigenic epitopes in human brain endothelial cells. *Journal of Neurochemistry*, *95*, 1201–1214.
  58. Abeylath, S. C., & Turos, E. (2008). Drug delivery approaches to overcome bacterial resistance to beta-lactam antibiotics. *Expert. Opin. Drug Delivery*, 5931–5949.
  59. Ulrich, A. S. (2002). Biophysical aspects of using liposomes as delivery vehicles. *Biosci. Rep*, *22*, 129–150.
  60. Sharma, A., & Sharma, U. . (1997). Liposomes in drug delivery: progress and limitations. *Int. J. Pharma*, *154*, 123–140.
  61. Gregoriadis, G. (1995). Engineering liposomes for drug delivery: progress and problems. *Trends Biotechnology*, *13*, 527–537.
  62. Schiffelers, R., Storm, G., & Bakker-Woudenberg, I. A. J. . (2001). Liposome-encapsulated aminoglycosides in pre-clinical and clinical studies. *J. Antimicrob. Chemother*, *48*, 333–344.
  63. Frank, M. (1993). The reticuloendothelial system and bloodstream clearance. *J Lab Clin Med*, *122*, 487–488.
  64. Woodle, M., Matthey, K., Newman, M., Hidayat, J., Collins, L., & Redemann, C. (1992). Versatility in lipid compositions showing prolonged circulation with sterically stabilized liposomes. *Biochim. Biophys Acta*, *1105*, 193–200.
  65. Papahadjopoulos, D., Allen, T. M., Gabizon, A., Mayhew, E., Matthey, K., & Huang, S. (1991). Sterically stabilized liposomes: improvements in pharmacokinetics and antitumor therapeutic efficacy. *Proc Natl Acad Sci USA*, *88*, 11460–11464.
  66. Spuch, C., & Navarro, C. (2011). Liposomes for Targeted Delivery of Active Agents against Neurodegenerative Diseases. *J. Drug. Deliv.*
  67. Noble, G. T., Stefanick, J. F., Ashley, J. D., Kiziltepe, T., & Bilgicer, B. (2014). Ligand-targeted liposome design: challenges and fundamental considerations. *Trends Biotechnology*, *32*, 32–45.
  68. Corley, P., & Loughrey, H. (1994). Binding of biotinylated-liposomes to streptavidin is influenced by liposome composition. *Biochim. Biophys Acta*, *1195*, 149.

69. Loughrey, H., Bally, M. B., & Cullis, P. R. (1987). A non-covalent method of attaching antibodies to liposomes. *Biochim. Biophys Acta - Biomembranes*, *901*, 157.
70. Torchilin, V. P., Khaw, B. A., Smirnov, V. N., & Habera, E. (1979). Preservation of antimyosin antibody activity after covalent coupling to liposomes. *Biochemical and Biophysical Research Communications*, *89*(4), 1114–1119.
71. Gupta, B., & Torchilin, V. P. (2007). Monoclonal antibody 2C5-modified doxorubicinloaded liposomes with significantly enhanced therapeutic activity against intracranial human brain U-87 MG tumor xenografts in nude mice. *Cancer Immunol. Immunother*, *56*, 1215–1223.
72. Bell, R. D., & Ehlers, M. D. (2014). Breaching the blood-brain barrier for drug delivery. *Neuron*, *81*, 1–3.
73. Akash, M. S. H., Rehman, K., Parveen, A., & Ibrahim, M. (2016). Antibody-drug conjugates as drug carrier systems for bioactive agents. *Int. J. Polym. Mater. Polym. Biomater*, *65*, 1–10.
74. Qin, J., Li, R., Raes, J., Arumugam, M., Burgdorf, K. S., Manichanh, C., ... Yamada, T. (2010). A human gut microbial gene catalogue established by metagenomic sequencing. *Nature*, *464*, 59–65.
75. Methods for dilution antimicrobial susceptibility tests for bacteria that grow aerobically. (2006). *Approved standard - Seventh edition. CLSI document M07-A7*.
76. Garcia, B., Shi, C., & Webster, T. J. (2017). Tat-functionalized liposomes for the treatment of meningitis: an in vitro study. *International journal of nanomedicine*, *12*, 3009–3021.
77. Thomas S. Hnasko, & Robert M. Hnasko. (2015). The western blot. *Springer protocols*.
78. Show, P. L., Ooi, C. W., & Ling, T. C. (2019). *Bioprocess Engineering: Downstream Processing*.
79. SH, H., KP, N., JA, M., KK, H., JP, S., T, H., ... HR, N. (2007). Rhizavidin from *Rhizobium etli*: the first natural dimer in the avidin protein family. *Biochem J*, *405*, 397–405.
80. DE, H., I, L. T., EA, M., JF, E., NM, G., RE, S., & PS, S. (2006). Cooperative hydrogen bond interactions in the streptavidin-biotin system. *Protein science*, *15*, 459–467.
81. Ansell, S. M., Harasym, T. O., Tardi, P. G., Buchkowsky, S. S., Bally, M. B., & Culli, P. R. (n.d.). Antibody Conjugation Methods for Active Targeting of Liposomes. In *Methods in Molecular Medicine*.
82. Kruger, N. J. (1994). The Bradford Method for Protein Quantitation. In *Basic Protein and Peptide Protocols. Methods in Molecular Biology<sup>TM</sup>*.
83. Neves-coelho, S., Eleut, R. P., Enguita, F. J., Neves, V., & Castanho, M. A. R. B. (2017). A New Noncanonical Anionic Peptide That Translocates a Cellular Blood–Brain Barrier Model. *Molecules*, *22*. doi:10.3390/molecules22101753
84. F, H., F, Y., J, P., KZ, L., LW, W., & XL, D. (2010). Immortalized mouse brain endothelial cell line Bend.3 displays the comparative barrier characteristics as the primary brain microvascular endothelial cells. *Zhongguo Dang Dai Er Ke Za Zhi*, *12*, 474–478.
85. Maier, R. M. (2009). Bacterial Growth. In *Environmental Microbiology* (pp. 37–54).
86. Yates, G. T., & Smotzer, T. (2007). On the lag phase and initial decline of microbial growth curve. *J Theoret. Biol.*, *244*, 511–517.

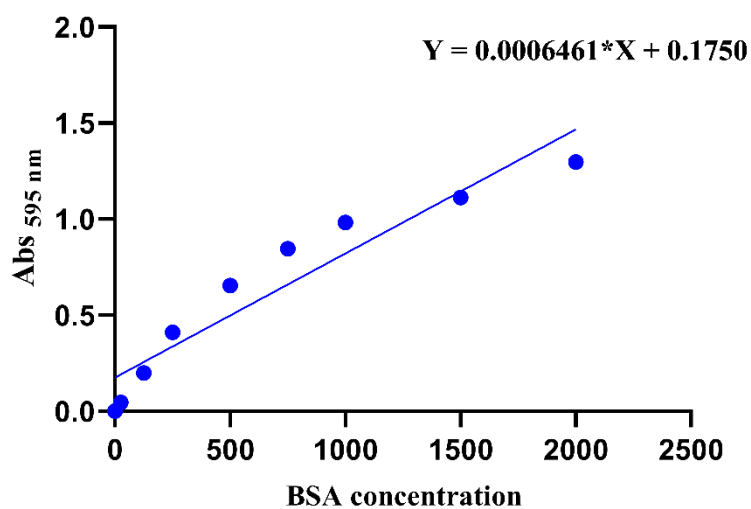
87. Hall, B. G., Acar, H., Nandipati, A., Barlow, M., & Easy, G. R. M. (2014). Growth Rates Made Easy. *Molecular Biology and Evolution*, *31*, 232–238.
88. Kolter, R., Siegele, D. A., & Tormo, A. (1993). The stationary phase of bacterial life cycle. *Annual Review of Microbiology*, *47*, 855–874.
89. Widdel, F. (2007). Theory and measurement of bacterial growth. *Di dalam Grundpraktikum Mikrobiologie*.
90. MJ, B., C, M., I, M.-B., MS, V., YV, B., C, G., ... N., C. (2017). programmed cell division delay preserves genome integrity during natural genetic transformation in *Streptococcus pneumoniae*. *Nature communications*, *8*, 1621.
91. I, W., K, H., & RE, H. (2008). Agar and broth dilution methods to determine the minimal inhibitory concentration (MIC) of antimicrobial substances. *Nature Protocols*, *3*, 163–175.
92. Prata, F., Cabral, M., Ventura, L., Ferreira, P. R., & Brito, M. J. (2018). MENINGITES AGUDAS BACTERIANAS Recomendações da Sociedade de Infecçologia Pediátrica e da Sociedade de Cuidados Intensivos Pediátricos da SPP. *Sociedade Portuguesa de Pediatria*.
93. Andrews, J. (2001). Determination of minimum inhibitory concentrations. *J Antimicrob Chemother*, *48*, 5–16.
94. Danaei, M., Dehghankhold, M., Ataei, S., Davarani, F. H., Javanmard, R., Dokhani, A., ... Mozafar, M. R. (2018). Impact of Particle Size and Polydispersity Index on the Clinical Applications of Lipidic Nanocarrier Systems. *pharmaceutics*, *10*.
95. Worldwinde, M. I. (2011). *Dynamic Light Scattering, Common Terms Defined*.
96. Putri, D. C., Dwiastuti, R., Marchaban, M., & Nugroho, A. . (2017). Optimization of mixing temperature and sonication duration in liposome preparation. *J. Pharm. Sci. Commun.*, *14*, 79–85.
97. Badran, M. (2014). Formulation and in vitro evaluation of flufenamic acid loaded deformable liposome for improved skin delivery. *Digest J. Nanometer. Biostruct.*, *9*, 83–91.
98. Hunter, R. J., Zhang, H., & Midmore, B. R. (2001). Zeta Potential of Highly Charged Thin Double-Layer Systems. *Journal of Colloid and Interface Science*, *237*, 147–149.
99. Nii, T., & Ishii, F. (2005). Encapsulation efficiency of water-soluble and insoluble drugs in liposomes prepared by the microencapsulation vesicle method, *298*, 198–205. doi:10.1016/j.ijpharm.2005.04.029
100. MH, E., KM, O., MJ, G.-N., & LC, P. (2003). Efficacy of liposome-encapsulated ciprofloxacin compared with ciprofloxacin and ceftriaxone in a rat model of pneumococcal pneumonia. *J Antimicrob Chemother*, *51*, 83–91.
101. Yajko, D. M., Madej, J. J., Lancaster, M. V, Sanders, C. A., Cawthon, V. L., Gee, B., ... Hadley, W. K. (1995). Colorimetric Method for Determining MICs of Antimicrobial Agents for *Mycobacterium tuberculosis*, *33(9)*, 2324–2327.
102. Jenkins, S., Lewis, J., & Kihara, J. (1991). Multicenter trial of a new colorimetric method for determining antibiotic MICs for gram positive bacteria, abstr. *Abstracts of the 91st General Meeting of the American Society for Microbiology*, 368.
103. CO, O., CH, N., & MN, M. (1994). Enhanced killing of methicillin-resistant *Staphylococcus aureus* in human macrophages by liposome-entrapped vancomycin and teicoplanin. *Infection*, *22*, 338–342.

104. AA, K., SA, A.-S., & Abd-Allah. (2004). Treatment of experimental osteomyelitis by liposomal antibiotics. *J Antimicrob Chemother*, *54*, 1103–1108.
105. VP, T. (2005). Recent advances with liposomes as pharmaceutical carriers. *Nat. Rev. Drug. Discovery*, *4*, 145–160.
106. Song, J., Dagan, R., Klugman, K. P., & Fritzell, B. (2012). The relationship between pneumococcal serotypes and antibiotic resistance. *Vaccine*, *30*(17), 2728–2737. doi:10.1016/j.vaccine.2012.01.091
107. Yahiaoui, R. Y., Bootsma, H. J., Heijer, C. D. J. Den, Pluister, G. N., Paget, W. J., Spreeuwenberg, P., ... Stobberingh, E. E. (2018). Distribution of serotypes and patterns of antimicrobial resistance among commensal *Streptococcus pneumoniae* in nine European countries, 1–10.
108. Alhariri, M., Azghani, A., & Omri, A. (2013). Liposomal antibiotics for the treatment of infectious diseases. *Expert. Opin. Drug Delivery*, (April 2014). doi:10.1517/17425247.2013.822860
109. Aslantürk, Ö. S. (2017). In Vitro Cytotoxicity and Cell Viability Assays: Principles, Advantages, and Disadvantages. In *Genotoxicity - A Predictable Risk to Our Actual World*.
110. Hussein, K., Park, K.-M., Kang, K.-S., & Woo, H.-M. (2016). Biocompatibility evaluation of tissue-engineered decellularized scaffolds for biomedical application. *Mater Sci Eng C*, *67*, 766–778.
111. Azimzadeh, O., Linne, U., & Nyalwidhe, J. O. (2007). Use of Biotin Derivatives to Probe Conformational Changes in Proteins Use of Biotin Derivatives to Probe Conformational Changes, (May 2016). doi:10.1074/jbc.M610921200
112. Papadia, K., Markoutsas, E., & Antimisiaris, S. G. (2014). A Simplified Method to Attach Antibodies on Liposomes by Biotin-Streptavidin Affinity for Rapid and Economical Screening of Targeted Liposome. *Journal of Biomedical Nanotechnology*, *10*, 1–6.
113. Sciences, M. L., Gil, S., Andrieux, K., Nicolas, V., Taran, F., Georgin, D., ... Couvreur, P. (2005). A relevant in vitro rat model for the evaluation of blood-brain barrier translocation of nanoparticles. *Cellular and Molecular Life Sciences*, *62*, 1400–1408. doi:10.1007/s00018-005-5094-3
114. Khan, A. R., Yang, X., Fu, M., & Zhai, G. (2018). RECENT PROGRESS OF DRUG NANOFORMULATIONS TARGETING TO BRAIN. *journal of controlled release*.
115. AL, K., K, M., VP, T., & L, H. (1990). Amphipathic polyethyleneglycols effectively prolong the circulation time of liposomes. *FEBS*, *268*, 235–237.
116. Y, L., DM, W., CM, T., K, T., & M., L. (2013). Surface charge of *Streptococcus pneumoniae* predicts serotype distribution. *Infection and Immunity*, *81*, 4519–4524.
117. Bácskay, I., Nemes, D., Fenyvesi, F., Váradi, J., Vasvári, G., Fehér, P., ... Ujhelyi, Z. (2017). Role of Cytotoxicity Experiments in Pharmaceutical Development. In *Citotoxicity*.
118. Peate, I. (2004). An overview of meningitis: signs, symptoms, treatment and support. *British Journal of Nursing*, *13*, 796–801.
119. CMC, R., & MCJ, M. (2018). A world without bacterial meningitis: how genomic epidemiology can inform vaccination strategy. *F1000Research*.
120. Andrea G. Albarraçín Orío, G. E. P., Cortes, P. R., Cian, M. B., & Echenique, J. (2011). Compensatory Evolution of pbp Mutations Restores Fitness Cost Imposed by B-Lactam

Resistance in Streptococcus. *PLOS pathogens*.

121. Hansen, John, T., & Koeppe, Bruce, M. (2004). *Netter's Atlas of Human Physiology*.
122. Zhang, J., Wang, K., Mao, Z., Fan, X., Jiang, D. L., Chen, M., & Dang, S. C. (2013). Application of liposomes in drug delivery development- focus on gastroenterological targets. *International journal of nanomedicine*, 8, 1325–1334.
123. Hnasko, T. S., & Hnasko, R. M. (2015). The Western Blot. In *ELISA: Methods and Protocols* (Vol. 1318, pp. 87–96). doi:10.1007/978-1-4939-2742-5
124. Neves, V., Aires-da-silva, F., Corte-real, S., & Castanho, M. A. R. B. (2015). Antibody Approaches To Treat Brain Diseases. *Trends Biotechnology*, 34, 36–48. doi:10.1016/j.tibtech.2015.10.005

## Supplementary data



Supplementary figure 1: Linear regression and equation of absorbance of the several BSA concentrations for Bradford method .

### Unloaded liposomes containing functional PEG – PEG-Maleimide and PEG-Biotine

Lipid compositions – DPPC:Chol:DSPE-PEG: DSPE-PEG-FA: DSPE-PEG/Biotine or Maleimide Molar ratio - (1.85:1.0.11:0.03:0.01)

Supplementary table 1: Physicochemical characterization of liposomal formulations

Formulation	Mean size (nm) (P.I.)	Zeta Potential (mV)	Lipid Concentration (μmol/ml)
Biotine	125±2 (<0.06)	- 3 ± 1	20
Maleimide	128±1 (<0.06)	- 2 ± 1	20